

**AGE-ASSOCIATED DIFFERENCES IN HUMAN HEMATOPOIETIC STEM CELL
PROLIFERATION CONTROL**

by

Colin Hammond

B.Sc., University of Victoria, 2013

A THESIS SUBMITTED IN PARTIAL FULFILLMENT OF

THE REQUIREMENTS FOR THE DEGREE OF

DOCTOR OF PHILOSOPHY

in

THE FACULTY OF GRADUATE AND POSTDOCTORAL STUDIES

(Experimental Medicine)

THE UNIVERSITY OF BRITISH COLUMBIA

(Vancouver)

August 2021

© Colin Hammond, 2021

The following individuals certify that they have read, and recommend to the Faculty of Graduate and Postdoctoral Studies for acceptance, the dissertation entitled:

Age-associated differences in human hematopoietic stem cell proliferation control

submitted by Colin Hammond in partial fulfillment of the requirements for

the degree of Doctor of Philosophy

in Experimental Medicine

Examining Committee:

Dr. Connie Eaves, Professor, Medical Genetics, UBC

Supervisor

Dr. Xiaoyan Jiang, Professor, Medical Genetics, UBC

Supervisory Committee Member

Dr. Martin Hirst, Professor, Microbiology and Immunology, UBC

Supervisory Committee Member

Dr. Kenneth Harder, Associate Professor, Microbiology and Immunology, UBC

University Examiner

Dr. Fabio Rossi, Professor, Medical Genetics, UBC

University Examiner

Additional Supervisory Committee Members:

Dr. Carl Hansen, Adjunct Professor, Physics and Astronomy, UBC

Supervisory Committee Member

Abstract

Hematopoietic stem cells (HSCs) comprise a functionally and molecularly heterogeneous population of cells that collectively maintain the lifelong production of mature blood cells. Known developmental changes in their properties include an early postnatal switch from a rapidly cycling high self-renewal state to a quiescent state with an overall reduced self-renewal potential. Additional age-associated alterations in mouse HSC properties have been predicted but these have remained poorly explored in human HSCs. Of recent interest has been the finding that most healthy humans of advancing age possess enlarged clones of normal blood cells marked by somatic mutations in genes commonly involved in hematopoietic malignancies. Together, these findings suggest that altered regulation of HSC cycling may be a feature that develops with advancing age in humans. To examine this possibility, an investigation of the HSC and progenitor compartments in healthy human donors aged 0-69 years was initiated. A first characterization of cells within the HSC-enriched subset characterized by a CD34⁺CD38⁻CD45RA⁻CD90⁺CD49f⁺ (*CD49f*⁺) phenotype showed that these cells are consistently present from birth to old age at similarly low frequencies. Functional assays showed their long-term and lympho-myeloid differentiation capacity *in vitro* and *in vivo* (in transplanted immunodeficient mice) to be similar but indicated a possible increased *in vivo* supportive requirement with age. Kinetic analyses of individually tracked *CD49f*⁺ cells further revealed a strong and progressive aging-related delay in completing their first and subsequent divisions *in vitro* that was exacerbated when the growth factor stimulus was reduced. Development of a method for simultaneous cell-cycle staging and multiplexed molecular analysis of single *CD49f*⁺ cells traced this delay to a mitogen-sensitive G₁ elongation which was also evident at slightly later stages of hematopoietic cell differentiation. This delay appeared related to a reduced immediate

growth factor-induced activation of AKT and β -catenin obtained in adult cells. These findings point to a newly identified intrinsic and pervasive, aging-related alteration in specific early signaling intermediates that are required to drive G₁ progression in HSCs (and their early progeny) and lay the foundation for further analyses of how this regulatory change may impact the acquisition of other aging-related phenotypes in the hematopoietic system.

Lay Summary

A small collection of cells (called “blood stem cells”) are responsible for continuously producing the blood cells needed throughout a person’s life. However, little is known about how aging may impact this process. To address this question, blood and bone marrow cells were obtained from healthy human donors ranging in age from birth to 69 years old. Characterization of the blood stem cells in these samples showed many of their features were unchanged by aging. However, one important difference found was that blood stem cells from older donors took longer to generate two daughter cells when stimulated to do so. This change was shown to be connected to the way that older blood stem cells respond to certain external growth signals. These results present a previously unknown feature of aging that may contribute to the acquisition of other effects of aging on blood cell production including the development of leukemia.

Preface

Chapter 2 outlines the materials and methods used in Chapters 3 and 4.

Chapter 3 is being prepared for publication. Connie Eaves and I designed all experiments. I performed all experiments with some assistance from Fangwu Wang, Vivian Wu, Glenn Edin, and Margaret Hale. Fangwu Wang and I performed the *in vitro* lympho-myeloid differentiation experiment. Vivian Wu and Glenn Edin assisted with the *in vivo* transplantation experiments and animal tissue collections. I performed all data analysis and figure generation. Some scripts used for the analyses were originally developed by David Knapp. Connie Eaves and I interpreted the data.

Chapter 4 is being prepared for publication. Connie Eaves and I designed all experiments. I performed all experiments, data analysis, and figure generation. Vivian Wu and Danlin Zeng assisted for some of the cell-tracking experiments. Some R scripts used for the analyses were originally developed by David Knapp. Connie Eaves and I interpreted the data.

This research conducted here was approved by the UBC Human Research Ethics Board (H19-00207) and Animal Research Ethics Board (A19-0029).

Table of Contents

Abstract.....	iii
Lay Summary	v
Preface.....	vi
Table of Contents	vii
List of Tables	xi
List of Figures.....	xii
List of Abbreviations	xiii
Acknowledgements	xviii
Dedication	xix
Chapter 1: Introduction	1
1.1 Cellular Basis for Hematopoietic Reconstitution	1
1.2 Hematopoietic Cell Transplantation Therapies	2
1.3 Organization of the Hematopoietic Compartment.....	3
1.4 Origin and Development-Related Changes of HSCs.....	6
1.5 Contribution of HSCs to Steady-State Hematopoiesis	8
1.6 Features of Aging Hematopoiesis.....	12
1.7 Heterogeneity of HSC Properties	17
1.8 Regulation of HSC Behaviour	20
1.8.1 Intrinsic Regulation.....	21
1.8.2 Extrinsic Regulation.....	24
1.9 Cell Cycle Regulation.....	29
1.10 Cell Cycle Regulation in HSCs	32

1.11 Thesis Objectives.....	34
Chapter 2: Materials and methods.....	40
2.1 Normal human blood and marrow samples.....	40
2.2 Sample processing and isolation of cells by FACS.....	40
2.3 Phenotype data analysis.....	41
2.4 Assessment of <i>CD49f</i> + cell progenitor activity in engineered stromal cell-containing LTCs.....	43
2.5 Xenotransplants and analysis of regenerated cells.....	45
2.6 Single-cell tracking of survival and proliferation kinetics <i>in vitro</i>	46
2.7 Cell-cycle transit culture time-course setup and plate preparation for SA capture.....	48
2.8 Acquisition of microscope images.....	50
2.9 Analysis of microscopy data.....	50
2.10 Phospho-flow sample preparation and analysis.....	53
Chapter 3: Age-independent conservation of human CD34+ hematopoietic cell phenotypic progenitor content and <i>CD49f</i>+ long-term multilineage output potential.....	59
3.1 Introduction.....	59
3.2 Results.....	60
3.2.1 The relative frequencies of multiple phenotypes of human hematopoietic CD34+ cells are largely conserved from birth to mid-late adulthood.....	60
3.2.2 The <i>CD49f</i> + subset displays greater source- than aging-associated differences in their phenotypic properties.....	62
3.2.3 The LTC-IC frequency within the <i>CD49f</i> + subset is high and independent of donor age.....	63

3.2.4	Age-independent retention of lympho-myeloid differentiation potential of <i>CD49f</i> ⁺ cells.....	65
3.2.5	Repopulating ability of <i>CD49f</i> ⁺ cells from CB and adult BM is similar in a co-xenotransplantation assay.....	66
3.3	Discussion.....	67
Chapter 4: Aging delays proliferation and cell-cycle transit rates of normal human <i>CD49f</i>⁺ cells.....		85
4.1	Introduction.....	85
4.2	Results.....	87
4.2.1	Demonstration of a progressive age-related delay in the GF-stimulated kinetics of <i>CD49f</i> ⁺ cell division <i>in vitro</i>	87
4.2.2	Development of a system for monitoring paired cell cycle state and molecular changes in individually tracked cells.....	88
4.2.3	Adult <i>CD49f</i> ⁺ cells display an elongated G ₁ -phase	89
4.2.4	Proliferation but not survival responses of adult <i>CD49f</i> ⁺ cells are more sensitive to reduced GF stimulation than CB <i>CD49f</i> ⁺ cells.....	92
4.2.5	Adult <i>CD49f</i> ⁺ cells display lower activation of AKT and β-catenin following exposure to a strong GF stimulus.	95
4.3	Discussion.....	97
Chapter 5: Discussion.....		117
5.1	Major Contributions.....	117
5.1.1	Direct functional comparison of human <i>CD49f</i> ⁺ cells across 7 decades of age ..	119

5.1.2	Development of a high-resolution platform for multiplexed analysis of rare cells	122
5.1.3	Identification of a mitogen-sensitive developmentally regulated G ₁ transit delay	123
5.2	Implications and future directions	125
5.3	Limitations of the current work	127
5.4	Concluding remarks	129
	Bibliography	130

List of Tables

Table 2.1 Abs for <i>CD49f</i> + cell sorting and CD45+CD34+ phenotypic analysis	54
Table 2.2 Phenotypic definitions of stem and progenitor subtypes	55
Table 2.3 Abs and channels for <i>in vitro</i> lineage assessment	56
Table 2.4 <i>In vitro</i> lineage output classifications	57
Table 2.5 Abs for <i>in vivo</i> lineage assessment.....	57
Table 2.6 Microscopy Abs for cell-cycle staging	58
Table 2.7 Abs for phospho-flow cytometry	58
Table 3.1 Summary of donor specific outcomes in LTC-IC assays	83
Table 3.2 Summary of donor specific outcomes for <i>in vitro</i> lympho-myeloid assays.....	84
Table 3.3 Summary of donors and mice used for <i>in vivo</i> transplant analysis	84
Table 4.1 Analyzed cells by timepoint for cell-cycle staging in 100% 3GF	115
Table 4.2 Analyzed cells by timepoint for cell-cycle staging in 1% 3GF	116

List of Figures

Figure 1.1 Models of the human hematopoietic hierarchy	36
Figure 1.2 Highlighted factors impacting primitive hematopoietic cell cycling and self-renewal activities.....	38
Figure 1.3 Highlighted factors regulating cell-cycle entry and progression.....	39
Figure 3.1 Representative gating of CD34+ subsets from different sources of normal human blood cells.....	73
Figure 3.2 Phenotypic heterogeneity of the normal human CD34+ compartment	75
Figure 3.3 Phenotypic heterogeneity of <i>CD49f</i> + cells according to donor age and source	77
Figure 3.4 High LTC-IC activity of <i>CD49f</i> + cells from different sources.....	78
Figure 3.5 Age-independent lympho-myeloid differentiation potential of <i>CD49f</i> + cells revealed in single-cell cultures.....	80
Figure 3.6 Equivalent <i>in vivo</i> repopulating ability of CB and BM <i>CD49f</i> + cells revealed in a co-transplant assay.....	81
Figure 4.1 Identification of a progressive age-related delay in <i>CD49f</i> + division kinetics <i>in vitro</i>	103
Figure 4.2 Development of a system for monitoring paired cell-cycle state and molecular changes in individually tracked human blood cells.....	105
Figure 4.3 <i>CD49f</i> + and CD34+CD38- cells display an age-related elongation of G ₁	107
Figure 4.4 Stimulation of adult <i>CD49f</i> + cell proliferation requires higher levels of 3GF	109
Figure 4.5 G ₁ progression delay is exacerbated in adult cells under low 3GF stimulation	111
Figure 4.6 Reduced AKT and β -catenin activation in young adult stem and progenitor cells following short-term 3GF stimulation.....	113

List of Abbreviations

2D	2 Dimensions
³ H-Tdr	Tritiated Thymidine
5-FU	5-fluorouracil
α-MEM	Alpha Minimum Essential Medium Eagle
Ab	Antibody
AGM	Aorta-Gonad-Mesonephros
AHR	Aryl-Hydrocarbon Receptor
BIT	Bovine Serum Albumin, Insulin, and Transferrin
BM	Bone Marrow
BrdU	Bromodeoxyuridine
CADM	Congruence Among Distance Matrices
CB	Umbilical Cord Blood
<i>CD49f+</i>	CD34+CD38-CD45RA-CD90+CD49f+
CDK	Cyclin-Dependent Kinase
CFU-S	Colony-Forming Units-Spleen
CMP	Common Myeloid Progenitor
CXCL12	CXC-Chemokine Ligand 12

DAPI	4',6-diamidino-2-phenylindole
DMSO	Dimethyl Sulfoxide
ECM	Extracellular Matrix
EdU	5-ethynyl-2'-deoxyuridine
EDTA	Ethylenediaminetetraacetic Acid
EHT	Endothelial-to-Hematopoietic Transition
EPO	Erythropoietin
FACS	Fluorescence-Activated Cell Sorting
FBS	Fetal Bovine Serum
FL	Fetal Liver
FLT3L	FMS-Like Tyrosine Kinase 3 Ligand
FSC	Forward Scatter
G-CSF	Granulocyte-Colony-Stimulating Factor
GFP	Green Fluorescent Protein
GF	Growth Factor
GMP	Granulocyte-Macrophage Progenitor
GVHD	Graft Versus Host Disease
HBSS	Hank's Balanced Salt Solution

HSC	Hematopoietic Stem Cell
IL	Interleukin
IMDM	Iscove's Modified Dulbecco's Medium
IQR	Interquartile Range
LDA	Limiting Dilution Analysis
LDL	Low-Density Lipoproteins
LMPP	Lymphoid-Primed Multipotent Progenitor
LTC-IC	Long-Term Culture Initiating-Cells
MCM	Mini-Chromosome Maintenance
MEP	Megakaryocyte-Erythroid Progenitor
miR	Micro-RNA
MLP	Multipotent Lymphoid Progenitor
mPB	Mobilized Peripheral Blood
MPP	Multipotent Progenitor
NHEJ	Non-Homologous End-Joining
NK	Natural Killer
NM	Neutrophils and/or Monocytes
NOD	Non-Obese Diabetic

NRG-W41	NOD- <i>Rag1</i> ^{-/-} - <i>IL2Rγc</i> ^{-/-} - <i>W⁴¹/W⁴¹</i>
PB	Peripheral Blood
PBS	Phosphate-Buffered Saline
PFA	Paraformaldehyde
PI	Propidium Iodide
PRC1	Polycomb Repressive Complex 1
PRC2	Polycomb Repressive Complex 2
Rb	Retinoblastoma
ROS	Reactive Oxygen Species
SA	Streptavidin
SCF	Stem Cell Factor
scRNA-Seq	Single-cell RNA-Sequencing
SEM	Standard Error of the Mean
SFM	Serum-Free Medium
SPF	Specific-Pathogen-Free
SSC	Side Scatter
TNF	Tumor Necrosis Factor
TPO	Thrombopoietin

UMAP

Uniform Manifold Approximation and Projection

VAF

Variant Allele Fraction

Acknowledgements

Thank you to Connie Eaves for her support and guidance through the years. Her enthusiasm and passion for science is infectious. Her mentorship has truly changed the way I think about and approach things.

Thank you also to my committee members: Martin Hirst, Xiaoyan Jiang, and Carl Hansen for your guidance in performing my research.

To the current and past members of the Eaves lab, thank you for making the lab life more enjoyable. Special thanks to David Knapp and Davide Pellacani for all their help and their tolerance to my questions, you both taught me so much.

I am also thankful for all the support I received at the TFL. The Eaves lab technicians Glenn, Margaret, and Darcy who kept the lab and all experiments moving forward. Thank you to everyone at Stem Cell Assay, especially to Helen and Dianne, for all your help. The staff of the ARC for their wonderful care of our mice. Wenbo and Guillermo of the flow core for all their help. And thank you to Asha, Vincent, Shera, Shelby, Alice, and Amanda for keeping everything else together.

Thank you to my family for their love and support. And lastly to my soon-to-be wife Kathleen: doing our PhDs simultaneously was not always easy, but it was always easier for having you there.

Dedication

To my family.

Chapter 1: Introduction

1.1 Cellular Basis for Hematopoietic Reconstitution

In the mid-1950's, recognition of the severe effects of modest doses of ionizing radiation on bone marrow cellularity and blood cell production stimulated research into medical interventions against this effect. A major advance was the discovery that infusions of cells from the spleen (Jacobson et al., 1951) or bone marrow (Lorenz et al., 1951) could be protective when provided shortly after exposure of rodents to otherwise lethal doses of irradiation. Tracking the origin of the cells reconstituted in the recipients of marrow obtained from donors bearing a signature chromosomal translocation revealed their origin from the donor cells infused and hence that the reconstitution was not attributable simply to a humoral effect as had been previously postulated (Ford et al., 1956).

These findings spurred the development of methods to identify the cells capable of reconstitution and prompted the use of a limiting dilution analysis (LDA) strategy to determine the number of viable hematopoietic cells required to rescue lethally irradiated mice (McCulloch & Till, 1960). In following experiments, irradiated mice receiving donor marrow were discovered to develop macroscopic spleen nodules containing rapidly proliferating cells including multiple lineages of differentiated blood cells (Till & McCulloch, 1961). These nodules were later shown to represent clonal populations in experiments in which the infused cells bore uniquely altered karyotypes due to irradiation of the donor (Becker et al., 1963). Moreover, because the number of spleen colonies produced in recipients was linearly related to the number of donor cells injected, the procedure was inferred to detect the cell of origin (Till &

McCulloch, 1961). However, as other properties of these cells remained uncharacterized, they were assigned the functional designation of ‘colony-forming units-spleen’ (CFU-S).

However, some of the features of these spleen colonies provided the basis for several concepts still widely associated with hematopoietic stem cells (HSC). These included their content of mature cells from multiple different lineages as well as highly variable numbers of daughter CFU-S that would give rise to similar spleen colonies in secondary recipients (Siminovitch et al., 1963; Wu et al., 1967, 1968). These results suggested that CFU-S are multipotent with highly variable abilities to “self-renew” - that is, to generate progeny that maintain the defining functional properties of the cells from which they derived. The CFU-S present in adult mice were also found to be resistant to treatments that kill dividing cells, suggesting that most might exist in a non-cycling “quiescent” state (Becker et al., 1965; Bruce et al., 1966). Two decades later, it was revealed that most cells with CFU-S activity do not have the sustained blood cell output indicative of more primitive hematopoietic cells that are also found in the marrow throughout life, but rather represent a downstream stage of a cellular hierarchy arranged in an order of progressively lessening hematopoietic potential (Reviewed in Eaves, 2015 and discussed further in section 1.3).

1.2 Hematopoietic Cell Transplantation Therapies

The therapeutic potential suggested by these early findings was immediately realized and the first successful use of bone marrow transplantation to abrogate the effects of otherwise lethal treatments for pediatric leukemia using cells from an identical twin donor to avoid rejection were reported in 1959 (Thomas et al., 1959). Although the eventual outcomes of these transplants

proved ultimately non-curative, they demonstrated the reappearance of cytologically normal cells in the marrow of the patients following transplantation and therefore the therapeutic potential of this approach. Subsequent advances in understanding the mechanisms of graft rejection and graft-versus-host disease (GVHD) now allow transplantation of hematopoietic cells into patients also from allogeneic (matched-related donors or matched-unrelated donors) as curative therapies not only for hematological malignancies but also multiple other conditions (Ljungman et al., 2010; Naldini, 2019). Methods for mobilizing clinically useful transplantable hematopoietic cells into the blood (Panch et al., 2017), the use of autologous hematopoietic transplants (Ljungman et al., 2010) and more recent coupling of these strategies with therapeutic genetic modification of the cells (reviewed in Naldini, 2019) are all now consequences of the early discoveries in the 1950's and 1960's.

1.3 Organization of the Hematopoietic Compartment

Hematopoiesis is now recognized to be a hierarchically organized cellular process spanning many cell divisions to produce huge numbers of generally short-lived mature blood cells from a relatively small number of cells with considerable self-sustaining ability. Cells with different functional characteristics such as regenerative potential and differentiation capabilities demonstrated *in vitro* and *in vivo* are placed within different regions of this hierarchy with those having the most durable regenerative activity, the HSCs, residing at the apex and the terminally differentiated mature cells at the end. Specific assays designed to detect the presence of individual cells at different regions of this hierarchy were later linked with various viable cell separation methods, of which fluorescence-activated cell sorting (FACS)-based isolation of cells

defined by their combinatorial surface marker profiles has now become the most powerful (Doulatov et al., 2012; Eaves, 2015; Figure 1.1 A/B)

Surface marker phenotypes are continuing to identify features that subset the hematopoietic compartments of mice and humans as well as an increasing number of other model organisms. However, differences in surface marker profiles between even the mouse and human systems has made finding analogues between them problematic. For example, the Sca-1 marker present on mouse HSCs has no human homolog (Bradfute et al., 2005). In addition, the expression of several markers on primitive subsets of mouse and human cells appear to be opposingly regulated. For instance, the CD34 sialomucin is expressed on very early as well as later stages of primitive human hematopoietic cells whereas it is not expressed on HSCs in the mouse (Baum et al., 1992; Nakauchi et al., 2000; Osawa et al., 1996) with an opposite scenario for CD38 (Bhatia et al., 1997; Randall et al., 1996). Nevertheless, the general conceptualisation of the hematopoietic hierarchy in both mice and humans as being organized as a series of distinct cell types with specific potentialities and molecular differences mostly concordant with unique surface marker phenotypes and a generally bifurcating lineage restriction process has persisted for several decades (Figure 1.1B). However, in the last few years, the weaknesses of this model in allowing further insights into the detailed mechanisms of hematopoietic differentiation control have become apparent. In particular, the coupled use of single-cell sequencing strategies and functional assays of individually-assessed index-sorted cells have revealed that the hierarchy rather resembles a continuum of cells with overlapping functional potentials and that phenotypic classifications are restricted to isolating cells within different, but overlapping stages of this continual and variable process (Belluschi et al., 2018; Buenrostro et al., 2018; Giustacchini et al., 2017; Karamitros et al., 2018; Knapp et al., 2018, 2019; Velten et al., 2017; Zhao et al., 2017;

Zheng et al., 2018). Cellular movement across this landscape is then representative of alterations in molecular states contributing to the differing inherent functional potentials of the cells (Buenrostro et al., 2018; Knapp et al., 2018, 2019; Velten et al., 2017; Figure 1.1C).

Phenotypes of adult mouse bone marrow cells that can individually sustain the lifetime production of a high proportion of the mature blood cells in a transplanted congenic recipient are now well established (Kent et al., 2009). However, identification of a phenotype that selectively enriches for human cells with similar properties has been more challenging in part because of the evolving appreciation for the limitations of the assays available. A phenotype shown in LDA experiments to produce progeny in primary and secondary immunodeficient mouse recipients is now considered to identify an analogous human HSC compartment with ~10% purity (Knapp et al., 2017, 2018; Notta et al., 2011). Direct clonal tracking of this CD34⁺CD38⁻CD45RA⁻CD90⁺CD49f⁺ phenotype, hereafter referred to as *CD49f*⁺ cells, as well as clonal analyses of populations regenerated after ≥ 6 months in xenotransplants, or within gene-therapy patients, has revealed extensive heterogeneity in the kinetics and cellular outputs of individual HSCs including the identification of HSCs which robustly contribute to only a single mature lineage, drawing into question the multipotent ‘requirement’ of HSC outputs (Aiuti et al., 2013; Belluschi et al., 2018; Biasco et al., 2016; Biffi et al., 2013; Cheung et al., 2013; Knapp et al., 2018; Ravin et al., 2016; discussed further in section 1.7). However, the mechanisms and stages of lineage restriction that account for this heterogeneity remain poorly understood. Nevertheless, cell phenotypes remain a useful tool for isolating populations enriched in specific functional abilities and thereby enable in-depth functional and molecular profiling, recognizing that such findings then require reconciliation with their relevance within the more diffuse concept of the hematopoietic hierarchy as a multidimensional continuum.

1.4 Origin and Development-Related Changes of HSCs

In mice, the embryonic origin of definitive HSCs, those responsible for the lifelong production of mature blood cells, has been identified to occur at embryonic day 10.5 in the aorta-gonad-mesonephros (AGM) region and by inference at the same site approximately 30 days post-conception in humans (Ivanovs et al., 2017; Rowe et al., 2016). The emergence of functionally defined HSCs in mice is driven by a *Runx1*-dependent endothelial-to-hematopoietic transition (EHT) and the resulting definitive HSCs are marked by expression of *HoxB4* (Rowe et al., 2016). However, an earlier wave of primitive blood cells with limited cellular outputs, including nucleated red blood cells and myeloid cells, arise earlier in the yolk sac within ‘blood islands’ and migrate to the liver ahead of the definitive HSCs (Ivanovs et al., 2017; Rowe et al., 2016). However, even in mice, it is still unclear if or how these two cell types may be developmentally related since it has been shown that yolk sac cells cultured on AGM-derived stroma can produce progeny that are capable of repopulating adult mice (Matsuoka et al., 2001). Once seeded by the incoming definitive HSCs, the liver remains the primary site for hematopoiesis in the developing fetal mouse with colonization of the bone marrow occurring later (Ivanovs et al., 2017; Rowe et al., 2016). While the human fetal liver (FL) is similarly colonized prior to the bone marrow (BM), limited hematopoiesis can be found in the BM as early as 10.5 weeks post-conception, developmentally prior to what is seen in the mouse (Charbord et al., 1996; O’Byrne et al., 2019). Interestingly, several functional properties of these initial definitive HSCs do not remain stable during development with distinct differences from HSCs found in adult sources.

In some of the earliest experiments looking at the CFU-S content of hematopoietic cells in the FL or the BM of adult mice, it was revealed that CFU-S in the FL were highly sensitive to high-specific activity tritiated thymidine ($^3\text{H-Tdr}$) and therefore were mostly in cycle while those in the adult BM were not (Becker et al., 1965). This property was later seen to extend into the HSC compartment with fetal HSCs remaining rapidly cycling until 3-4 weeks post-birth where they were found to then switch rapidly, within a week, to the mostly quiescent state of adult HSCs (Bowie et al., 2006, 2007a). Evidence of a similar developmentally controlled switch in the cycling behavior of human and baboon HSCs has been inferred to occur in the first 1-3 years after birth through observation of a change in the rate of telomere decay in short-lived terminally differentiated blood cells (Baerlocher et al., 2007; Sidorov et al., 2009). However, the cells within the CD34+ stem and progenitor compartment in normal human umbilical cord blood (CB) are already mainly quiescent, perhaps indicative of a differently timed developmental switch in mice and humans (Wilpshaar et al., 2000). However, it is important to note that despite human CB containing relatively abundant frequencies of stem and progenitor cells, these must represent a small fraction of the body's total, with many still in the liver and already in the BM. Additionally, studies have previously shown a selection against or an inability of cycling stem/progenitor cells to enter the circulation (Bowie et al., 2006; Morrison et al., 1997; Ponchio et al., 1995). Nevertheless, it seems clear that, in both the mouse and human systems, the hematopoietic cells from the FL have enhanced regenerative properties when transplanted relative to those from the adult, with human CB being intermediate (Holyoake et al., 1999; Nicolini et al., 1999; Rebel et al., 1996). This enhanced regenerative capacity of fetal HSCs appears to be linked to a heightened self-renewal activity driven by expression of Lin28b and an increased sensitivity to Stem Cell Factor (SCF; Audet et al., 2002; Bowie et al., 2007b; Copley et

al., 2013). In this context, Lin28b functions to inhibit the *let-7* family of micro RNAs (miRs) which leads to higher levels of Hmga2. Overexpression of Lin28 or Hmga2 in adult mouse BM enhanced self-renewal to levels similar to those of fetal HSC, conversely HSC from the FL of *Hmga2*^{-/-} mice had reduced self-renewal activity (Copley et al., 2013). In humans, the repressive *LET-7* family members are more highly expressed in adult BM CD34+CD38-CD45RA-CD90+ cells, followed by those from CB, then lowest in FL with the opposite trend observed for LIN28B (Cesana et al., 2018). This study also found that while HMGA2 levels were lowest in adult BM, both FL and CB expressed high levels but displayed differential abundance of HMGA2 isoforms: a longer isoform in FL and shorter in CB suggesting differential splicing precedes transcriptional downregulation (Cesana et al., 2018). Altogether, these findings suggest that the LIN28b-LET-7-HMGA2 axis is a conserved mechanism regulating some of the altered features that adult HSCs display and distinguish them soon after birth from the rapid cycling and high self-renewal properties of the FL HSCs from which they develop.

1.5 Contribution of HSCs to Steady-State Hematopoiesis

Due to the very large number of new blood cells produced daily to sustain normal physiological requirements, it has been of long-term interest to determine the role of HSCs in maintaining this output under homeostatic conditions. As noted, early investigations indicated that the majority of adult cells capable of regenerating the hematopoietic system are quiescent (Becker et al., 1965; Bruce et al., 1966) and this was later supported by experiments showing that prolonged administration of bromodeoxyuridine (BrdU) was required to label the DNA of these cells. The rate at which the BrdU signal was lost in different populations was then used to determine the relative frequency at which these populations divided. From these experiments it

was estimated that adult mouse HSCs continuously and asynchronously enter the cell cycle during normal steady-state hematopoiesis at an estimated rate of 6-8% per day (Cheshier et al., 1999; Kiel et al., 2007). However, it has since been shown that the administration of BrdU necessary to label the DNA of the cells is sufficient to induce BM stress which enhances the rate of entry of HSCs into the cell cycle (Wilson et al., 2008). Subsequent strategies using an inducible histone H2B coupled to green fluorescent protein (GFP) were developed to avoid this and to specifically mark primitive populations. This strategy revealed that HSCs with high self-renewal activity divide less frequently *in situ* but could be rapidly stimulated into the cell cycle following an *in vivo* administration of 5-fluorouracil (5-FU) or G-CSF (Foudi et al., 2009; Morcos et al., 2020; Wilson et al., 2008) but could then return to dormancy (Wilson et al., 2008). This reversible activation of the HSC compartment has also been documented in response to a chronic inflammatory stimulus provided by administration of interleukin-1 (IL-1) which likewise stimulates HSC cycling at the expense of self-renewal activity followed by a reversal of this effect upon IL-1 withdrawal (Pietras et al., 2016). HSCs therefore regularly, but variably complete cell divisions and represent a fraction of cells that can be induced into a proliferative state by mechanisms that stimulate a rapid output of mature blood cells.

To determine the proportion of mature cells arising from HSCs under steady-state conditions, various clonal tracking techniques in mice have been deployed and have arrived at different conclusions. A study by Sun et. al. using the Sleeping Beauty hyperactive transposase system determined that steady-state hematopoiesis was maintained by thousands of long-lived progenitor clones each of which minimally contributed to the overall mature cell population (J. Sun et al., 2014). However, subsequent studies argue this methodology had an insufficient detection threshold and did not specifically label the HSC fraction. Use of an inducible label

under control of the *Tie2* locus granted higher specificity in labeling HSCs although at a low efficiency (~1% of HSCs labeled; Busch et al., 2015). Nevertheless, this method demonstrated that ~30% of HSCs contribute albeit infrequently to hematopoiesis (~1/110 dividing per day, with an assumed total of ~17,000 HSCs in a mouse), but mainly through contribution to shorter-term, but still long-lived, multipotent progenitors which greatly amplify their outputs (Busch et al., 2015). This was extended through use of a similar strategy with an inducible label expressed under the *Pdzk1ip1* locus which is expressed in mouse but not human HSCs. This alternative strategy enabled the labeling of ~30% of HSCs after induction (Sawai et al., 2016). In contrast to the previous studies, this strategy also demonstrated a higher continuous contribution of the HSC compartment to the output of mature cells, with the majority of these being derived from HSCs within 9 months. This finding was further underscored by the increased rate at which HSC contributed to the mature cell population when the mice were exposed to a poly:I-C-driven inflammatory stimulus (platelets and myeloid cells arising from labeled HSCs reached ~70% by 32 weeks in non-treated mice versus the same proportion reached around week 16 in poly:I-C-treated mice). Taken together, these latter results support the view that HSCs act both to maintain steady-state hematopoiesis and act as a reservoir in cases of BM stress.

In the human system, direct labeling of HSCs to assess their steady-state contributions *in situ* has been a technical challenge. However, time course tracking of the data obtained from patients in ongoing gene therapy trials has enabled many individual clones to be tracked via their unique viral insertion sites. These data show that a predominant contribution of the transplanted HSCs to steady-state hematopoiesis can be achieved within ~6 months and may continue for at least an additional 2.5 years (Biasco et al., 2016). Tracking of somatic transversions occurring in *CD49f*⁺ cells and linking those to mature cells with the same nucleotide transversion in normal

adults under steady-state conditions has similarly indicated long-term contribution to multiple mature lineages by the *CD49f*⁺ HSC compartment (Wang et al., 2020). In both cases, the contribution from the HSC compartment was also determined to be polyclonal. However, deep sequencing studies performed on blood taken from normal adults of varying ages now reveals that older persons frequently contain a readily detectable portion (variant allele fraction (VAF) >0.1) of their circulating (very short-lived) neutrophils that contain unique somatic mutations indicating their origin from a more limited pool of primitive hematopoietic cells (Genovese et al., 2014; Jaiswal et al., 2014). Interestingly, these mutations were most frequently found in genes associated with leukemias, primarily *TET2*, *DNMT3A*, and *ASXL1* (Genovese et al., 2014; Jaiswal et al., 2014) and persons bearing these mutated clones were at increased risk of developing a hematologic cancer (hazard ratio >10; Genovese et al., 2014; Jaiswal et al., 2014). An indication of this type of perturbed but non-neoplastic growth, recently termed “clonal hematopoiesis of indeterminate potential” (CHIP) had been previously suggested by occasional evidence of highly skewed ratios of G6PD alleles (on the X-chromosome) in normal older women who were G6PD heterozygotes (Champion et al., 1997; Fey et al., 1994). More recent analyses have found that the presence of such mutant clones with enhanced growth potential, but are otherwise apparently phenotypically normal is nearly ubiquitous in healthy adults over 50 years old and that clones bearing *DNMT3a* mutations can be detectable decades earlier (McKerrell et al., 2015; Young et al., 2016). The presence of these somatic clones in the blood measured years apart also strongly suggests an origin within the HSC compartment (Young et al., 2016). This aging-associated rise in oligoclonal maintenance of tissues by mutant but non-transformed cells has also been found to extend to other tissues beyond the blood system (Yizhak

et al., 2019), most notably in the skin (Martincorena et al., 2015), esophagus (Martincorena et al., 2018), and endometrium (Suda et al., 2018).

In summary, the HSC compartment acts both as a continuous source of cells that, while individual clones contribute at a very low rate, meets the needs of steady-state blood cell renewal requirements, in addition to serving as a reservoir able to respond rapidly to stimuli that signal for increased needs. However, as individuals age, the appearance of mature cells arising from HSCs bearing somatic mutations in leukemia-associated genes becomes increasingly evident. These findings add to the interest in obtaining an improved understanding of the functional and molecular properties of HSCs that change with age and the mechanisms responsible for their appearance.

1.6 Features of Aging Hematopoiesis

The process of aging is seen in many organisms and has been associated with the appearance of several hallmarks common across many tissues. These include changes in the (epi)genome that include increased mutational loads, shortened telomeres, and altered epigenomic features. In addition, alterations to metabolism and proteostasis are widely recognized (López-Otín et al., 2013). Functional evidence of an accumulation of cells with senescent features and reduced regenerative activity of the stem cell compartment have also been commonly associated with aging in several tissues, including the skin, muscle, intestine, brain, and blood (López-Otín et al., 2013). Despite the shared nature of these changes across different tissues, exactly what is driving their acquisition at a cellular level remains unclear. Elevation in the plasma levels of several inflammatory cytokines including IL-6, tumor necrosis factor (TNF),

and IL-1 β in the elderly is thought to contribute to the acquisition and progression of at least some aging-related features and the development of diseases in a process termed “inflamm-aging” (Franceschi et al., 2006, 2018; Geiger et al., 2013).

It is also appreciated that DNA replication is imperfect, leading to the accumulation of somatic mutations over time, estimated at a frequency of ~40 novel mutations per year in adult stem cell populations across different human tissues (Blokzijl et al., 2016). In addition, telomeres undergo progressive shortening with each cell division, and when these become critically short it leads to chromosomal fusions, translocations, and aneuploidy (Aubert & Lansdorp, 2008). These findings support a model in which damage to the genome is a major driver of acquiring aging phenotypes. Further support for this concept is that mutations in genes influencing DNA replication and repair including telomere maintenance are responsible for many progeroid diseases which are characterized by multiple symptoms of premature aging (Carrero et al., 2016; López-Otín et al., 2013). As well, mouse models with deficient DNA base-excision repair, non-homologous end-joining (NHEJ), or telomere maintenance also show signs of premature aging of the blood system characterized by the appearance of anemias, lymphopenias, and decreased functional abilities of their stem and progenitor cells (Allsopp et al., 2003; Lee et al., 1998; Nijnik et al., 2007; Prasher et al., 2005; Rossi et al., 2007). In addition, telomerase deficiencies in humans have visible disease phenotypes (Blasco, 2005), which are not immediately seen in laboratory mice due to their possession of much longer telomeres requiring several generations before effects are observed (Allsopp et al., 2003; Blasco et al., 1997; Lee et al., 1998). In addition, increased γ H2AX foci and intracellular reactive oxygen species (ROS) have also been observed in CD34⁺CD38⁻ cells from older humans and in those regenerated in hematopoietic

cell transplant patients (Yahata et al., 2011), reinforcing a likely link between aging features and genomic stability.

However, increased DNA damage alone is unlikely to be responsible for aging in the hematopoietic system. While aged HSCs in mice were found to have higher levels of mutations (Moehrle et al., 2015), γ H2AX foci (Rossi et al., 2007), and a corresponding increase in DNA breaks, this damage was repaired when the aged cells were stimulated to cycle, ending up at levels similar to those seen in the HSCs of younger mice (Beerman et al., 2014). This outcome was also accompanied with finding that the DNA damage response is not compromised in aged HSCs, with repair proceeding efficiently in both aged and younger HSCs (Moehrle et al., 2015). Furthermore, the genes found to be most commonly mutated in age-related CHIP are not DNA damage response genes but are more involved in mechanisms regulating the epigenome (*DNMT3A*, *TET2*, *ASXL1*) and splicing (*SF3B1*, *SRSF2*), suggesting that malfunctioning DNA damage responses are not a primary driver of normal aging.

Advancing age in both mice and humans is associated with several changes in the composition and function of mature blood cells. These include decreases in the number of circulating lymphocytes, reduced immune responses, increases in the appearance of anemia (Geiger et al., 2013; Guralnik et al., 2004; Ogawa et al., 2000), and an increasing prevalence of CHIP (Jaiswal & Ebert, 2019). In mice, an altered balance of mature lymphoid and myeloid progeny has been shown to be associated with a selectively reduced output of lymphoid progenitors and the appearance of an increasing proportion of HSCs that predominantly or exclusively produce myeloid progeny (Benz et al., 2012; Cho et al., 2008; Dykstra et al., 2007, 2011; Yamamoto et al., 2018). Aging in mice has also been canonically associated with a

somewhat counterintuitive increase in the frequency of phenotypic HSCs while the overall regenerative ability of the hematopoietic compartment declines (Beerman et al., 2010; de Haan et al., 1997; Dykstra et al., 2011; Flach et al., 2014; Morrison et al., 1996; Rossi et al., 2005; Sudo et al., 2000). Importantly, some of these aging-related functional alterations have been linked to cell-extrinsic effects caused by changes in the tissue environment of the aging host rather than being attributable exclusively to intrinsic alterations in the HSCs. For example, transplants of BM from old mice into young recipients produced a less biased output of myeloid progeny and a higher level of chimerism than was seen when transplanted into older hosts (Ergen et al., 2012). Conversely, young BM transplanted into old mice produced a lower overall chimerism and a reduced output of T cells (Ergen et al., 2012). Similar results have also been obtained when the outputs of more purified HSC populations from mice of different ages were compared (Kuribayashi et al., 2021; Rossi et al., 2005; Young et al., 2021). These effects were attributed in part to an increased level of Ccl5/Rantes in the older mice (Ergen et al., 2012) and a decreased level of Igf1 appearing by middle-age (Young et al., 2021). However, this variable but apparent shift in these heterochronic transplants was ultimately incomplete and old BM transplanted into young hosts still showed reduced overall engraftment, an increased proportion of myeloid progeny, and a lower proportion of lymphoid cells, suggesting persistent intrinsic alterations in these cells with aging (Kuribayashi et al., 2021; Rossi et al., 2005; Young et al., 2021).

Comparison of the epigenomic states of young and old HSCs in mice has demonstrated hypermethylation of genes regulated by the Polycomb Repressive Complex 2 (PRC2; Beerman et al., 2013; D. Sun et al., 2014), broader genomic coverage of both the active H3K4me3 and repressive H3K27me3 histone marks, and reduced expression of several epigenetic modifiers (D. Sun et al., 2014). Additional features of HSCs from older mice include reduced polarity resulting

from increased Cdc42 activity (Florian et al., 2012), altered autophagy, an overactive oxidative phosphorylation metabolism, and elevated ROS (Ho et al., 2017). Taken together, it seems likely that the processes causing the acquisition of aging features reflect the contribution of a combination of many systems with varying impacts and temporal regulation.

Although laboratory strains of inbred mice have been very useful for revealing many features of mammalian cell aging, very few studies examining how age affects human HSC properties have, as of yet, been reported. Similarities between the mouse and human systems so far noted include an age-associated expansion of hematopoietic cells with a primitive phenotype (Kuranda et al., 2011; Nilsson et al., 2016; Pang et al., 2011) and a relatively reduced chimerism obtained when transplanted into immunodeficient mice (Pang et al., 2011). Less clear is whether human HSCs from older donors display an age-related reduced output of lymphoid cells given the singular report of selectively reduced B lymphoid output in xenografts of an HSC-enriched subset of cells from older donors (Pang et al., 2011) that was not confirmed in another study (Kuranda et al., 2011). Additionally, data from human patients receiving hematopoietic transplants have not been consistent in associating a poorer recovery with hematopoietic cell transplants obtained from older donors. For example, although autologous transplants in older patients were associated with reduced multi-lineage recoveries than younger patients (Woolthuis et al., 2014) and recipients of allogeneic transplants between HLA-matched pairs were also found to show reduced rates of overall survival with increasing donor age in three studies (Finke et al., 2012; Kollman et al., 2001, 2016), a similar relationship was not found in another such study (Rezvani et al., 2015). Unfortunately, these studies are confounded by the use of differing categorizations of young and old donors, different rates of GVHD apparent between transplants

of related and unrelated donors, and the use of different conditioning regimens (Finke et al., 2012; Kollman et al., 2001, 2016; Rezvani et al., 2015).

Long-term clonal tracking of autologously transplanted young and old rhesus macaques has however, yielded potentially more informative results. These investigations found an increase in the proportion of clones that mainly produced mature B lymphoid cells or mature myeloid cells in aged macaque recipients whereas long-term clones in younger macaque hosts were mainly bi- or multi-potent (Yu et al., 2018). Aged macaques also displayed a gradual decrease in the number of clones which contributed over time, suggesting possible clonal exhaustion or altered cycling control relative to the more stable number of contributing clones observed in the younger macaques (Yu et al., 2018). In summary, much evidence points to the accrual of functionally important changes in human HSCs during aging, but their precise nature and underlying mechanisms remain largely unexplored.

1.7 Heterogeneity of HSC Properties

Single-cell transplants of very primitive mouse hematopoietic cells over the last 20 years have repeatedly demonstrated an extensive heterogeneity in the regenerative activity they display. Tracking the outputs of single HSCs in syngeneic transplants revealed differences in their repopulating kinetics, lineage output capabilities, and self-renewal activities (Benz et al., 2012; Carrelha et al., 2018; Dykstra et al., 2007; Lu et al., 2011; Muller-Sieburg et al., 2004; Sanjuan-Pla et al., 2013; Sieburg et al., 2006; Yamamoto et al., 2013, 2018). The repeated demonstration of sustained outputs from HSCs of mature cells of a single lineage for long periods of time also contradicts the long-held concept of HSCs as a relatively homogeneous

multipotent population (Dykstra et al., 2007; Sanjuan-Pla et al., 2013; Yamamoto et al., 2013). Additionally, these features appear to be intrinsically regulated and transmitted with relative stability through many HSC self-renewal divisions resulting in similar mature outputs being detected even in serial transplantation experiments. These findings have strongly suggested that stably sustained epigenomic features determine the unique patterns of differentiation outputs their progeny display (Benz et al., 2012; Dykstra et al., 2007; Yu et al., 2016). Shifting of these functional behaviours during aging, such as the shift towards an increased proportion of lymphoid-deficient HSCs and megakaryocyte/platelet-restricted HSCs, have also been connected to alterations in the epigenome using single-cell techniques (Grover et al., 2016; Kowalczyk et al., 2015; Mann et al., 2018; Yu et al., 2016).

In the human system, single-cell transplants of HSCs have historically been difficult due to the lower prospective purity of long-term repopulating cells obtainable. These remain obtainable at a purity of ~10% for human CB using the *CD49f*⁺ phenotype which has, nevertheless, begun to open up possibilities for exploring their molecular and functional heterogeneity (Knapp et al., 2017, 2018; Notta et al., 2011). Clonal tracking studies of bulk *CD34*⁺ stem and progenitor cells or individually DNA barcoded *CD49f*⁺ cells have similarly demonstrated their extensive heterogeneity, paralleling the findings from analyses of long-term repopulating cells from mice (Aiuti et al., 2013; Biasco et al., 2016; Biffi et al., 2013; Cheung et al., 2013; Knapp et al., 2018; Ravin et al., 2016). Heterogeneity in the clonal outputs of single human HSC-enriched populations *in vitro* have also been documented (Belluschi et al., 2018; Knapp et al., 2018, 2019; Notta et al., 2016). Tracking of the proliferation kinetics of subsets of *CD49f*⁺ cells from CB with differing *in vivo* repopulating ability demonstrated similar but separable kinetics observed within the first 3 divisions *in vitro* (Belluschi et al., 2018; Knapp et

al., 2018). In addition, these *CD49f*⁺ cell subsets were found to display different patterns of signaling activation in response to the same cytokine stimuli with different cytokines eliciting different proportions of *CD49f*⁺ cells to display an activation response (Knapp et al., 2016). The use of single-cell profiling techniques has also demonstrated that heterogeneity within the *CD49f*⁺ subset also extends to the entire human CD34⁺ population supporting the concept that the hematopoietic cell differentiation process is best modeled as a continuum of cells that may transit through overlapping molecular states and functional potentials rather than via a highly restricted series of changes that define discrete cell types (Belluschi et al., 2018; Buenrostro et al., 2018; Knapp et al., 2018, 2019; Pellin et al., 2019; Velten et al., 2017; Zheng et al., 2018; Figure 1.1C). Importantly, this model supports that certain transitions through this continuum would be marked by identifiable changes in the cellular transcriptome, DNA methylation profile, or chromatin accessibility features indicative of significant functional changes (Belluschi et al., 2018; Bock et al., 2012; Buenrostro et al., 2018; Farlik et al., 2016; Pellin et al., 2019; Velten et al., 2017; Zheng et al., 2018). Adding further heterogeneity to human HSC data has been the finding of strong donor-specific DNA methylation patterns overwhelming methylation differences between closely related but nevertheless functionally distinct HSC subsets (Hui et al., 2018; Knapp et al., 2018). However, these did not preclude the identification of differences in DNA methylation profiles which were able to separate *CD49f*⁺ subsets that differed in their ability to serially transplant immunodeficient mice, unlike transcriptomes from single-cell RNA-sequencing (scRNA-Seq) or multiparameter proteomic profiling (Knapp et al., 2018).

Recent studies have also identified additional cell-surface markers that enable functionally distinct subsets of CB *CD49f*⁺ cells to be prospectively isolated. For example, the presence of CD33 on *CD49f*⁺ cells in CB was found to mark a population containing the long-

term repopulating cells capable of initiating serial transplants in immunodeficient mice (Knapp et al., 2018). Additionally, a CLEC9A^{hi}CD34^{low} phenotype was found to isolate a subset of CB CD49f⁺ cells enriched for multipotent lineage outputs *in vivo* and contained a higher proportion of long-term repopulating cells than those of the CLEC9A^{low}CD34⁺ fraction (Belluschi et al., 2018). However, the extent to which these two more recently described subsets may overlap is not yet known. It is also not yet known whether or how well these additional phenotypes may similarly enrich for functional HSCs from donors of different ages. This extensive heterogeneity now appreciated to exist in all features so far examined in the CD49f⁺ population, including the diversity of their regenerative activity, underscores the importance of single cell analyses to analyze the molecular mechanisms underlying the functional properties of HSCs.

1.8 Regulation of HSC Behaviour

A cell's functional state at a particular point in time reflects the states of a series of highly interconnected regulatory networks that include temporally associated features of their genomes, epigenomes, transcriptomes, proteomes, metabolic states, and structural organization. The components of these networks can also influence one another and be profoundly influenced by elements in the environment external to the cell. It is the culmination of these influences that determine the timing and likelihood of a cell displaying a particular behaviour. Of prime interest here is whether a cell with HSC potential when stimulated to divide will self-renew by producing a least one daughter cell that retains the original potential. Indeed, the role of individual elements and cellular states in regulating these outcomes has been of high interest ever since CFU-S were first identified more than half a century ago.

1.8.1 Intrinsic Regulation

As discussed in section 1.4, the Lin28b-let-7-Hmga2 axis appears to be a conserved mechanism influencing an alteration in HSC self-renewal activity that distinguishes fetal and adult HSC behaviour (Cesana et al., 2018; Copley et al., 2013). However, this is far from the only mechanism influencing developmental changes in HSC self-renewal behaviour (Babovic & Eaves, 2014). In the mouse, *Sox17* has been identified as a transcription factor required in fetal HSCs, but is dispensable for adult HSC functions (Kim et al., 2007), although *Sox17* can act to increase the self-renewal activity of adult HSC and activate several fetal HSC genes when overexpressed (He et al., 2011). Retroviral overexpression of *HOXB4* in mouse BM cells has also been connected with increased self-renewal activity of HSCs (Antonchuk et al., 2002; Sauvageau et al., 1995). This expanded self-renewal activity could be further improved by using a fusion of Nup98 with Hoxb4 or Hoxa10 which was found to be related to the homeodomain of the *Hox* gene (Ohta et al., 2007). However, this effect was greatly reduced when applied to human cells and only modestly expanded CB long-term culture-initiating cell (LTC-IC) numbers *in vitro* (Sloma et al., 2013). Several other transcription factors including Evi-1 (Goyama et al., 2008; Zhang et al., 2011), Gfi1 (Hock et al., 2004; Zeng et al., 2004), Gata2 (de Pater et al., 2013; Rodrigues, 2005; Rodrigues et al., 2012), and Gata3 (Frelin et al., 2013; Ku et al., 2012) have also been implicated with roles in maintaining HSC homeostasis in mice.

Interestingly, the effects of several of these factors have been linked to alterations in the regulation of HSC proliferation with increased cycling typically associated with reduced HSC function (Hock et al., 2004; Zeng et al., 2004; Zhang et al., 2011). This finding agrees well with the results of HSC labeling studies in mice that have suggested that HSC dormancy correlates

with the most durable repopulating activity in transplanted recipients (Foudi et al., 2009; Wilson et al., 2008). It is further supported by findings of cell-cycle regulator manipulation causing impacts on HSC homeostasis that link sustained proliferative activity with the loss of self-renewal ability (reviewed in Pietras et al., 2011; discussed further in 1.10). However, this is not always the case. For example, loss of Gata3 was found to reduce both HSC responsiveness to proliferative stimuli and their ability to self-maintain (Ku et al., 2012). Additionally, knockdown of miR126 in human hematopoietic cells increased both their cycling and self-renewal activity without signs of exhaustion via a de-repression of the PI3K/AKT/GSK3- β signaling axis (Lechman et al., 2012). Similarly, CDK6, a regulator of early G₁ entry and progression which is expressed at low levels in human HSCs and at higher levels in progenitor cells with less durable outputs is consistent with the extended time required for HSC to exit quiescence (Laurenti et al., 2015); and yet, forced overexpression of CDK6 was found to reduce the time required for HSC to exit quiescence while also increasing their self-renewal activity without affecting their differentiation behaviour (Laurenti et al., 2015). Together these findings suggest a complex relationship between HSC cycling and self-renewal control that allows different factors to differently modulate these two responses (Fig. 1.2).

As mentioned above in section 1.7, certain alterations in the epigenomic landscapes of cells within the hematopoietic hierarchy can reflect and may help dictate their different functional potentials. Comprehensive profiling of histone marks and the corresponding enhancer states in mouse hematopoietic stem and progenitor cells have identified a number of dynamic changes in enhancer use between different subsets of cells defined by classical cell surface phenotypes. These in turn, have implicated cell-type-specific transcription factor regulators of cellular identity based on their expression and motif accessibility at active enhancers (Lara-

Astiaso et al., 2014). Potential HSC regulators thus identified included *Meis1*, *Hoxa9*, and *Erg*, all of which had previously been indicated as key regulators of HSC function (Lara-Astiaso et al., 2014; Wilson et al., 2011). In single-cell sequencing studies of the human hematopoietic stem and progenitor compartments, movement away from the HSC state has been associated with gradual priming of lineage-associated programs and loss of HSC-associated programs (Buenrostro et al., 2018; Farlik et al., 2016; Pellin et al., 2019; Velten et al., 2017; Zheng et al., 2018; Figure 1.1C). Tracking of transcription factor motif accessibility during the transition away from the HSC compartment showed early loss of GATA motif accessibility which preceded the loss of HOX motif accessibility at later steps (Buenrostro et al., 2018). Loss of HOX motif accessibility also appears to correspond with reduced expression of *GATA3* and *HOX* gene family members at the stage when HSCs are exiting the HSC compartment (Velten et al., 2017). The role of epigenomic alterations therefore appears to be linked to opposing functions of maintaining or transitioning away from an HSC state. It might then be expected that deregulation of certain epigenomic modulators would influence HSC function.

In agreement with this prediction is the finding that, in mice, modulation of *Tet2*, *Dnmt3a*, *Dnmt1*, and *Bmi1* all have apparent impacts on HSC self-renewal and differentiation activity (Wilkinson et al., 2020; Fig. 1.2). Conditional loss *in vivo* of *Tet2*, which acts to hydroxylate 5-methylcytosines, resulted in an expansion of the HSC compartment and eventually their acquisition of a myeloproliferative phenotype (Moran-Crusio et al., 2011). Deletion of *Dnmt3a* was also found to markedly increase the self-renewal activity of mouse HSCs, with progeny remaining detectable over 12 rounds of serial transplantation (Challen et al., 2012; Jeong et al., 2018). Conversely, loss of *Dnmt1* resulted in the acquisition of defective self-renewal and differentiation properties of HSCs (Trowbridge et al., 2009). *Bmi1*, a member of the

PRC1 complex implicated in the expansion of repressive H3K27me3 marks, has similarly been identified as disrupting HSC self-renewal and enhancing lymphoid differentiation when knocked out in mice and conversely found to cause enhanced HSC self-renewal activity when overexpressed (Iwama et al., 2004; Oguro et al., 2010; Park et al., 2003). The high frequency of expanded clones bearing loss-of-function *TET2* and *DNMT3A* mutations found in aging humans with CHIP likewise suggests the associated acquisition of a growth advantage by these cells (Jaiswal & Ebert, 2019). In contrast, the similar effects resulting from *TET2* and *DNMT3A* loss-of-function mutations is unexpected given that these genes would appear to act via opposing mechanisms; that is *TET2* being responsible for the hydroxylation of 5-methylcytosine, promoting their removal, and *DNMT3A* being responsible for depositing methyl groups on cytosine. Alteration of H3K27me3 levels similarly have been found to have opposing contextual impacts. Gain of H3K27me3 has been identified from gain-of-function mutations of *EZH2*, the catalytic member of the PRC2 complex, in B cell lymphomas (McCabe et al., 2012) whereas reduced H3K27me3 from inactivation of *EZH2* is more common in myeloid malignancies (Ernst et al., 2010). It is then clear that the regulation of epigenomic states is fundamental to the maintenance of core HSC and normal hematopoietic activities.

1.8.2 Extrinsic Regulation

The majority of HSCs inhabit the BM throughout adult life where they are embedded in a complex tissue environment that contains many non-hematopoietic cells as well as later stages of differentiated blood cells and extracellular matrix (ECM) components. The non-hematopoietic cell types include fibroblasts, osteoblasts, adipocytes, endothelial cells, and neural cells which form many interconnections as well as expressing and secreting many hematopoietic cell-

responsive factors (Crane et al., 2017). Three main non-cell-autonomous factors implicated as key regulators of HSC maintenance are SCF, thrombopoietin (TPO), and CXC-chemokine ligand 12 (CXCL12; Crane et al., 2017). SCF binds to its receptor KIT which is expressed on both mouse and human HSCs and on some downstream progenitors (Escribano et al., 1998; Ikuta & Weissman, 1992). Both soluble and membrane-bound forms of SCF are present in the BM, and deletion of the membrane-bound form in *Sl/Sl^d* mutant mice was found to inhibit the formation of spleen colonies by transplanted CFU-S and their self-renewal (McCulloch et al., 1965; Sutherland et al., 1970). Additional studies in mice bearing mutations in *Kit* that impaired intracellular signaling similarly showed reduced CFU-S and HSC self-renewal abilities thereby implicating SCF as a signaling factor important for sustaining and/or activating an important pro-survival or pro-quiescence response in HSCs (Miller et al., 1996; Thorén et al., 2008). Similarly, mice lacking TPO signaling (either through loss of *c-Mpl*, the receptor for TPO, or TPO itself) also had reduced CFU-S and HSC activities (Kimura et al., 1998; Qian et al., 2007). Loss of TPO signaling in the latter case appeared to deplete the HSC compartment by increasing their cycling activity, suggesting a role for TPO in maintaining HSC quiescence (Qian et al., 2007). CXCL12 interaction with the CXC-chemokine receptor 4 (CXCR4) appears to similarly be involved in maintaining HSC quiescence and retention in the BM (Cashman et al., 2002; Sugiyama et al., 2006; Tzeng et al., 2011). Disruption of this interaction using a selective CXCR4 antagonist (AMD3100/Plerixafor) results in mobilization of human CD34+ hematopoietic cells into the PB from the BM (Liles et al., 2003). Beyond these factors, many additional growth factors (GFs) have been identified with positive as well as direct effects on primitive hematopoietic cells.

In vitro studies of the responsiveness of adult human BM LTC-IC to various GFs alone or in combination identified combinations that support the expansion of LTC-IC numbers ~10-

fold within 10 days in a serum-free culture with SCF, fms-like tyrosine kinase 3 ligand (FLT3L), and IL-3 (Petzer et al., 1996). In contrast none of these GFs alone elicited this result. The expansion obtained was also dose-dependent with peak effects achieved using 300 ng/mL of SCF and FLT3L plus 60 ng/mL of IL-3 (Zandstra et al., 1997). Interestingly, expansion of the adult BM LTC-ICs required higher levels of these GFs than the expansion of downstream colony-forming cells (CFCs) indicating differential requirements for cells at different levels of the hematopoietic hierarchy (Zandstra et al., 1997). Importantly, the ratio of SCF and FLT3L to IL-3 was connected to the degree of LTC-IC expansion achieved. When IL-3 levels were selectively elevated, LTC-IC expansion was greatly reduced or even contracted underscoring the likelihood that the relative strengths of signals induced by different GFs can impact their effects on primitive hematopoietic cell activities (Zandstra et al., 1997). Recent studies of *CD49f*⁺ cells from human CB have also demonstrated the separable effects of GFs on their survival, proliferation, and maintenance of repopulating ability (Knapp et al., 2016, 2017). Use of a 5 GF cocktail composed of SCF, FLT3L, IL-3, IL-6, and G-CSF robustly activated members of the AKT, MAPK, and STAT pathways as well as β -catenin, with strong support of survival and proliferation *in vitro*, and was also able to maintain serial repopulating ability of these cells for up to 3-weeks (Knapp et al., 2016, 2017). However, individual factors from this cocktail were variably able to support *CD49f*⁺ cell survival and were ultimately insufficient to stimulate division (Knapp et al., 2017). Combinations of any two of these factors restored survival *in vitro* but only certain combinations restored proliferation. However, these combinations, which had different abilities to regulate the survival and proliferation of the *CD49f*⁺ cells *in vitro* had no discernible effect on their ability to serially transplant immunodeficient mice after culture, thereby indicating a clear separation of the control of these functions *in vitro* from other

requirements which modulate the maintenance of HSC regenerative properties (Knapp et al., 2017).

An ability of several GFs to antagonize HSC functions has also been reported. For example, addition of TNF- α to a GF combination that otherwise stimulates an expansion of human LTC-ICs was found to reduce LTC-IC numbers following an induced proliferation and increased production of macrophages (Petzer et al., 1996). Inhibitory effects on human CD34+ cell cycling *in vitro* have also been observed including effects by macrophage inflammatory protein (MIP-1)- α , transforming growth factor (TGF)- β , and monocyte chemoattractant protein (MCP)-1 (Bonnet et al., 1995; Cashman et al., 1998; Mayani et al., 1995). As mentioned above, the pro-inflammatory cytokines Ccl5/Rantes and IL-1 appear to push mouse HSC into cycle and towards myeloid differentiation resulting in reduced regenerative activity during chronic exposure (Ergen et al., 2012; Pietras et al., 2016) again suggestive of a general negative impact of inflammation on HSC functionality. These findings may well explain the deleterious effects on HSCs often encountered in culture systems that result in the production of many inhibitory cytokines, such as TGF- β , IL-10, MCP-1, and Ccl5/RANTES among others, and hence require their systematic dilution or removal to improve the yields of functional HSCs (Csaszar et al., 2012).

Two small molecules have been identified which demonstrate abilities to expand the outputs of human cells with repopulating activity in transplanted immunodeficient mice. StemRegenin1 (SR1) is a purine derivative identified in a screen of 100,000 heterocyclic compounds tested for their ability to expand CB CD34+ cell numbers *in vitro*. Subsequent experiments showed that their exposure to supportive GFs plus SR1 yielded a population with

accelerated short- to intermediate-term multilineage repopulating activity in immunodeficient mice (Boitano et al., 2010). SR1 was found to be an antagonist of the aryl-hydrocarbon receptor (AHR) which in turn modulates several cell-cycle regulators, including CXCR4, and several hematopoietic transcription factors (Boitano et al., 2010; Singh et al., 2009). The second factor, UM171 was also identified through a screening approach as able to expand even more primitive human hematopoietic cell numbers *in vitro*, shown to be in an AHR-pathway independent manner (Fares et al., 2014, 2017). Later studies identified several additional effects of UM171 including the modulation of pro- and anti-inflammatory processes (Chagraoui et al., 2019) and enhanced degradation of the CoREST complex to allow the re-establishment of H3K4me2 and H3K27ac marks promoting the maintenance of a primitive epigenomic state (Chagraoui et al., 2021). The relative success of these small molecules again points to the role of multiple mechanisms contributing to the maintenance of a primitive HSC state when they are exposed to highly mitogenic combinations of GFs.

Given the intrinsic and functional differences that have been identified as occurring in HSCs during development and aging, it is surprising that there are few studies exploring whether HSCs in hosts of different ages have acquired altered responsiveness to different extrinsic stimuli. In mice it was observed that FL HSCs are more sensitive to SCF and can complete self-renewal divisions at lower concentrations than those which are required by adult HSCs (Audet et al., 2002; Bowie et al., 2007). In human CD34+ cells, the inhibitory effects of MIP-1 α , TGF- β , and TNF- α were similar between CB and FL (Mayani et al., 1995). However, conditions found to expand adult LTC-IC *in vitro* were inefficient at expanding their comparators from CB, suggesting these cells may require different levels of activation or require different combinations of pathways to be activated (Zandstra et al., 1998). Such differences in the GF-mediated

response requirements of HSCs from CB and adult donors could thus be an important consideration in the development of improved therapeutic strategies using these different HSC sources.

1.9 Cell Cycle Regulation

The cell cycle remains broadly subdivided into 4 different phases based on the original discovery that DNA synthesis is largely confined to a period that is separated from mitosis by 2 time gaps (Howard & Pelc, 1951), hence the later terms of M, G₁, S, and G₂ to denote these phases. G₀ was later recognized as a distinct state in which cells appear post-mitotically arrested but nevertheless remain responsive to stimuli and can proceed towards division when appropriately stimulated (Cheung & Rando, 2013). Quiescence in stem cells appears to be an actively maintained state since modulation of several different transcription factors, epigenetic modulators, or cell cycle regulators act to reduce the proportion of stem cell populations in G₀ (Cheung & Rando, 2013; Hao et al., 2016; Hock et al., 2004; Laurenti et al., 2015; Pietras et al., 2011; Wilkinson et al., 2020; Zeng et al., 2004; Zhang et al., 2011). Transition into and through the cell cycle to ultimately complete a division is regulated by a complex balance of cyclins, cyclin-dependent kinases (CDKs), CDK inhibitors, retinoblastoma (Rb) family members, as well as the proper assembly and function of many other protein complexes (Deegan & Diffley, 2016; Hao et al., 2016; Pietras et al., 2011; Satyanarayana & Kaldis, 2009; Sherr, 2000; Fig. 1.3).

Key early steps that initiate the entry and early passage of cells through G₁ involve the actions of CDK3/cyclin C and CDK4 and CDK6 in concert with cyclin D to hyperphosphorylate and thereby inactivate Rb, followed by the activation and subsequent effects of CDK2/cyclin E

in late G₁ (Hao et al., 2016; Pietras et al., 2011; Satyanarayana & Kaldis, 2009; Sherr, 2000). The hyperphosphorylation of Rb disrupts its inhibition of the E2F family of transcription factors that enable the expression of E2F-responsive genes required for G₁ exit and S-phase entry (Hao et al., 2016; Pietras et al., 2011; Satyanarayana & Kaldis, 2009; Sherr, 2000). Signaling activation through the PI3K/AKT and MAPK pathways by mitogens also acts to push cells through G₁ in part through stabilization of c-Myc which in turn transcribes many target genes including *Ccnd2* (cyclin D2) and represses *Cdkn1a*, *Cdkn1b*, and *Cdkn2b* (encoding the CDK inhibitors p21, p27, and p15 respectively; García-Gutiérrez et al., 2019; Hume et al., 2020).

P15, p16, p18, and p19 (p14 in humans) act to block the association of CDK4 and CDK6 with cyclin D and thereby prevent the hyperphosphorylation of Rb (Hume et al., 2020; Satyanarayana & Kaldis, 2009; Sherr, 2000). Non-phosphorylated Rb is then able to continue repressing the transcription of genes required for DNA synthesis through its interaction with the E2F-family of transcription factors and its role in recruiting histone deacetylases and chromosomal remodeling SWI/SNF complexes to E2F-target promoters (Sherr, 2000). P21, p27, and p57 also act to inhibit CDK2-cyclin complexes preventing S-phase entry and progression (Hume et al., 2020; Satyanarayana & Kaldis, 2009; Sherr, 2000). For example, even in the presence of mitogenic signaling, DNA damage can activate p53 to increase p21 and repress CDK2, thereby blocking S-phase entry (Hume et al., 2020; Sherr, 2000).

Because the cyclin D family members are relatively short-lived (Sherr, 1993; Yang et al., 2017), they require continual translation downstream of mitogenic signals to outcompete the binding of CDK inhibitors with CDK4/6. Formation of CDK4/6-cyclin D complexes also serves to sequester the CDK inhibitors p21 and p27 thereby relieving their repression of CDK2-cyclin E

complexes (García-Gutiérrez et al., 2019; Hume et al., 2020; Sherr, 2000). Conversely, collapse of CDK4/6-cyclin D complexes releases p21 (and p27) thereby preventing CDK2/cyclin E phosphorylation of Rb and arresting the cell in G1 (García-Gutiérrez et al., 2019; Hume et al., 2020; Sherr, 2000). Loading of mini-chromosome maintenance (MCM) helicase complexes to replication origins also occurs in G1 with aid from CDKs (Deegan & Diffley, 2016). Transition into S-phase activates the MCM helicase unwinding of DNA initiated by CDK2 complexed with cyclin A and initiation of DNA replication (Hume et al., 2020; Satyanarayana & Kaldis, 2009; Sherr, 2000). CDK1 activity with cyclin A and cyclin B drives G2 and M-phase progression respectively (Satyanarayana & Kaldis, 2009).

Despite the important roles of each of these positive and negative cell cycle regulators, there are high levels of redundancy in their functions. For example, the knockout of any single cyclin D family member has been shown to have relatively mild effects whereas knockout of all 3 results in late embryonic lethality (Kozar et al., 2004). Similarly, compensatory roles of Cdk4 and Cdk6 are seen in single knockout mice that remain viable, whereas embryonic lethality is seen in mice lacking both Cdk4 and Cdk6 (Malumbres et al., 2004; Tsutsui et al., 1999). Similarly, loss of Cdk2 appears to be compensated by an ability of Cdk1 to bind to cyclin E (Aleem et al., 2005). Loss-of-function of cell cycle inhibitors are also not lethal (apart from p57 which causes early postnatal death), but typically lead to increased susceptibility to tumour formation as well as causing other tissue-specific alterations (Hao et al., 2016; Pietras et al., 2011; Sherr, 2012).

1.10 Cell Cycle Regulation in HSCs

Conditions that drive continued cycling of adult HSCs have been generally, but not exclusively, associated with loss of their regenerative activity (see section 1.8 and Fig. 1.2). Direct modulation of cell cycle regulators has been found to exert varying impacts on the hematopoietic system. For example, mice lacking *p21* display increased cycling of primitive hematopoietic cells that display a reduced self-renewal activity and an increased sensitivity to cytotoxic agents (Cheng et al., 2000). Conversely genetic ablation of *p18* in mice results in their production of HSCs with increased self-renewal activity in the absence of large increases in their turnover rate (Gao et al., 2015; Yuan et al., 2004). Similarly, human hematopoietic cells with increased *CDK6* expression showed moderate improvements in their self-renewal activity as measured by their regenerative activity in serially transplanted immunodeficient mice (Laurenti et al., 2015). *P27*-deficient mice also displayed improved repopulating efficiency in primary transplants compared to wild-type cells, however this did not translate into greater serial transplantability, which was explained as the effect primarily impacting progenitors downstream of the HSC compartment (Cheng et al., 2000; Gao et al., 2015). Conversely, conditional knockout of *p57* in the hematopoietic cells of adult mice reduced not only the frequency of primitive hematopoietic cells that were quiescent but also their repopulating and self-renewal activities in transplant recipients (Matsumoto et al., 2011). Together, these results suggest an important role of CDK inhibitors acting on CDK2 in the maintenance of HSC self-renewal activity, with an opposite effect obtained by increasing Cdk4/6 activity.

Stimulation of HSCs to divide in response to specific GFs has identified the involvement of several signaling pathways with differing impacts. The AKT and MAPK pathways in

particular have been identified as key connections between GF receptor activation and initiation of a proliferative response. For example, stimulation of CB *CD49f*⁺ cells *in vitro* with SCF in the absence of other cytokines or serum was found to activate MAPK signaling, whereas FLT3L activated AKT and MAPK, with IL-3 primarily activating STAT5 (Knapp et al., 2016). However, stimulation by these factors individually resulted in varying support of survival and negligible levels of *CD49f*⁺ cell division and a combination of any two efficiently restored survival but provided variable support for completing a first division (Knapp et al., 2017). Together, these findings reveal the importance of activating multiple pro-mitogenic pathways to elicit the efficient recruitment of quiescent HSCs to complete a division. Use of small molecule inhibitors in this system further demonstrated the important contribution of AKT signaling not only in supporting *CD49f*⁺ cell survival but also stimulating their division, with both being reduced in the presence of triciribine (Knapp et al., 2016). AKT has been found to phosphorylate and inhibit GSK3 as well as directly phosphorylating β -catenin (Verheyen & Gottardi, 2010), suggesting a potential synergy between these pathways. It is thus of interest that exposure of CB *CD49f*⁺ cells *in vitro* to a GSK3 inhibitor in concert with FLT3L stimulation (activating AKT and MAPK in these cells) improved both their survival and their proliferation, suggesting that β -catenin activation may be an important mediator of the unique biological responses of these cells to GF stimulation (Knapp et al., 2016). This finding is also supported by evidence that miR126 also inhibits multiple targets of the PI3K/AKT/GSK3 pathway in human HSCs causing an attenuation of their response to external signals thereby promoting HSC quiescence (Lechman et al., 2012).

Interestingly, very little is known about how aging may impact the regulation of HSC proliferation. Certain negative regulators of cell cycle progression, including *p18* and *p21*, have

been found to be increased in the HSCs of adult mice as compared to their fetal counterparts (Bowie et al., 2007). HSCs in aged mice have also been found to express increased levels of *p16*, *p21*, and reduced levels of several cyclins (*Ccnb2*, *Ccnd1*, and *Ccne1*; Flach et al., 2014; Janzen et al., 2006). A slight delay in the onset of the first division by aged mouse HSCs has also been reported to occur in association with their reduced expression of MCM helicase components and heightened replicative stress (Flach et al., 2014). However analogous mechanistic studies in human HSCs are lacking.

1.11 Thesis Objectives

The investigations outlined in this thesis were prompted by the paucity of information about mechanisms that regulate human HSC survival and proliferation in the adult. These were performed with the anticipation that the findings would inform strategies to enhance adult HSC handling for therapeutic applications as well as enable advances in our understanding of their transformation into adult leukemias. To this end I designed and adapted a series of functional assays to characterize and compare previously undefined properties of *CD49f*⁺ cells obtained from healthy human donors of ages ranging from 0-69 years. These studies tested the hypothesis that intrinsically manifested, aging-associated changes in *CD49f*⁺ cells would result in an altered rate or lineage composition of their output as well as the survival and proliferative responses of these cells to GF stimulation.

The lack of information of the properties of adult sources of *CD49f*⁺ cells compared to the more extensive characterization of these cells isolated from CB, suggested a useful first step would be to address this gap. For this purpose, I planned to undertake a multi-parameter

phenotypic analysis of multiple samples obtained from CB and normal adult human donors of BM or G-CSF-mobilized PB (mPB). In addition to determining the presence and frequency of *CD49f*⁺ cells within the *CD34*⁺ cell population isolated from each of these sources, I also sought to determine their relative content of 7 other canonical progenitor subsets defined by combinatorial surface marker phenotypes. I also asked whether using the Uniform Manifold Approximation and Projection (UMAP) algorithm (Becht et al., 2019; McInnes et al., 2018) to examine high-dimensionality relationships of these markers would reveal donor age- or source-associated phenotypic differences within the *CD49f*⁺ cell compartment. In parallel, I planned to use functional tests to examine and compare the differentiated cell outputs of the different sources of *CD49f*⁺ cells in transplanted immunodeficient mice and in 2 different 6-8-week stromal cell-containing co-culture systems that support the long-term generation of lymphoid and/or myeloid cells. The results of these experiments are presented in Chapter 3.

The results obtained in Chapter 3 revealed an age-related delay in the ability of *CD49f*⁺ cells from older donors to produce detectable clones of progeny in the stromal cell-containing co-cultures. This raised the question as to whether a similar delay would be evident in the early proliferative behaviour of these cells when they were stimulated to divide by exposure to a highly mitogenic combination of GFs, and, if so, whether this would be found to be related to an aging-associated alteration in the responsiveness of these cells to GF stimulation. These questions required the development and application of methods to investigate these responses at single-cell resolution to accommodate the high degree of heterogeneity known to be present in the HSC compartment. The methods developed to address these questions and the results thereby obtained are presented in Chapter 4.

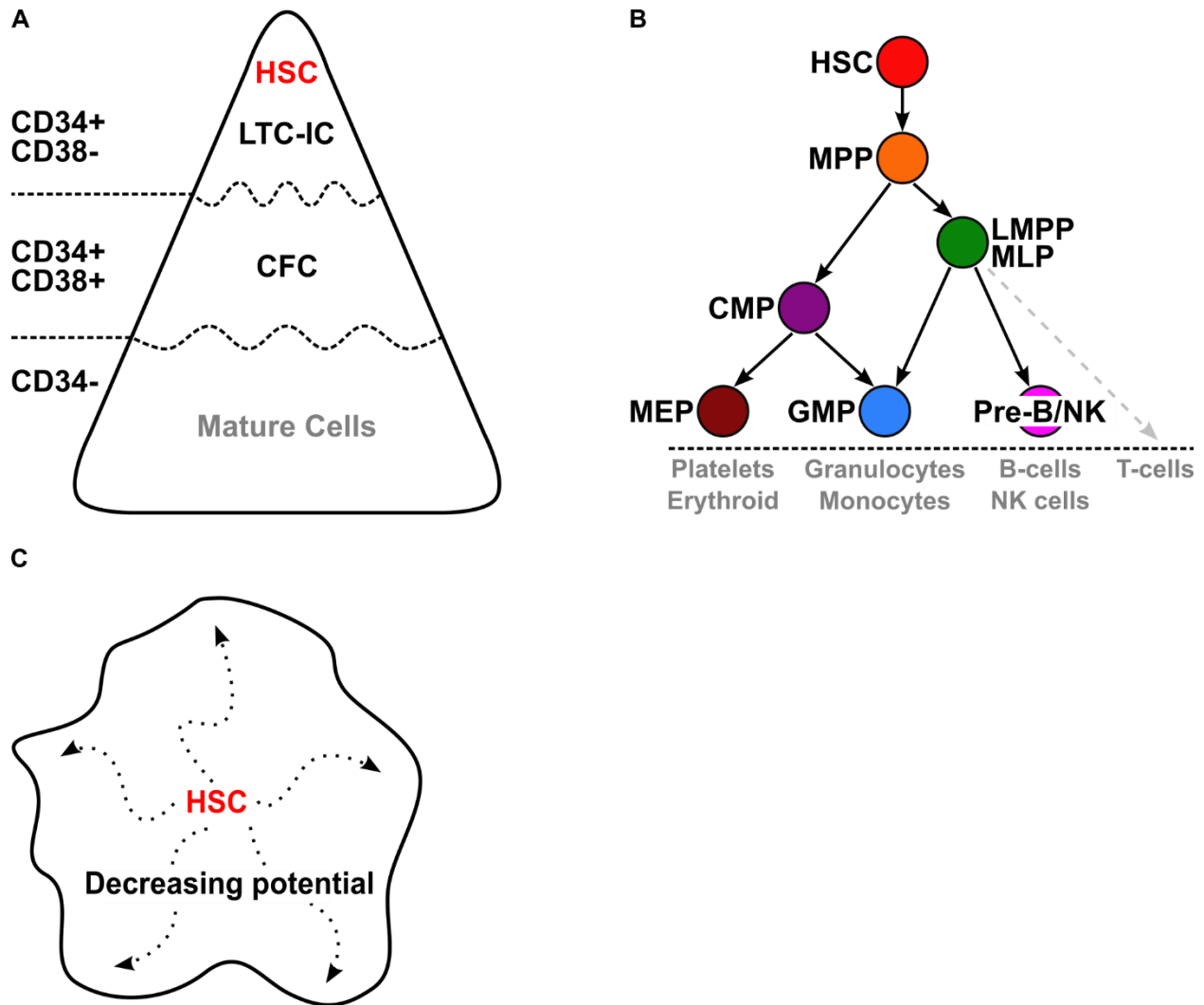


Figure 1.1 Models of the human hematopoietic hierarchy. A) Model of hematopoietic hierarchy based upon functionality displayed *in vitro* or *in vivo*. These functionalities remain broadly enriched using the surface markers displayed on the left. B) Discretized model with phenotypically defined progenitor subpopulations (MPP: multipotent progenitor, LMPP: lymphoid-primed multipotent progenitor, MLP: multipotent lymphoid progenitor, CMP: common myeloid progenitor, MEP: megakaryocyte-erythroid progenitor, GMP: granulocyte-macrophage progenitor, Pre-B/NK: Pre-B/Natural Killer (NK) cells). Arrows display cell-type transitions inferred from experimental observations. C) Continuum model from single-cell analytical strategies. Lineage commitment is progressive with loss of features associated with the

functionally defined self-renewal property that distinguishes HSCs. Directionality primes towards different lineage potentials in as of yet poorly defined alternative trajectories undertaken at variable rates and frequencies. Particular functional potentials are enriched, but individual cellular potentials remain highly heterogeneous, in different regions of this space.

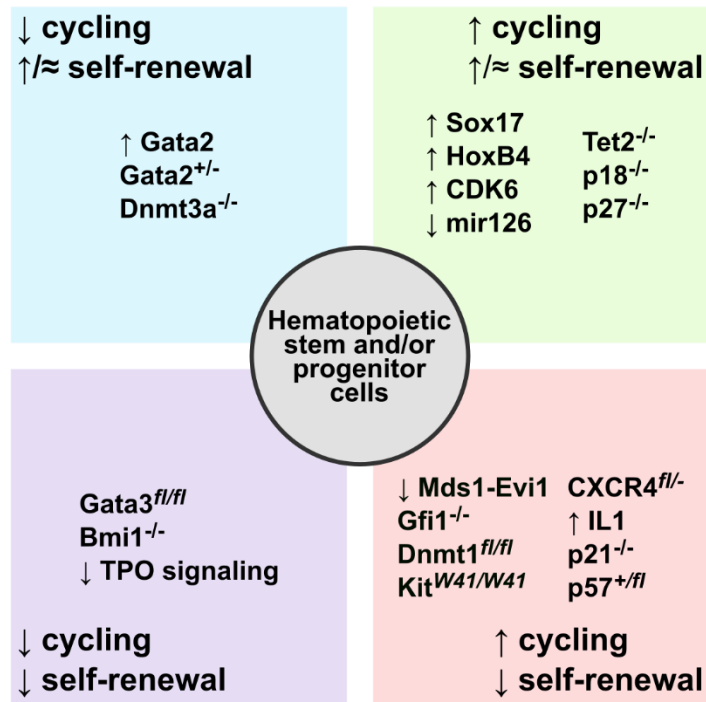


Figure 1.2 Highlighted factors impacting primitive hematopoietic cell cycling and self-renewal activities. Arrows indicate increased or decreased relative levels of the indicated factor (i.e. ↑ indicates overexpression, ↓ indicates knock-down). Specific genetic perturbations are as indicated.

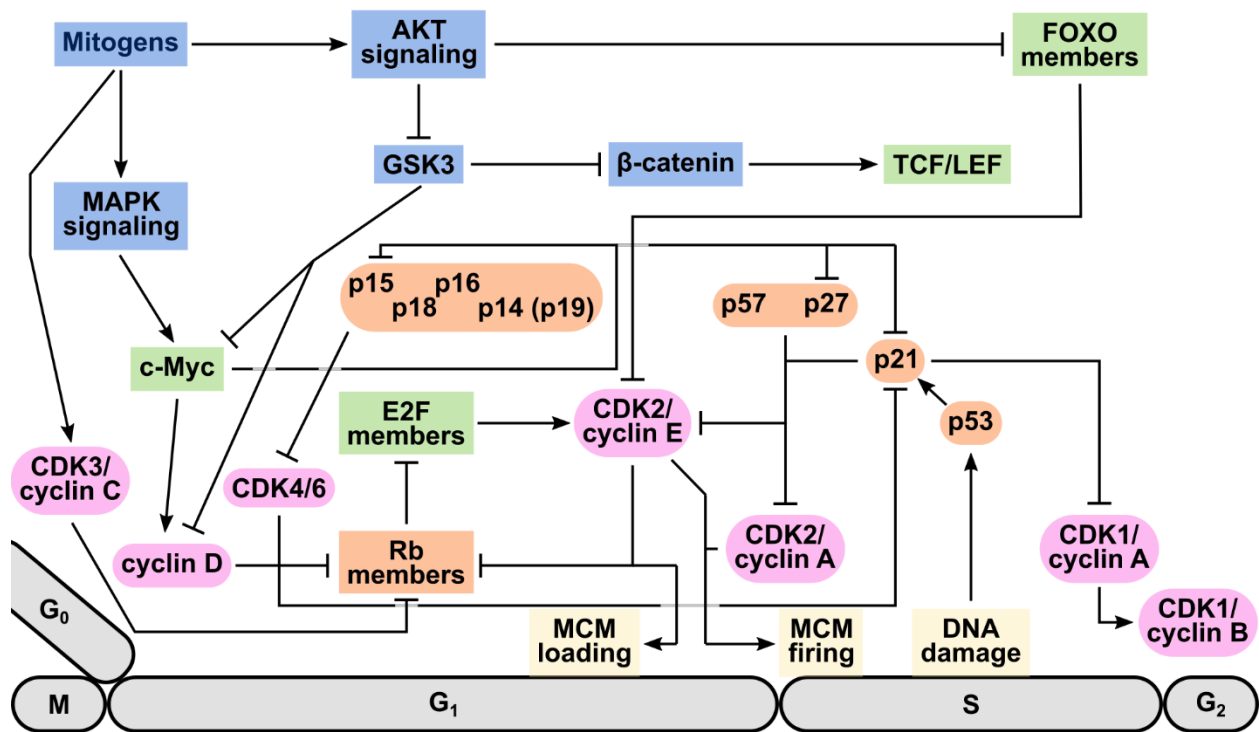


Figure 1.3 Highlighted factors regulating cell-cycle entry and progression. Lines ending with arrowheads indicate a positive effect, conversely, lines ending with bars indicate a negative effect. Grey portions of lines are used to distinguish origins of overlapping lines. Grey ovals indicate phases of the cell cycle, pink ovals are cyclins and CDKs, orange indicates negative regulators of cell-cycle progression, green indicates transcription factors, blue indicates signaling messengers, and yellow indicates processes. Positions of the indicated processes, as well as the cyclins and CDK complexes, are roughly above the portion of the cell-cycle where they or their activities occur.

Chapter 2: Materials and methods

2.1 Normal human blood and marrow samples.

Anonymized heparinized samples of CB, adult BM, or adult G-CSF-mPB cells were obtained from hematologically normal donors with informed consent. Adult samples were designated as either young when from donors 18-45 years old or aged when from donors >50 years old. All cells were obtained and used in experiments according to approved University of British Columbia Research Ethics Board, Biosafety, and Animal use protocols (in accordance with Canadian Council on Animal Care guidelines).

2.2 Sample processing and isolation of cells by FACS.

The low-density (<1.077 gm/ml) cells in fresh CB and BM samples were isolated by centrifugation at 800 g on Lymphoprep™ (#07861) with or without co-removal of CD11b+CD3+CD19+ cells using the RosetteSep™ reagent from STEMCELL Technologies, (Vancouver, BC, Canada, #15266) to obtain an initial enrichment of the CD34+ population. The cells thus isolated were then enriched to a purity of >70% using the EasySep™ reagents and magnet also from STEMCELL Technologies (#18056) and then used immediately or after cryopreservation in 10% dimethyl sulfoxide (DMSO; Origen Biomedical, Austin, Texas, USA, #CP-100) and 90% fetal bovine serum (FBS; Millipore-Sigma, Oakville, Ontario, Canada, #F1051). Leukapheresis samples of mPB were directly cryopreserved in FBS and DMSO and then CD34+ cells isolated using EasySep™ as above after thawing.

Frozen CB, BM, or mPB cells were thawed by drop-wise addition to Iscove's Modified Dulbecco's Medium (IMDM; STEMCELL Technologies, #36150) supplemented with 10% FBS and 10 $\mu\text{g}/\text{mL}$ DNase I (Millipore-Sigma, D4513). CD34⁺ cell-enriched populations were then suspended in Hanks' Balanced Salt Solution (HBSS; STEMCELL Technologies, #37150) supplemented with 5% human serum (Millipore-Sigma, H4522) and 1.5 $\mu\text{g}/\text{mL}$ anti-human CD32 antibody (Clone IV.3; STEMCELL Technologies, #60012) and then stained with designated Abs for 1-2 hrs on ice. Cells were then washed with HBSS with 2% FBS, 10 $\mu\text{g}/\text{mL}$ DNase, and resuspended in the same with added 1 $\mu\text{g}/\text{mL}$ propidium iodide (PI) (Millipore-Sigma, #537059) prior to analysis or sorting on a Becton Dickinson (Mississauga, Ontario, Canada) FACSAria™ Fusion, FACSAria™ III sorter, or FACSymphony™ instrument. Sorted cells were collected according to designated phenotypes after pre-gating as PI-negative (viable) singlets as bulk suspensions in Protein LoBind® tubes (Eppendorf, Mississauga, Ontario, Canada, #022431081) containing HBSS + 2% FBS or in 96-well plates (VWR, Edmonton, Alberta, Canada, #167008) pre-filled with an indicated medium. Assays of single cells were initiated by sorting them directly into the individual wells of Terasaki (Greiner, Monroe, North Carolina, USA, #654102) or 96-well plates prefilled with an indicated 0.2 μm filtered medium.

2.3 Phenotype data analysis.

Resulting flow cytometric profiles were analyzed in R using a combination of the 'flowCore' package (Hahne et al., 2009) and custom scripts. Cells were categorized as outlined in Table 2.2. Dimensionality reduction was performed using the UMAP algorithm (Becht et al., 2019; McInnes et al., 2018) within the R package 'umap'. Data from the measurements of 13-parameters, (FSC-A, SSC-A, CD45, CD34, CD38, CD45RA, CD90, CD49f, CD33, CD10,

CD117, CD123, and CD135; Table 2.1) recorded on individual CD45+CD34+ cells in each sample were initially converted to Z-scores (mean set to 0) using the R function 'scale'. Samples with multiple data files (recorded on separate occasions) had each occasion scaled independently. The resulting scaled data from over 10^6 CD45+CD34+ cells from normal CB, BM, and mPB donors was then reduced to 2-dimensions using the 'umap' function with default settings. Distance relationships of the progenitor subtypes were calculated as outlined in (Knapp, Kannan, et al., 2017). Briefly, 2-dimensional (2D) kernel density estimates for each cell subtype were calculated using the 'kde2d' function in the R package 'MASS' and then converted into probability density functions (sum of density = 1). Pairwise dissimilarities of the probability density functions were then calculated by taking half of the sum of the absolute difference in the probability density distributions, and pairwise similarities (proportion of the density distributions that overlapped) were then set to 1 minus this value for each subtype being analyzed. Calculated differences were visualized by applying the 'hclust' function in R. To determine if relationships between progenitor subtypes were maintained between the different sources of normal human CD45+CD34+ cells, the R function 'CADM.post' in the 'ape' package was used to perform a congruence among distance matrices (CADM) test (Campbell et al., 2011). UMAP reduction was also performed on just the *CD49f*+ cells from all samples starting from the same scaled data to give insight into age-related differences in this single phenotypic subset. Pairwise similarities were calculated as above.

To compare pairwise differences in the levels of parameters, null distributions of medians were generated via bootstrap re-sampling of cells within each cluster (bootstrap performed with replacement generating 10^4 median values from random samples of 50 cells for each iteration). Overlap of observed medians from each of the other clusters with the null distribution was then

used to indicate the probability that the observed median could arise in the null distribution. This process was repeated generating a null distribution from each cluster for comparison with the observed medians of each other cluster for each fluorescent parameter in the UMAP.

2.4 Assessment of *CD49f*⁺ cell progenitor activity in engineered stromal cell-containing LTCs.

These experiments were all initiated with single cells sorted as above into the 60 inner wells of a collagen-coated Nunc 96-well plate preloaded with equal mixtures of 1.7×10^4 irradiated mouse fibroblasts (5×10^4 total/well). In one set of experiments, the irradiated fibroblasts consisted of M210B4 cells engineered to express human IL-3 and G-CSF, *sl/sl* mouse embryo fibroblasts engineered to express human SCF, IL-3, and *sl/sl* mouse embryo fibroblasts similarly engineered to express human FLT3L. Each well was also preloaded with 100 μ l of MyeloCult H5100 (STEMCELL Technologies, #05150) supplemented with freshly dissolved 10^{-6} M hydrocortisone (Millipore-Sigma, #3867). Plates were incubated at 37 °C in 5% CO₂ in air with weekly assessment for the presence of highly refractile cells prior to half-medium changes performed after 2, 3, 4, and 5 weeks of incubation. After 6 weeks, the cultures were again visually assessed, and then the half-media change performed with the further addition of 50 ng/mL SCF (a gift from Amgen), 20 ng/mL each of GM-CSF and IL-3 (gifts from Novartis), IL-6 (a gift from Cangene) and G-CSF and 3 U/mL erythropoietin (EPO; STEMCELL Technologies) without inclusion of hydrocortisone. Incubation was continued for an additional 2 weeks and then the contents of each well finally categorized visually as “highly proliferative” (cultures containing a confluent or nearly confluent layer of highly refractile round cells), “proliferative” (fewer but >50 such cells seen), and “negative” (<50 such cells evident). Cultures

seen to contain >50 highly refractile round cells before the week 8 assessment but were then found to be negative at week 8 were categorized as “transient”.

In a second set of experiments, a protocol designed to detect a broader range of lineage outputs from single index-sorted *CD49f*⁺ cells was adopted. For these, the cells were deposited into the 60 inner wells of a Nunc 96-well plate already containing 9×10^3 MS-5 cells (a gift from Dr. Laure Coulombel, Inserm, Paris, France) and 300 each of irradiated M210B4 mouse fibroblasts engineered to express human IL-3 and G-CSF, *sI/sI* mouse fibroblasts engineered to express human SCF, IL-3 and FLT3L, and 100 μ L of α -Minimum Essential Medium Eagle (α -MEM; STEMCELL Technologies, #36450) containing 2 mM L-glutamine (Thermo Fisher, #35050061), and 10^{-4} M β -mercaptoethanol (Millipore-Sigma, 805740). This medium was supplemented with 15% FBS, 50 ng/mL SCF, 10 ng/mL FLT3L (a gift from Immunex) and 3 U/mL EPO (STEMCELL Technologies, #90257) for the first 2 weeks. For the next 3 weeks, 7.5% FBS with the same GFs was added and then, for the last week 7.5% FBS with 3 U/mL EPO was added. These cultures were incubated also at 37 °C in 5% CO₂ in air with weekly half-medium changes and again assessed weekly for the presence of >50 highly refractile round cells. At week 6, all wells that had been found to contain >50 refractile cells at any time point were trypsinized (STEMCELL Technologies, #07400), and the harvested cells were then stained with the panel of Abs shown in Table 2.3. Lineage contents were assessed by flow cytometry and assigned as outlined in Table 2.4.

2.5 Xenotransplants and analysis of regenerated cells

CD34-enriched CB cells from a large pool (>3,000 donors) were incubated at 37°C in 5% CO₂ in air for 16 hr in serum-free media (SFM) composed of IMDM, 20% Bovine Serum Albumin, Insulin, and Transferrin (BIT) with added 40 µg/mL low-density lipoproteins (LDL; STEMCELL Technologies), 10⁻⁴ M β-mercaptoethanol, and 1% L-glutamine supplemented with 100 ng/mL SCF and FLT3L (gift from Immunex), 20 ng/mL IL-3 and IL-6 and G-CSF, as well as 35 nM UM171 and 750 nM SR1 (gifts from Dr. Guy Sauvageau, IRIC, University of Montreal, Montreal PQ). Cells were then incubated for 6 hrs in the same medium containing 10⁶-10⁷ infectious units/mL of a *MNDU3* lentivirus containing a GFP cDNA driven by a *PGK* promoter (Imren et al., 2014; a gift from Dr. Keith Humphries, Terry Fox Laboratory, BC Cancer, Vancouver BC). The cells were then washed and cultured for a further 48 hrs in the same media as above without virus. PI-negative GFP⁺ cells were isolated on a FACSAria™ III and pooled with freshly isolated *CD49f*⁺ cells from 2 individual CB or 2 young adult BM donors at a ratio of 10⁴ GFP⁺ cells:300 *CD49f*⁺ cells. The resulting pools were then injected via the tail vein into 12-16 week old female non-obese diabetic (NOD)-*Rag1*^{-/-}-*IL2Rγc*^{-/-}-*W^{A1}/W^{A1}* (NRG-W41) mice exposed 1-6 hours previously to a sublethal whole-body dose of 200 cGy of ¹³⁷Cs γ-rays delivered over a few minutes. The NRG-W41 strain was chosen due to previous studies suggesting enhanced chimerism of transplanted human cells into mice bearing mutated *c-kit* alleles (Cosgun et al., 2014; McIntosh et al., 2015; P. H. Miller et al., 2017; Yurino et al., 2016). Mice used for xenografting experiments were bred and maintained in the BC Cancer Research Centre Animal Resource Centre under aseptic specific-pathogen-free (SPF) conditions.

Following transplantation, mice were monitored at weeks 4, 8, 12, 16, 20, and 30 via BM aspirations of alternating femurs for evidence of human blood cell chimerism using the Abs outlined in Table 2.5. Mature red blood cells in the aspirate samples were first lysed in 0.8% NH_4Cl + 0.1mM ethylenediaminetetraacetic acid (EDTA; STEMCELL Technologies, #07850) then samples were processed, stained, and analyzed by flow cytometry as outlined in section 2.2. Analysis of the changing levels of several human hematopoietic cell phenotypes over time in the transplanted mice was performed in R. Human chimerism was calculated as the sum of the percentages of human CD45^+ cells (detected by two different anti-human CD45^+ Abs targeting different epitopes) and human CD45-GPA^+ cells detected in the total viable single cell population obtained in the BM aspirate samples. Lineage chimerism was similarly determined as the proportion of myeloid ($\text{CD45}^+\text{CD34-CD33}^+$), B-lymphoid ($\text{CD45}^+\text{CD34-CD19}^+$), and erythroid (CD45-GPA^+) cells in the total viable mouse BM sample. Mice without total human engraftment above 0.005% (combined GFP⁺ and GFP⁻ human engraftment) of the total viable mouse BM across all timepoints were excluded from downstream analysis, 2 such mice were excluded this way. Data shown are geometric means with standard deviations. Pairwise differences were examined at each timepoint using the Student's *t* test. Correlations were assessed by calculating a linear model of \log_{10} -transformed chimerism values for GFP⁻ and GFP⁺ cells within each sample analyzed.

2.6 Single-cell tracking of survival and proliferation kinetics *in vitro*

Clonal tracking of CD49f^+ cells was performed on single CD49f^+ cells sorted as above into separate wells of a Terasaki plate containing 20 μL of 0.2 μm filtered SFM + 300 ng/mL SF, 300 ng/mL FLT3L and 60 ng/mL IL3 (3GF). Serial 10-fold dilutions of this initial 3GF

concentration in SFM were used for the 3GF dose-response experiments. Following sorting of single-cells as described in section 2.2, plates were kept on ice for 30-60 min after which each well was visually assessed to determine the presence or absence of a viable single highly refractile cell. Plates were then wrapped with a thin band of Parafilm™ between the lid and the bottom of the plate, and each plate was then placed inside of a 15 cm round petri dish with 6x 35 mm dishes each containing 2-3 mL of autoclaved distilled water to reduce media evaporation throughout the period of culture in a humidified atmosphere of 5% CO₂ in air at 37°C. Each well was then manually assessed 1-2x daily for 7 days for cell viability (high refractility, cell size, and membrane integrity) and cell division. The number of divisions completed by each cell at the end of the experiment was calculated as follows from the number of viable cells: 1 cell = no divisions, 2 cells = 1 division, 3-4 cells = 2 divisions, 5-8 cells = 3 divisions, 9-16 cells = 4 divisions, 17-32 cells = 5 divisions, and >32 cells = 5+ divisions. Initial observation of a division was adopted as the time the division occurred. If >1 division occurred in a well between monitoring timepoints, the divisions were treated as having occurred at times equally spaced between the observation timepoints. Wells were no longer assessed for divisions after reaching >5 division cycles (>32 cells). Wells that were never observed to have a viable single cell in them through the course of the experiment were excluded from downstream analyses.

Analysis of survival and proliferation kinetics was performed in R. Survival was calculated using the functions ‘Surv’ and ‘survfit’, and statistical differences were calculated with a log-rank test using the ‘survdif’ function in the ‘survival’ package. Proliferation kinetics were calculated on viable cells using the ‘drc’ package (Ritz et al., 2015) to generate dose-response curves of proliferation as a function of time. Contributions of individual samples to the curves were weighted based on the number of cells analyzed in each sample. Reported median

division times are the calculated ED50 values of the corresponding weighted curve generated for each corresponding data set. Errors bars reflect the standard error of the mean (SEM) of ED50 values for samples originating from the same group. Pairwise statistical comparisons of ED50 values (null hypothesis being that the ratio of ED50 for 2 groups = 1) of the weighted curves was performed using the 'compParm' function of the 'drc' package. Dose-response curves for survival and proliferative ability were generated as above with pairwise ED50 calculations reflecting differences in the concentrations of 3GF required for 50% of *CD49f*⁺ cells from each group to maintain survival or complete ≥ 1 division within 7 days of culture.

2.7 Cell-cycle transit culture time-course setup and plate preparation for streptavidin (SA) capture

Bulk CD45⁺CD34⁺CD38⁻ (200-500) and *CD49f*⁺ (50-100) cells were sorted into separate wells of Nunc round-bottom 96-well plates containing 100 μ L of SFM + 300 ng/mL SF + 300 ng/mL FTL3L + 60 ng/mL IL3 + 10 μ M 5-ethynyl-2'-deoxyuridine (EdU) or 100 μ L of SFM + 3 ng/mL SF + 3 ng/mL FTL3L + 0.6 ng/mL IL3 + 10 μ M EdU and incubated for 24, 40, 52, or 64 hr at 37 °C in 5% CO₂ in air. After the allotted time, the cells in each well were individually harvested and washed twice with HBSS + 2% FBS and transferred into Protein LoBind[®] tubes, centrifuged at 300 g for 5min, aspirated to minimal volume and then transferred to the individual wells of a SA-coated 384-well plate (Thermo Fisher, #15504 or Greiner, #781990). Prior to loading, wells of the 384-well plate were coated with 1 μ g/mL α -CD44-biotin (Biolegend, #103004) in IMDM overnight at 4 °C. Wells were then washed 2x with IMDM removing all volume immediately prior to loading the cells prepared as described above. Cells for the 0 hr timepoint were sorted directly into wells of a 384-well plate prepared as above with

the addition of SFM+3GF. After cells were transferred into the 384-well plate they were centrifuged at 300 g for 3-5min, then promptly fixed with 4% paraformaldehyde (PFA) in phosphate-buffered saline (PBS) for 30 min at room temperature, then washed 3x with HBSS + 2% FBS before storing at 4 °C. Once all time points were transferred and fixed, cells were permeabilized and RNA removed with 0.5% Triton X-100 + 200 µg/mL RNaseA (Invitrogen, #12091-021) in HBSS + 2% FBS for 15 min at 37 °C, then washed 2x with PBS + 2% FBS and resuspended in 0.1% Triton X-100 in PBS + 2% with 1.5 µg/mL α -human CD32 and 5% human serum. Cells were then stained with an α -CDK2 Ab (Cell Signaling Technologies, #2546S), then washed 2x with PBS + 2% FBS and stained with a goat α -rabbit-AF594 secondary Ab (Thermo Fisher, #A-11012) for 30 min on ice. Cells were then washed 3x with PBS + 2% FBS and stained with an α -human CD45-AF488 Ab (Biolegend, #304017) and an α -CDK6-AF647 Ab (Abcam, #EPR4515) for 1 hr on ice. Cells were then washed 2x with PBS + 2% FBS and resuspended in the same buffer containing 2 µg/mL 4',6-diamidino-2-phenylindole (DAPI; Millipore-Sigma, #32670) and then imaged (see imaging acquisition details in section 2.9). Following imaging, fluorescence was quenched by adding 2x quenching solution (9% H₂O₂ + 50 mM NaOH (Millipore-Sigma, #H1009 and #795429 respectively) in PBS) and storing the samples overnight at 4 °C. The extent of quenching achieved was assessed by washing the wells 2x with PBS + 2% FBS, resuspending them in 2 µg/mL DAPI and imaging the plate with the same microscope settings used in the preceding imaging step. When the degree of quenching appeared incomplete, new quenching solution was added, and the plate left at room temperature for another 1-4 hr and then imaged again as previously described. Subsequent antibody staining, imaging, and quenching was performed as described above (all Abs used are listed in Table 2.6).

EdU staining was performed using the Click-It™ EdU AF594 kit (Invitrogen, #C10354) according to the manufacturer's guidelines.

2.8 Acquisition of microscope images

384-well plates were imaged on a Nikon A1-si microscope with a 10x objective and images acquired by setting the focus on the centre of each well and stitching a large image (overlap set to 5%) such that the entire bottom of the well was captured and combined into a single large image. Images were captured at ¼ frames/sec as the average of 2 captures. To capture total fluorescence from each cell, the pinhole diameter was set to 255.4 µm. Voltages for each channel were adjusted separately for each imaging panel. Determination of quenching completion was performed using the voltage settings of previously acquired panels.

2.9 Analysis of microscopy data

Acquired images were quantified in FiJi using custom macro scripts. Images were loaded using the 'Bio-Formats Importer' plugin using default parameters. Background subtraction was performed using a rolling ball radius of 25.0 pixels and then a gaussian blur (sigma radius = 1 pixel) was applied. Event regions were selected on the DAPI channel using the 'Robust Automatic Threshold Selection' plugin with the following settings: noise = 20, lambda = 3, and min = 150. To separate identified regions containing multiple events, regions were shrunk slightly using the 'erode' command. Then the 'Adjustable Watershed' command (tolerance = 0.1) was used. The resulting regions were analyzed using the "Analyze Particles" command with the following settings: size = 5-200 and circularity = 0.8-1.00 and exported as a '.csv' files.

Representative images in Figure 4.2 are from a portion of a single well imaged at 10x as above

for each imaging cycle. Images channels for this figure had the following thresholds set in FiJi: DAPI = 0-4095, AF488 = 500-4095, AF594 = 1000-4095, AF700 = 1000-4095, Transmitted = 0-2500.

Downstream quantification was performed in R also using custom scripts. Wells acquired in the same imaging stage were combined and event specific information between imaging panels was maintained by calculating a well-by-well affine transformation formula and applying this to the positions of the events in the subsequent imaging stages to ‘stitch’ the events to those identified in the initial imaging stage. This required identifying landmark regions maintained in the same well between panels using the ‘Extract SIFT Correspondences’ plugin in FiJi with the following settings: `initial_gaussian_blur = 1`, `steps_per_scale_octave = 3`, `minimum_image_size = 64`, `maximum_image_size = 1024`, `feature_descriptor_size = 4`, `feature_descriptor_orientation_bins = 8`, `closest/next_closest_ratio = 0.92`, `filter_maximal_alignment_error = 25`, `minimal_inlier_ratio = 0.05`, `minimal_number_of_inliers = 7`, and `expected_transformation = Rigid`. Resulting landmark positions were used to calculate a well-specific affine transformation using the ‘AffineTransformation’ function in the ‘`vec2dtransf`’ package in R (German Carillo, <https://cran.r-project.org/web/packages/vec2dtransf/index.html>). The affine transformation was then applied to the events in the subsequent imaging stage and the adjusted event positions were matched to the events of the initial imaging stage by calculating pairwise Euclidean distances between the events using the ‘`cdist`’ function in the ‘`rdist`’ package (Nello Blaser, <https://cran.r-project.org/web/packages/rdist/index.html>). Unique matches between events were then assigned by identifying events with the minimum distance between the two images. Poor quality matches were removed by setting a maximum distance between matched events as $5 \times$ median distance of

the minimum distance of matches or a distance ≥ 50 pixels. In rare events of the SIFT landmarks identified between two images generating an affine transformation which resulted in a low number of high-quality matches, an affine transformation using the median values of the affine transformations calculated for all of the other wells in the same experiment was used. Events that were not matched through all imaging stages (and therefore not present throughout all imaging acquisitions) were removed from downstream analysis.

To remove auto-fluorescent debris and separate cells from acquired events, an ‘Autofluorescence’ parameter was calculated as the sum of the fluorescence of the AF488, AF594, and AF647 channels acquired following fluorescence quenching of the first imaging stage and a circularity parameter calculated as $(\text{perimeter}^2 / (4 * \text{area})) / \pi$. Fluorescent channels apart from DAPI (DNA content) were then transformed using $\text{asinh}(x/150)$, after which all channels were converted to Z-scores (mean=0) using the function ‘scale’ with default parameters (each experiment scaled independently). Resulting data was converted to a ‘flowFrame’ structure using the ‘Biobase’ (Huber et al., 2015) and ‘flowCore’ (Hahne et al., 2009) packages to allow for visualization and 2D gating. Events with high ‘Autofluorescence’ and circularity values outside of -2 to 2 were excluded, and cells were identified using a combination of CD45 and DAPI fluorescence. Identified cells from each experiment were then combined and their associated DAPI, CD45, CDK2, CDK6, Ki67, pRb, and EdU parameters were collapsed into 2D using the ‘umap’ function. Kmeans clustering was performed to split the resulting UMAP distribution into 3 regions. The proportion of each cell type within a region at a given timepoint was calculated to assess movement of the cells through the cell cycle. Statistical differences between these proportions were calculated using Holm-corrected Kruskal-Wallis rank sum tests.

Comparison of intensities of individual parameters was performed using Holm-corrected Wilcoxon tests.

2.10 Phospho-flow sample preparation and analysis

CD34⁺ cell-enriched samples of CB and young adult BM were thawed as previously described in 5 mL Protein LoBind® tubes (Eppendorf, #0030108302) and then washed 2x in PBS without FBS. Cells were then stained with an eFluor™ 780 fixable viability dye (Invitrogen, #5016966) for 30 min on ice, then washed 1x in PBS + 20% FBS and resuspended in SFM. Cells were then incubated at 37 °C in 5% CO₂ in air for 180 min total, with addition of 3GFs to the cells 0, 5, 15, or 30 min prior to the end of the culture period. Cells were then fixed with 1.6% PFA for 10 min at room temperature, washed 1x with PBS + 2% FBS, then permeabilized by adding -80 °C 100% MeOH dropwise while vortexing gently. Cells were then washed and resuspended in PBS without FBS and barcoded with Pacific Blue succinimidyl ester (Thermo Fisher, #P10163) at 0 µg/mL, 0.002 µg/mL, 0.02 µg/mL, or 0.2 µg/mL for 30 min at room temperature while being shielded from light. Cells were then washed 1x with PBS + 10% FBS, then pooled together into a single tube and resuspended in PBS + 2% FBS + 1.5 µg/mL α-human CD32 + 5% human serum and stained with the Abs outlined in Table 2.7 for 60-120 min. Thereafter, the cells were washed and stained with a goat α-rabbit-AF594 secondary for 15 min. Cells were then washed again and analyzed on a BD FACSymphony™.

Flow cytometric analysis was performed in R as described above. Viable single cells were gated as CD45⁺CD34⁺CD38⁻CD45RA⁻ cells or *CD49f*⁺ cells and results for cells treated under different conditions were identified based on their assigned Pacific Blue barcode

intensities. Fluorescent intensities of each intracellular marker were converted to Z-scores (mean=0) using the ‘scale’ function in R on a sample-by-sample basis. Data was then pooled by sample age-group and differences in marker intensity for each stimulated time point from their corresponding unstimulated condition was performed by generating null distributions of medians via bootstrap re-sampling of cells from each condition as outlined in section 2.3.

Table 2.1 Abs for *CD49f*+ cell sorting and *CD45*+*CD34*+ phenotypic analysis

Antigen	Clone	Colour	Company
CD10	HI10a	PerCP-Cy5.5	Biolegend
CD33	WM53	PECF594	BD
CD34	561	BV421	Biolegend
CD38	HIT2	BV711	Biolegend
CD45	HI30	AF700	Biolegend
CD45RA	HI100	BV605	Biolegend
CD49f	eBioGoH3	FITC	eBioscience
CD90	5E10	PECy7	BD
CD117	104D2	APC	eBioscience
CD123	6H6	APC-ef780	eBioscience
CD135	BV10AH42	PE	Invitrogen

Table 2.2 Phenotypic definitions of stem and progenitor subtypes

Subtype	Phenotype
HSC	CD45+CD34+CD38-CD45RA-CD90+CD49f+
MPP	CD45+CD34+CD38-CD45RA-CD90-CD49f-
LMPP	CD45+CD34+CD38-CD45RA+CD10-
MLP	CD45+CD34+CD38-CD45RA+CD10+
PreB/NK	CD45+CD34+CD38+CD45RA+CD10+
CMP	CD45+CD34+CD38+CD45RA-CD135+
GMP	CD45+CD34+CD38+CD45RA+CD135+
MEP	CD45+CD34+CD38+CD45RA-CD135-

Table 2.3 Abs and channels for *in-vitro* lineage assessment

Antigen	Clone	Colour/Channel	Company
CD7	M-T701	FITC	BD
CD10	MEM-78	BB700	BD
CD11b	M1/70	BV711	Biolegend
CD14	61D3	PECy7	eBioscience
CD15	HI98	V500	BD
CD19	SJ25C1	PE	eBioscience
CD33	WM53	PECF594	BD
CD34	581	AF700	BD
CD45	HI30	APC-ef780	eBioscience
CD56	CMS5B	APC	eBioscience
CD235a	HI264	Pacific Blue	Biolegend
Empty	NA	V 610/20-A	NA

Table 2.4 *In vitro* lineage output classifications

Class	CD45	CD34	CD33/ CD11b	CD14/ CD15	CD10&19 or CD56 or CD7
Lineage Negative	+	+/-	-	-	-
NM	+	+/-	+	+	-
Lymphoid	+	+/-	-	-	+
Mixed	+	+/-	+	+	+

Table 2.5 Abs for *in vivo* lineage assessment

Antigen	Clone	Colour	Company
CD3	OKT3	SuperBright 600	eBioscience
CD15	HI98	PECy7	BD
CD19	SJ25C1	PE	eBioscience
CD33	WM53	PECy7	eBioscience
CD34	581	AF700	BD
CD38	HIT2	BV711	Biolegend
CD45	HI30	APC-ef780	eBioscience
CD45	2D1	APC	eBioscience
CD235a	HI264	Pacific Blue	Biolegend

Table 2.6 Microscopy Abs for cell-cycle staging

Antigen	Clone	Colour	Company
CD45	HI30	AF488	Biolegend
pRb (pS807/pS811)	J112-906	AF647	BD
CDK2	78B2	NA	CST
CDK6	EPR4515	AF647	Abcam
Ki67	B56	AF488	BD

Table 2.7 Abs for phospho-flow cytometry

Antigen	Clone	Colour	Company
pAKT (pS473)	M89-61	PE	BD
pSTAT5 (pY694)	47	PECy7	BD
pERK1/2 (pT202/pY204)	20A	AF647	BD
Non-phospho (active) β -Catenin	D13A1	NA	CST
CD45	HI30	BUV395	BD
CD34	581	BB700	BD
CD38	HIT2	BV711	Biolegend
CD45RA	HI100	BV605	Biolegend
CD90	5E10	AF700	Biolegend
CD49f	eBioGoH3	FITC	eBioscience

Chapter 3: Age-independent conservation of human CD34+ hematopoietic cell phenotypic progenitor content and CD49f+ long-term multilineage output potential.

3.1 Introduction

As reviewed in Chapter 1, many aspects of the unperturbed process of hematopoiesis are demonstrably affected by aging. This includes a consistent decreased output and functional decline of mature lymphoid cells accompanied by increasing anemia, the appearance of clonal expansions bearing leukemia-associated mutations (CHIP) and overt malignancy (Guralnik et al., 2004; Jaiswal & Ebert, 2019; Ogawa et al., 2000). Studies in the mouse suggest that some of these changes may arise from altered numbers of certain progenitors and stem cell subsets that are aging-related, including a reduced output of mature lymphocytes that correlate with decreased numbers of lymphoid progenitors and an increasing proportion of HSCs producing myeloid-restricted progeny (Benz et al., 2012; Cho et al., 2008; Dykstra et al., 2007, 2011). Evidence of cell intrinsic mechanisms of aging have been suggested to be due to an observed accumulation of DNA damage, metabolic changes, and epigenetic alterations affecting the functionality of HSCs (Geiger 2013). Analogous studies in humans have been more limited but are supported by reports of an aging-associated accumulation of immunophenotypic primitive cell subsets (Kuranda et al., 2011; Nilsson et al., 2016; Pang et al., 2011).

Here we focused on comparing a number of biological properties of cells defined by the CD49f+ cell phenotype – a CB subset highly enriched in cells found to display the regenerative properties in xenograft transplantation assays used to define human HSCs (Belluschi et al., 2018; Knapp et al., 2017, 2018; Notta et al., 2011). To date, however, very few functional studies of

cells with this phenotype isolated from normal adult donors have been described and are limited to a suggested ~5-40-fold decline in their repopulation potential as compared to those present in CB (Huntsman et al., 2015; Wang et al., 2019). It was therefore of interest to more fully characterize the human CD34⁺ stem and progenitor cell compartment present in normal human donors spanning 7-decades of life and use a variety of long-term *in vitro* and *in vivo* assays to compare the proliferative and lineage output activities of the CD49f⁺ fraction of these cells.

3.2 Results

3.2.1 The relative frequencies of multiple phenotypes of human hematopoietic CD34⁺ cells are largely conserved from birth to mid-late adulthood.

An initial series of experiments was undertaken to determine how the phenotypic composition of the CD34⁺ cell compartment might change in healthy humans from birth through adulthood. For this survey, ~ 10⁶ CD34⁺ cells isolated from CB, mPB, and BM samples obtained from a total of 33 individuals were assigned to 8 well-described phenotypic subtypes (Doulatov et al., 2010, 2012; Karamitros et al., 2018; Knapp et al., 2019) using the same panel of 11 Abs (Table 2.2, Fig. 3.1A-C). The average frequencies of most of these subtypes were found to vary markedly between individual donors (Fig. 3.2A), without obvious differences trending with the age of the donor or the source of the CD34⁺ cells analyzed (BM vs PB, Fig. 3.2A). Overall, CMPs were the dominant progenitor subtype in most samples, closely followed by GMPs, although this difference did appear to reverse with age in the BM samples (median values of 39% CMPs (interquartile range (IQR) 30-44%) and 23% GMPs (IQR 19-35%) in the young adult BM samples vs 28% (IQR 22-34%) and 38% (IQR 30-42%) respectively in the aged adult

BM samples). However, in the PB, the frequency of GMPs decreased with increasing age whereas the CMP frequency remained relatively stable (i.e., 16% GMPs (IQR 12-19%) in CB, 10% (IQR 8.5-31%) in young adult mPB, and 4.5% (IQR 2.8-4.7%) in the aged adult mPB samples, with median CMP proportions staying between 47%-53% for each group).

As a more agnostic approach to identify potential source-specific differences, UMAP dimensionality reduction was then applied to the same 11 surface marker-based phenotype data in combination with the simultaneously measured FSC and SSC properties culminating as 13 mean-scaled parameters (Becht et al., 2019; McInnes et al., 2018). This yielded a 2D distribution characterized by a large central cluster with two areas of high cellular density and 3 regions branching out from or separated from the main central cluster (Fig. 3.2B). The distributions of the 5 different sources of CD45+CD34+ cells showed a high degree of overlap in this 2D UMAP display (Figure 3.2C). Hierarchical clustering of the 8 canonical phenotypically-defined subtypes obtained using their UMAP density distributions and their resultant spatial relationships were generally consistent with the literature; with expected closest associations of the *CD49f*+ cells with MPPs, a high proximity of LMPPs with MLP cells, CMPs with MEPs, and GMPs with Pre-B/NK cells (Fig. 3.2D; Buenrostro et al., 2018; Knapp et al., 2019; Velten et al., 2017; Zhao et al., 2017). Importantly, the spatial relationship of these subtypes was maintained when the analyses were restricted to the cells obtained from separate age or source groups (CADM test, $P < 0.005$). However, the cells within each phenotype also displayed heterogeneity within UMAP space with CMP and GMP cells having particularly heterogeneous distributions (Fig. 3.2E).

To further examine the phenotypes underlying the UMAP distribution, K-means clustering was then used to segregate the CD45+CD34+ UMAP distribution into 6 regions (Fig.

3.2F). This analysis revealed one group of cells (Region 1) distinguished by their relatively elevated levels of CD90 and CD34 and low levels of CD38, consistent with the phenotypic properties of *CD49f*⁺ cells. Interestingly, the cells in all 3 regions comprising the central UMAP cluster (regions 1-3) showed higher levels of CD117 (KIT) than the cells in regions 4 and 5 which were located further away from the central cluster. Increasing levels of expression of CD45RA by the cells in regions 3, 4, and 5 was also associated with a location remote from the central cluster. Higher CD10 expression by the cells in region 4 and elevated expression of CD123 by the cells in region 5 suggest their more restricted identities as cells adopting lymphoid and myeloid fates, respectively. The cells in region 6 comprised 2.3% of the total CD45⁺CD34⁺ compartment and were well separated from the remaining cells. The profile of cells within this region included very high expression of CD49f, CD90 and CD123, with low expression of CD34, CD38, CD45RA, and CD117, and a broad range of expression of CD45 - a phenotype suggestive of persisting rare CD34⁺ contaminants (such as maturing blood and/or endothelial cells).

3.2.2 The *CD49f*⁺ subset displays greater source- than aging-associated differences in their phenotypic properties.

To determine the extent of similarity between cells sharing the defining *CD49f*⁺ phenotypic properties that are present in different sources and/or donors of different ages, we again used UMAP, but applied it exclusively on this subset from each group. This gave 2 connected but spatially distinct clusters in a 2D UMAP distribution (Fig. 3.3A). Interestingly, these 2 clusters were found to be separated based on the source of the *CD49f*⁺ cells rather than the age of the donor, although *CD49f*⁺ cells from young adult BM donors were somewhat

intermediate between the 2 clusters (Fig. 3.3B). This was similarly observed from a pairwise overlap assessment of their UMAP density distributions which also placed *CD49f*⁺ cells from CB, young adult mPB, and aged adult mPB together and separate from those isolated from the BM (Fig. 3.3C). Examination of the markers underlying this distribution pointed primarily to differences in the levels of CD45, CD34, and CD90 expression, with BM *CD49f*⁺ cells from young or aged adult donors showing consistently higher expression of these markers than their counterparts isolated from the PB (Fig. 3.3D). CD38 expression was also lower in BM *CD49f*⁺ cells than in cells isolated from the PB. Additional differences were observed in the levels of the 3 growth-factor receptors examined (CD117, CD123, and CD135), however, none of the latter appeared to be changed consistently with the source or age of the donor examined.

3.2.3 The LTC-IC frequency within the *CD49f*⁺ subset is high and independent of donor age.

To compare the growth potential of *CD49f*⁺ cells obtained from differently aged donors, they were assessed for their LTC-IC content in 8-week cultures initiated with single cells deposited into separate wells of a 96-well plate containing irradiated mouse fibroblasts engineered to produce several human growth factors (Fig. 3.4A; Hogge et al., 1996; Knapp et al., 2018; Sutherland et al., 1989). In addition, the cells were pre-stained with the same large panel of Abs used for the phenotype comparisons and index-sorted to allow subsequent correlation of their LTC-IC activity with their initial phenotypic properties.

Cells in this assay were then defined as “highly proliferative”, “proliferative”, or “negative” according to the amount of progeny they produced after 6 weeks under standard LTC

conditions and another 2 weeks following the addition of multiple GFs to promote the generation of expanded numbers of terminally differentiating myeloid cells. *CD49f*⁺ cells that produced readily detectable progeny before 8 weeks but were negative later were classified as “transient” (see section 2.4 for details). The resulting distribution of these outcomes was significantly different for all groups examined (pairwise Fisher’s exact test, $P < 0.001$; Fig. 3.4B; Table 3.1). This included a progressive decrease in the frequency of *CD49f*⁺ cells classified as “transient” LTC-ICs as a function of donor age (mean values of 19% in CB, 14% in young adult BM, and 3% in aged adult BM). However, despite these differences, the frequency of LTC-ICs with obvious cell outputs at 8 weeks within the *CD49f*⁺ subset was found to be independent of the age of the donor as ~50% of this phenotype (Fig. 3.4C). Nevertheless, the rate at which readily detectable numbers of progeny became evident was significantly delayed as a function of the increasing age of the donor (pairwise Komolgorov-Smirnov tests, all $P < 0.0001$). Thus, by week 3, 88% of CB LTC-ICs had already produced visible progeny, whereas only 40% of the BM LTC-ICs from young adults, and 30% of BM LTC-ICs from the aged adult group were detectable at this time. The magnitude of this delay is amplified in the observation that 36% of the LTC-ICs from the aged adult BM samples did not produce any detectable progeny until the final week 8 assessment, in contrast to the corresponding values of 9% and 3.5% within total LTC-ICs detected from the young adult BM and CB samples respectively, suggesting considerable age-associated changes in how LTC-IC proliferative responses are regulated.

Use of the index sorting data to analyze potential phenotype-associations with the growth patterns displayed by *CD49f*⁺ cells in the LTC assays showed that CB *CD49f*⁺ cells categorized as highly proliferative LTC-ICs have elevated levels of CD33, CD34, and CD90 (Fig 3.4C) in agreement with a previous report (Knapp et al., 2018). However, of these markers, only CD33

was elevated on highly proliferative LTC-ICs from young adult BM donors, suggesting CD34 and CD90 expression levels become less predictive of *CD49f*⁺ functional potential with increasing donor age.

3.2.4 Age-independent retention of lympho-myeloid differentiation potential of *CD49f*⁺ cells.

A next set of experiments was designed to determine whether the lympho-myeloid lineage outputs seen in older humans might be reflected in an aging-related change in the potentialities of their *CD49f*⁺ cells using a modified 6-week LTC system (see section 2.4 ; Fig. 3.5A). This LTC assay was previously shown to detect these potentialities in CB *CD49f*⁺ cells at a high frequency, and at relative frequencies similar to those displayed by clonally tracked CB *CD49f*⁺ cells transplanted into immunodeficient mice (Knapp et al., 2019). In the present experiments, the lineage content of clones produced in these modified 6-week LTCs were assessed by flow cytometry and categorized as either “mixed” (neutrophil and/or monocytes (NM) and lymphoid), “NM”, “lymphoid”, or “lineage negative” (clones of CD45⁺ cells that were negative for the lineage markers assessed and listed in Table 2.4; Fig. 3.5B).

As found in the 8-week LTC-IC assays, there was no difference in the overall frequency of cells with detectable outputs in this 6-week assay system (Table 3.2). Examining the proportions of *CD49f*⁺ cells which produced detectable clones in this system, we similarly found that more of the CB *CD49f*⁺ cells produced only transient outputs (21%) than was seen from the young adult BM (3%) or aged adult BM (1%). This culminated in a modest but significantly different spectrum of lineage outputs from the *CD49f*⁺ cells from CB as compared to those from

either young or aged adult BM samples (pairwise Fisher's exact test, $P < 5 \times 10^{-8}$), but not between the latter 2. Most notably, the frequency of clonogenic *CD49f*⁺ cells that were able to produce lymphoid progeny (either alone or with NM cells) in the 6-week cultures did not decrease with increasing age of the donor, in fact they increased with the age of the donor (from 47% in the CB cells, to 59% and 68% in the BM of young and aged adult donors respectively).

3.2.5 Repopulating ability of *CD49f*⁺ cells from CB and adult BM is similar in a co-xenotransplantation assay.

A final set of *in vivo* xenotransplant experiments was then undertaken to compare the cell output properties of *CD49f*⁺ cells from 2 CB and 2 young adult BM donors (Table 3.3). Previous LDA of adult *CD49f*⁺ cells with repopulating activity in immunodeficient mice have reported a decrease in the frequency of these cells of ~5-40-fold compared to CB (Huntsman et al., 2015; Wang et al., 2019). As an alternative strategy, we adopted a co-transplantation design in which the "test" *CD49f*⁺ cells were mixed with GFP-transduced CB cells (derived from a large pool of normal CB *CD34*⁺ cells) with the expectation that these might serve to interact with or produce factors that might be critical to optimizing the differentiated cell output of limiting numbers of adult *CD49f*⁺ cells. To this end, sub-lethally irradiated NRG-W41 mice were transplanted with a combination of 300 *CD49f*⁺ cells, from either CB or young adult BM donors, mixed with 10^4 GFP-transduced CB cells (selected for GFP expression 2 days post-transduction) and the proportion of human chimerism in the mouse BM was assessed at weeks 4, 8, 12, 16, 20, and 30 (Fig. 3.6A & B).

All mice showing detectable repopulation from the GFP⁺ CB cells also contained detectable GFP⁻ progeny from the input *CD49f*⁺ cells. Overall levels of human GFP⁻ cells regenerated from CB and young adult BM *CD49f*⁺ cells were not significantly different at any time post transplant, although this assessment was also compromised by the extensive heterogeneity in the levels of engraftment observed in the individual mice in both groups in both pairs of experiments undertaken (Fig. 3.6C). These included a consistently detectable average, albeit individually variable, number of myeloid, B-lymphoid, and erythroid cells in the progeny of both sources of input *CD49f*⁺ cells (Fig 3.6D-F). No T cells were detected in any mouse for 20 weeks, however, at week 30 progeny of 1 CB and 1 young adult BM donor contained detectable, but low levels, of T cells. Interestingly, there was no correlation between the combined outputs from the CB *CD49f*⁺ cells with the GFP⁺ outputs in the same mice across all timepoints ($R^2=5.4 \times 10^{-4}$, $P=0.91$, Figure 3.6G), whereas the output of the young adult *CD49f*⁺ cells was highly correlated with the GFP⁺ cell outputs in the same mice ($R^2=0.56$, $P=5.5 \times 10^{-7}$, Fig. 3.6H). This suggests that the presence of the additional co-injected GFP⁺ CB cells may have a previously undefined positive effect (either directly or indirectly mediated) in promoting the regenerative activity of adult *CD49f*⁺ cells that is not required by *CD49f*⁺ CB cells themselves.

3.3 Discussion

The last decade has brought the identification of an extremely rare *CD49f*⁺ subset within both CB and adult sources that contains cells with the most prolonged hematopoietic regenerative activity (Belluschi et al., 2018; Huntsman et al., 2015; Knapp et al., 2017, 2018; Notta et al., 2011; Wang et al., 2019). The use of single-cell profiling techniques has also demonstrated extensive heterogeneity not only in the *CD49f*⁺ subset but the larger CD34⁺

stem/progenitor fraction (Belluschi et al., 2018; Buenrostro et al., 2018; Knapp et al., 2019; Velten et al., 2017; Zheng et al., 2018). These findings, in turn, have renewed interest and enabled attempts to characterize how the functional properties of these highly potent cells may change over time, both in comparison to analogous cells in model organisms and in the mechanisms regulating their proliferation and differentiation. In the studies described here, cells isolated from the PB or BM of healthy donors spanning 7 decades of age were subjected to a detailed phenotypic profiling and functional analyses of the cell output activities of their *CD49f*⁺ subset was assessed *in vitro* and *in vivo* at high resolution.

Somewhat expected was the large degree of inter-donor heterogeneity of several classically defined progenitor phenotypes comprising the *CD34*⁺ population even between donors of the same age group and sources of *CD34*⁺ cells. Nevertheless, analyses of relatively small numbers of individual samples allowed many significant age-related and age-independent differences to be discriminated. Unexpected was the consistently sustained proportion of *CD49f*⁺ cells as 1-2% of the entire *CD34*⁺ population over the full range of ages and sources of cells examined. This stands in contrast to previous studies of mouse and human samples where an increase in the representation of phenotypic HSCs as a function of donor age has been reported (Kuranda et al., 2011; Pang et al., 2011; Rossi et al., 2005). However, it should be noted that previous human studies used a broader phenotypic classification with a lower frequency of functional HSCs. Also unexpected was the finding that the lympho-myeloid output of *CD49f*⁺ cells manifested in both *in vitro* and *in vivo* settings designed to strongly elicit these potentialities was not diminished with age. This again contrasts with the results of previous studies in mice and humans indicating that lymphoid cell outputs decrease with advancing age (Nilsson et al., 2016; Pang et al., 2011; Rossi et al., 2005). However, at least in mice, the HSC appears to be the

stage at which this defect is sustained, but it is not manifested until a later stage of lymphoid restricted cell differentiation (Benz et al., 2012). Studies in humans have reported conflicting results regarding the changing proportions of lymphoid progenitors during aging, here we saw variation between some age groups and sources but nothing indicative of a specific age-related decrease (Kuranda et al., 2011; Nilsson et al., 2016; Pang et al., 2011). Interestingly, experiments with mice have indicated that the environment of the aged BM is less supportive of lymphoid production, and that lymphoid output from older hematopoietic cells can be partially restored by transplantation of “old” HSCs into younger hosts (Ergen et al., 2012) or in hosts given IGF1 (Young et al., 2021). Beyond the expected intra-donor heterogeneity of *CD49f*⁺ cells, we also found an unexpected association of the phenotypic properties examined here to correlate more strongly with whether the *CD49f*⁺ cells were present in the PB or BM rather than the age of the donor of the sample. Taken together, these new findings reflect the recognized challenges in reconciling differences between the mouse and human systems in identifying key shared properties of hematopoiesis. Additionally recognized is the still obligate reliance on relating findings to the entire CD34⁺ compartment that cannot take into account any absolute numerical changes in stem or progenitor cells related, for example, to a hypocellularity of the human BM that has been observed with advancing age (Ogawa et al., 2000).

Despite the relatively few markers examined in our UMAP comparison of human CD34⁺ phenotypes, we also observed a similar continuum of cells with different progenitor classes having overlapping distributions rather than forming into discrete clusters. This is consistent with many recent studies that have used an enlarged range of single-cell molecular profiling parameters (Buenrostro et al., 2018; Knapp et al., 2019; Velten et al., 2017; Zheng et al., 2018) reinforcing the concept of more heterogeneous differentiation trajectories than historically

envisaged (Knapp et al., 2019; Laurenti & Göttgens, 2018). One example confirmed here was a developmentally sustained preservation of the extensive heterogeneity in the CMP and GMP subsets likely reflective of their phenotypic classification isolating mixtures of cells with different lineage output potentials (Karamitros et al., 2018; Knapp et al., 2019; Notta et al., 2016). Analysis of different regions of the UMAP distribution identified several markers that suggest a movement of *CD49f*⁺ and MPP cells towards myeloid or lymphoid commitment. These include increased CD123 and CD10 expression, respectively as indicative of commitment to these lineages as predicted by their later specific association with the downstream progenitors of these lineages (Doulatov et al., 2010; Görgens et al., 2013; Manz et al., 2002). However, the regions with the highest levels of expression of these markers represent only a portion of the total GMP and Pre-B/NK progenitor populations suggesting that higher levels of expression of these markers may be representative of cells even more restricted to their respective lineages. Lower CD117 expression was also observed in cells in these outlying regions consistent with this marker playing an important role in earlier cell types (Kent et al., 2008; Thorén et al., 2008).

Interestingly, although no frequency difference was observed between *CD49f*⁺ cell content in the CD34⁺ compartment, those that were isolated from the BM were phenotypically different from those isolated from the PB regardless of donor age. The surface markers CD45, CD34, and CD90 were more highly expressed on *CD49f*⁺ cells from the BM than from the PB. Higher expression of CD34 and CD90 by BM *CD49f*⁺ cells may serve to aid *CD49f*⁺ cells to interact with or remain in the niche, due to their adhesion properties (AbuSamra et al., 2017; Barker et al., 2004). CD90 has also been indicated as a potential player in mediating HSC production of immature progenitors, with antibody inhibition of CD90 resulting in reduction of CFCs with high proliferative potential (Mayani & Lansdorp, 1994). Despite these phenotypic

differences, *CD49f*⁺ cells from CB and adult BM were similarly enriched for ~50% LTC-IC in our single-cell assay. By analyzing the input surface marker expression of *CD49f*⁺ cells we confirmed that the most highly proliferative CB clones detected in the 8-week LTC-IC assays had heightened expression of CD33, CD34 and CD90 (Knapp et al., 2018). However, only CD33 was similarly more highly expressed on the highly proliferative LTC-ICs from young adult BM. CD34 and CD90 levels were not predictive for the functionality of young or aged adult BM *CD49f*⁺ cells, perhaps due to our observation of these cells already having heightened expression of these markers as compared to CB *CD49f*⁺ cells. Perhaps heightened CD34 and CD90 levels on CB *CD49f*⁺ cells are indicative of cells that have recently entered circulation from the BM and have not yet reduced expression of surface proteins that are also involved in adhesion interactions. Parabiosis experiments in mice have demonstrated a consistent small proportion of HSCs that migrate through the blood to extramedullary tissues (Wright, 2001). Very recent work has also identified that these HSCs outside of the BM have upregulated gene sets involved in the actomyosin cytoskeleton suggesting these cells have alternative mechanical properties than those in the BM (Mende et al., 2020).

The observation of decreasing proportions of transient clones in our *in vitro* assays with increasing donor age is likely related to the overall delay when clonal outputs from 8-week LTC-ICs could be visualized. This is consistent with the output kinetics seen in the 6-week multi-lineage LTCs where a high proportion of clonogenic CB *CD49f*⁺ cells only produced progeny transiently, whereas these were more rarely seen emanating from clonogenic young or aged adult BM *CD49f*⁺ cells assessed in parallel. Previous reports of adult *CD49f*⁺ cells having a low frequency of and poor output from long-term repopulating cells *in vivo* (Huntsman et al., 2015; Wang et al., 2019) led us to develop a co-transplantation system where *CD49f*⁺ cells from single

CB or young adult BM donors were co-transplanted with GFP-transduced CB CD34⁺ cells into immunodeficient mice. We observed no difference in the total or specific lineage output from CD49f⁺ cells from CB or young adult BM donors over a 30-week period of assessment.

However, we saw a sharp contrast in that the overall output of the young adult CD49f⁺ cells was highly correlated with the output of the GFP-transduced CB cells in the same mice while no such correlation was observed for the CB CD49f⁺ cells. Together, these results suggest a differential requirement of conditions that support an optimal regenerative activity from adult as compared to neonatal CD49f⁺ cells. This in turn highlights potential inefficiencies of current immunodeficient mouse strains for comparing the innate stem cell properties of differently aged sources of human hematopoietic cells.

In summary, the results presented here reveal the relative stability of the phenotypes present in the CD34⁺ compartment of the PB and BM of healthy humans from birth to the 7th decade of life and in the unexpected retention of the functionally assessed B-lymphoid and myeloid output potential of the CD49f⁺ subset they contain. We also demonstrate clear age-associated changes in the speed with which their differentiated cell outputs are activated in stromal-cell-containing co-cultures, the frequency of CD49f⁺ cells which produce transient clones under these conditions *in vitro*, and the different dependence of their regenerative activities *in vivo* on the presence of other types of normally regenerating human hematopoietic cells. Taken together, these findings delineate a new spectrum of HSC functional properties that are differentially affected by aging.

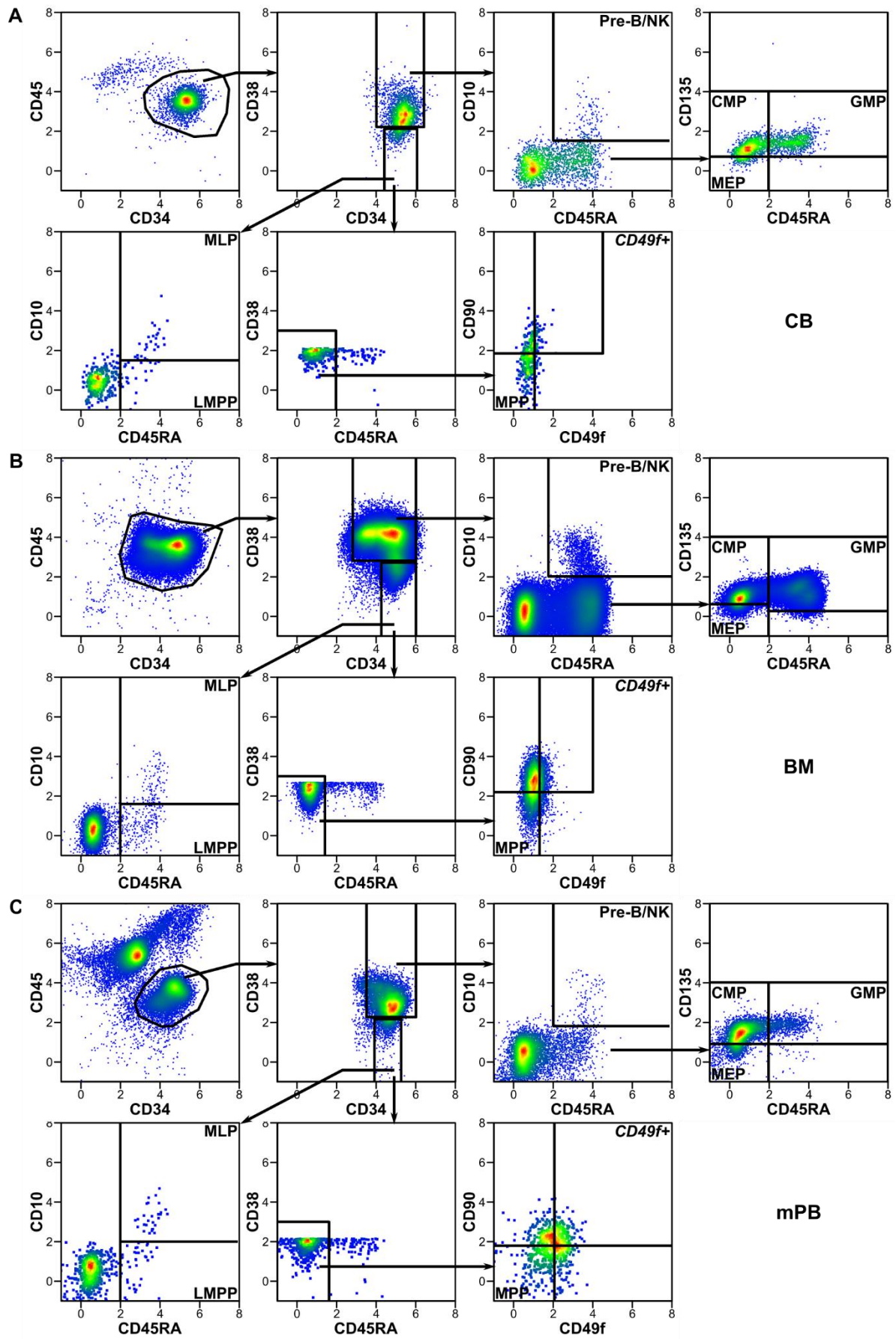


Figure 3.1 Representative gating of CD34+ subsets from different sources of normal human blood cells. Example gating of indicated CD34+ stem and progenitor subsets for CB (A), BM (B), and mPB (C). Axis scales for fluorescent markers are represented as $\text{asinh}(x/150)$.

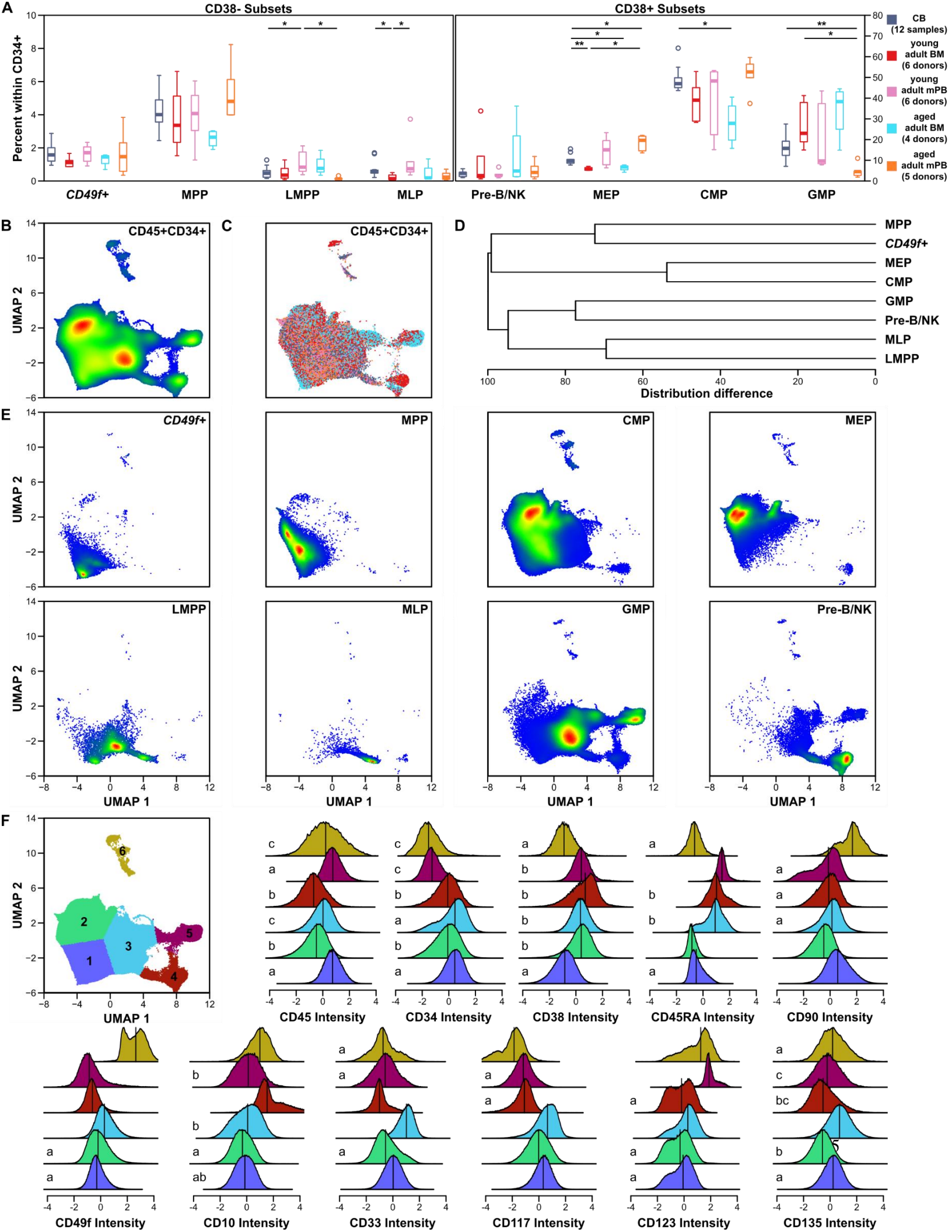


Figure 3.2 Phenotypic heterogeneity of the normal human CD34+ compartment. A) Frequency of CD34+CD38- progenitor (*left*) and CD34+CD38+ progenitor (*right*) subsets in total CD34+ cells from different sources of normal human blood cells (Holm-corrected pairwise Wilcox tests, * $P < 0.05$, ** $P < 0.01$). B) Pseudocoloured 13-parameter UMAP representation of pooled CD45+CD34+ cells from different sources. C) Visualization of 10 000 CD45+CD34+ cells from each source. D) Hierarchical clustering of phenotypic subsets based on pairwise differences in their density distributions in UMAP space. E) Pseudocoloured distributions of indicated phenotypic subsets across UMAP space. F) Relative intensities of fluorescent markers between K-means identified UMAP clusters. Letters beside histograms indicate groups which were not significantly different from each other.

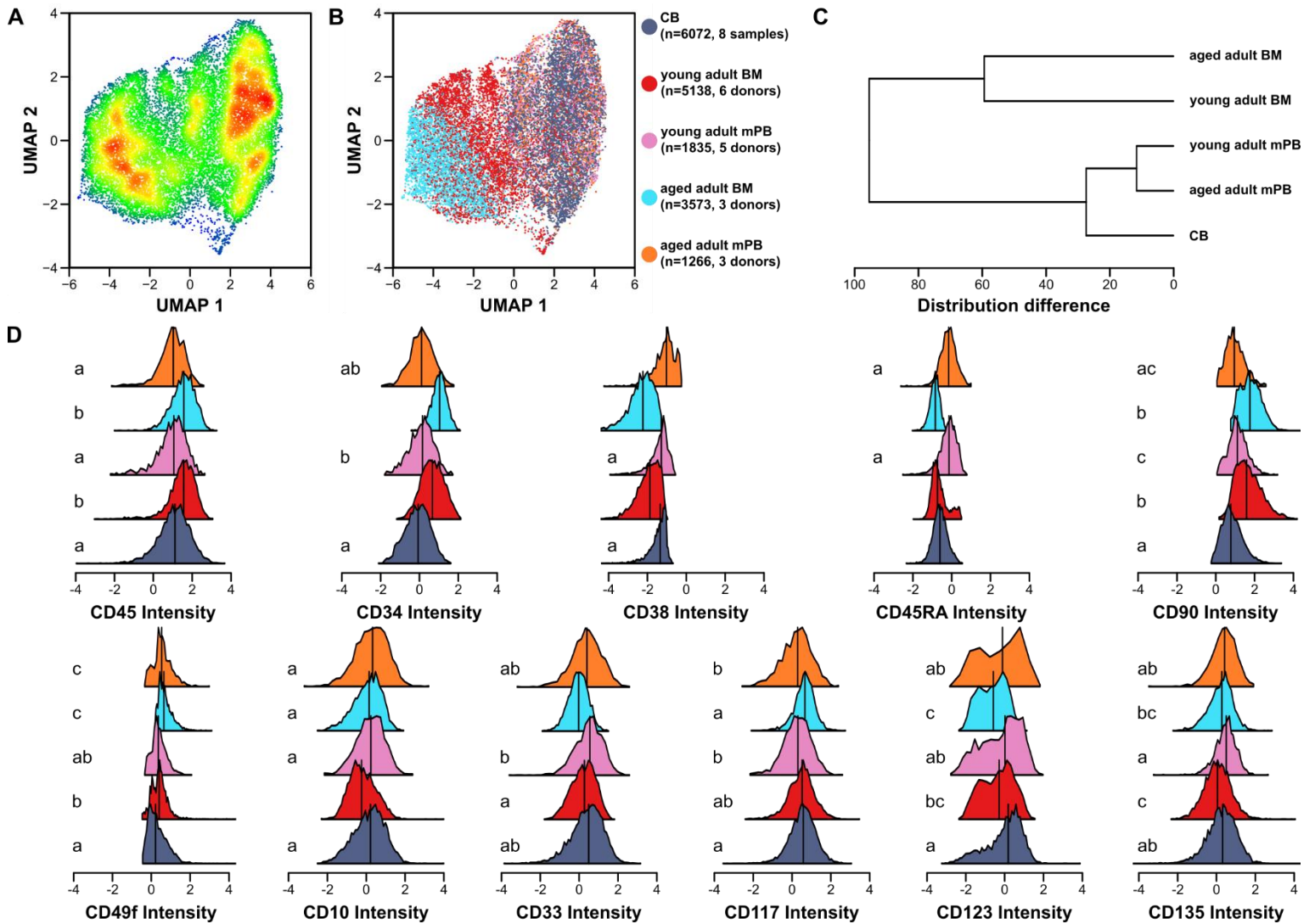


Figure 3.3 Phenotypic heterogeneity of $CD49f^+$ cells according to donor age and source.

Pseudocoloured (A) and source-specific (B) 13-parameter UMAP representations of pooled $CD49f^+$ cells from different normal donors. C) Hierarchical clustering of $CD49f^+$ cells from each source based upon pairwise differences in their density distributions in UMAP space. D) Relative intensities of fluorescent markers between sources of $CD49f^+$ cells. Letters beside histograms indicate groups which were not significantly different from each other.

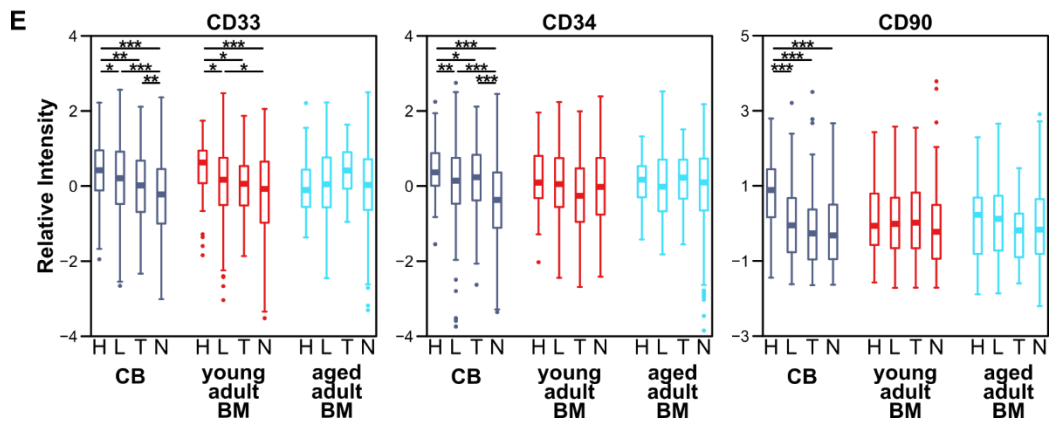
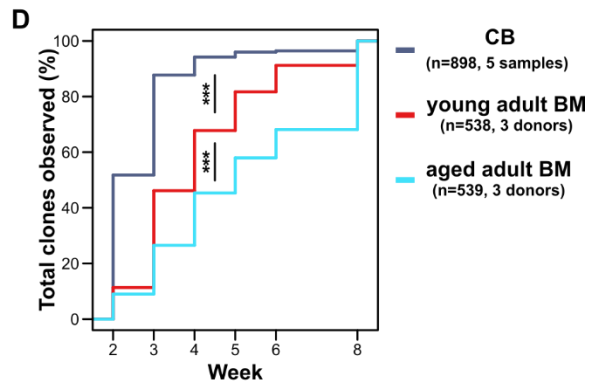
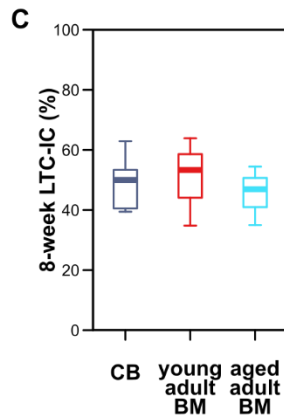
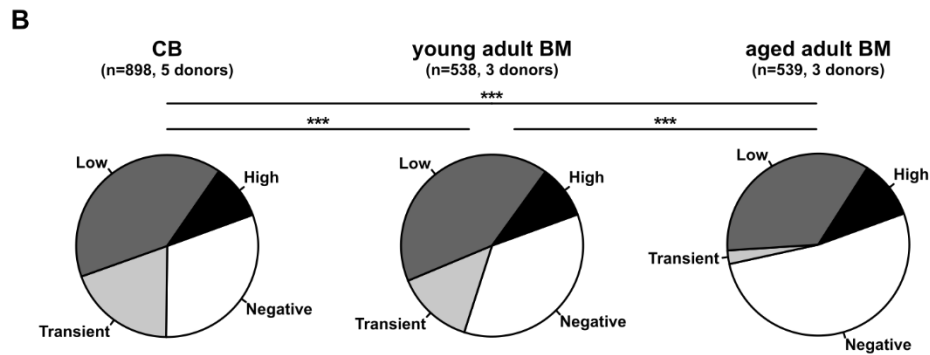
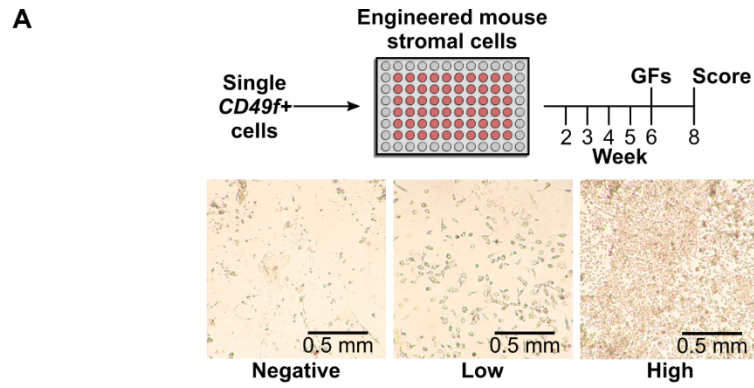


Figure 3.4 High LTC-IC activity of *CD49f*⁺ cells from different sources. A) Experimental design of single-cell LTC-IC assay. B) Distribution of clonal outputs from each donor age-group (***P*<0.001, Fisher's exact test). C) Relative intensities of CD33 (*left*), CD34 (*centre*), and CD90 (*right*) expression on *CD49f*⁺ cells with different clonal outputs (**P*<0.05, ***P*<0.01, ****P*<0.001, Holm-corrected Student's t-test). D) Proportion of *CD49f*⁺ cells that are 8-week LTC-IC from each age-group. E) Empirical cumulative distribution of clonal appearance over time (***P*<0.001, Komoglerov-Smirnov test).

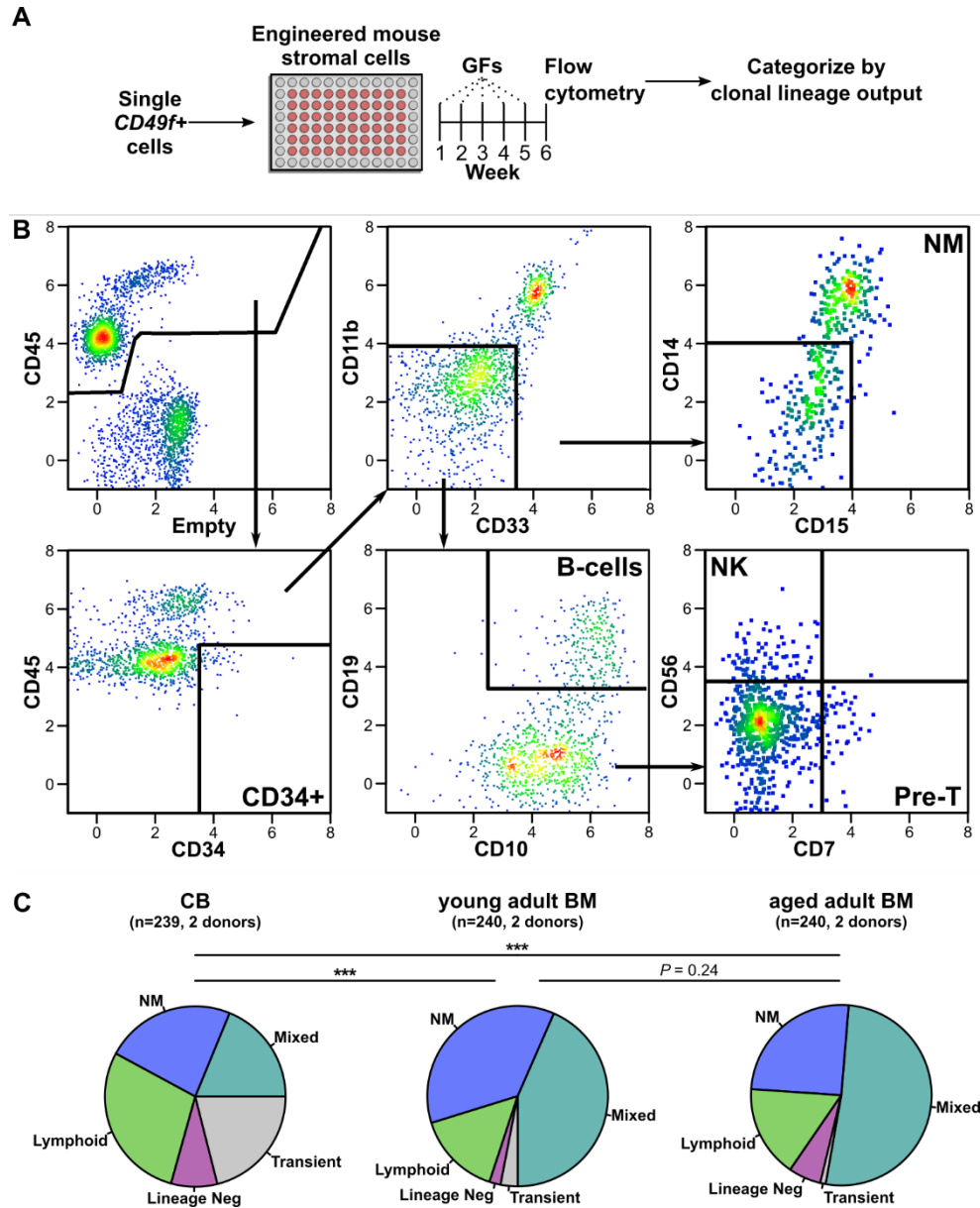


Figure 3.5 Age-independent lympho-myeloid differentiation potential of *CD49f*⁺ cells

revealed in single-cell cultures. A) Experimental design of single-cell multilineage LTC assay.

B) Representative gating strategy of indicated lineages following harvest.

C) Combined clonal outputs of *CD49f*⁺ cells from each indicated group (***) $P < 0.001$, Fisher's exact test).

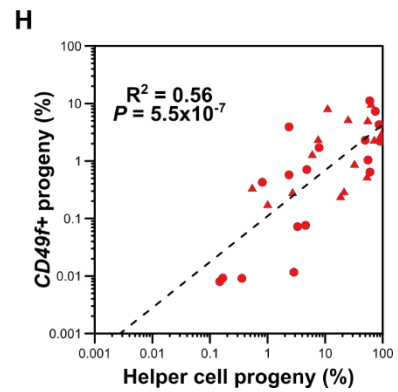
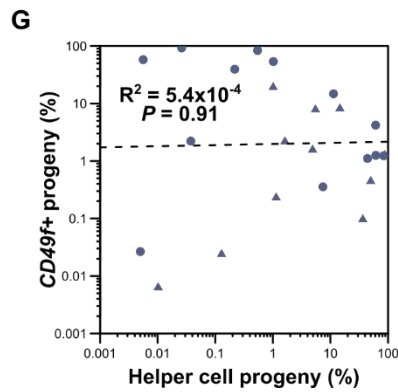
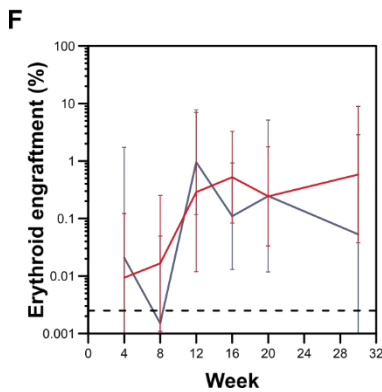
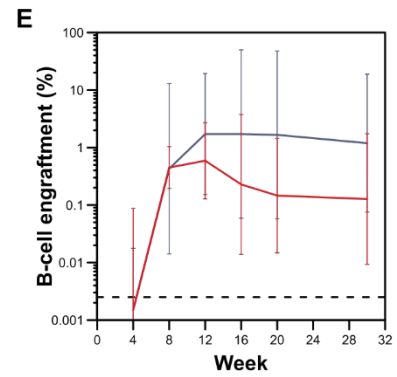
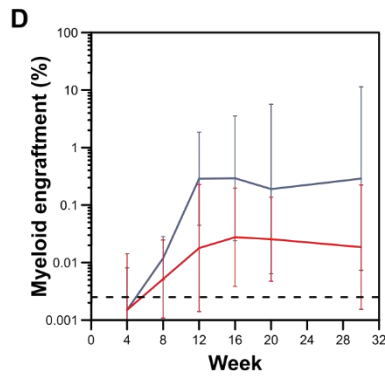
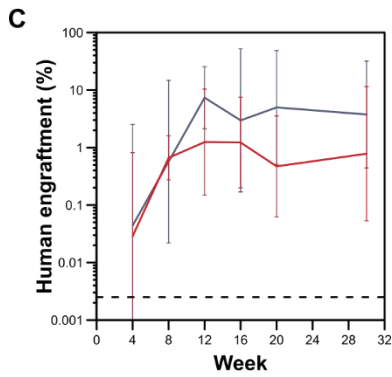
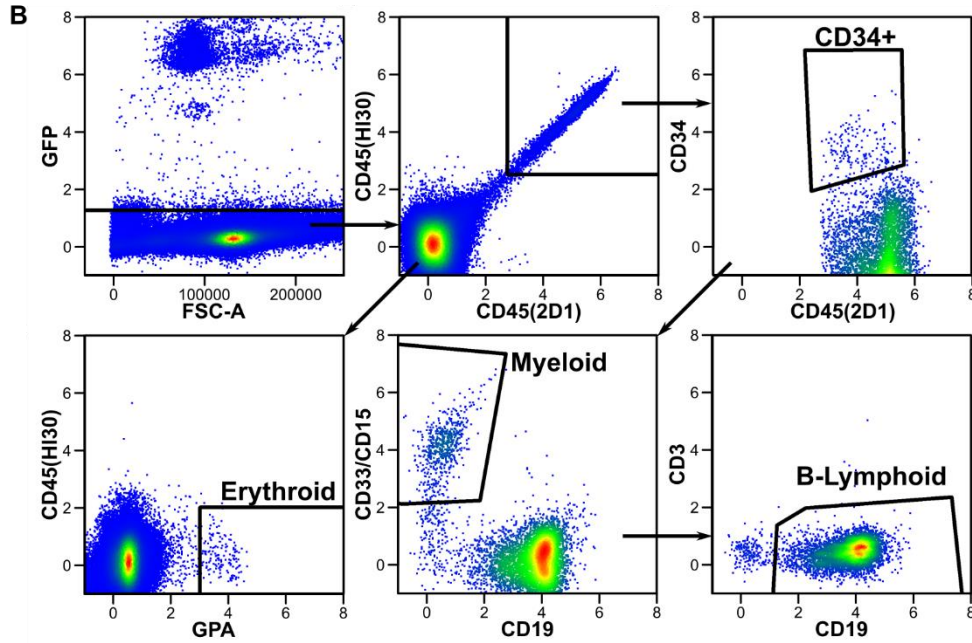
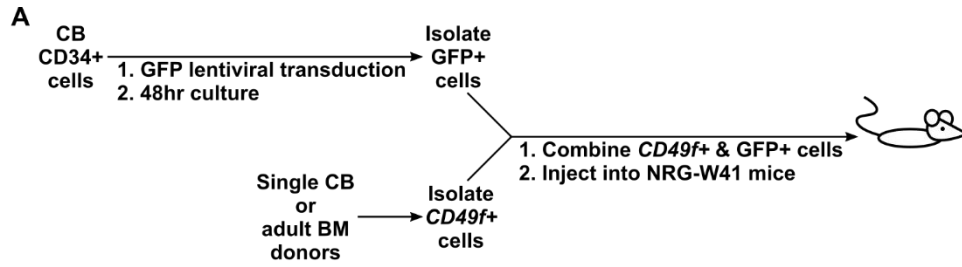


Figure 3.6 Similar *in vivo* repopulating ability of CB and BM *CD49f*⁺ cells revealed in a co-transplant assay. A) Experimental design of co-transplantation experiment. B) Representative flow cytometry analysis of BM aspiration from an engrafted mouse. Overall percentages of GFP-human (C), myeloid (D), B-lymphoid (E), and erythroid (F) cells from input CB (navy) and young adult BM (red) *CD49f*⁺ cells in viable mouse BM. Lines indicate geometric mean of all mice in each group. Bars indicate geometric mean*geometric standard deviation and geometric mean/geometric standard deviation. Linear correlation of GFP- chimerism with GFP+ chimerism for CB (G) and young adult BM (H). Points indicate an individual mouse at a single timepoint. Symbols indicate mice transplanted with different single donors.

Table 3.1 Summary of donor specific outcomes in LTC-IC assays

Sample	Age	Group	Number of cells			
			Negative	Transient	Proliferative	Highly Proliferative
1	NA	CB	72	35	65	8
2	NA	CB	63	46	67	4
3	NA	CB	52	37	119	32
4	NA	CB	45	10	50	13
5	NA	CB	44	46	59	31
6	29	Young adult BM	90	26	44	18
7	31	Young adult BM	35	30	102	13
8	36	Young adult BM	66	18	76	20
9	53	Aged adult BM	83	12	70	14
10	61	Aged adult BM	82	0	62	36
11	56	Aged adult BM	115	2	57	6

Table 3.2 Summary of donor specific outcomes for *in vitro* lympho-myeloid assays

Sample	Age	Group	Number of cells					
			Negative	Transient	NM	Lymphoid	Lin Neg	Mixed
1	NA	CB	62	6	16	13	7	16
2	NA	CB	45	22	15	25	4	9
3	33	Young adult BM	84	1	16	3	2	14
4	31	Young adult BM	57	2	20	12	0	29
5	58	Aged adult BM	50	0	14	12	3	40
6	56	Aged adult BM	86	1	12	5	3	13

Table 3.3 Summary of donors and mice used for *in vivo* transplant analysis

Sample	Age	Group	Number of mice					
			Week 4	Week 8	Week 12	Week 16	Week 20	Week 30
1	NA	CB	2	2	2	2	2	2
2	NA	CB	2	2	2	2	2	2
3	33	yBM	3	3	3	3	3	3
4	36	yBM	3	3	3	3	3	2 [†]

[†]Mouse died prior to week 30.

Chapter 4: Aging delays proliferation and cell-cycle transit rates of normal human *CD49f*⁺ cells.

4.1 Introduction

Hematopoiesis is a hierarchically organized process that supports the lifelong production of mature blood cells from relatively small numbers of cells with considerable self-sustaining ability. The stepwise changes that accompany and regulate this process in HSCs and their immediate progeny at the single-cell level are now recognized to be complex and highly variable, even when restricted to analysis at a single timepoint (Laurenti & Göttgens, 2018). However, factors that alter the cycling dynamics of HSC appear to be related to their functional potential. Label-retention studies in mice have demonstrated that throughout adult life under steady-state conditions, some HSCs are continuously, but infrequently, recruited from a quiescent state into cycle (Foudi et al., 2009; Morcos et al., 2020; Wilson et al., 2008) through HSC-intrinsic regulatory mechanisms and their interactions with specific environmental cues (Hao et al., 2016; Pietras et al., 2011). Intrinsic regulation of HSC proliferation and self-renewal is also controlled developmentally. Fetal mouse HSCs are highly proliferative and transition to an adult-like cycling activity abruptly between 3 and 4 weeks after birth (Bowie et al., 2007). A similar abrupt change in the cycling activity of HSCs in baboons and humans has been inferred to occur in the first 3 years of life based upon the rate of telomere decay measured in the short-lived neutrophils they ultimately produce (Baerlocher et al., 2007; Sidorov et al., 2009). In addition to the proportion of cycling HSCs found to be changed postnatally, the time required to complete a first division by HSCs when they are maximally stimulated *in vitro* has been found to correlate with the longevity of their regenerative potential in functional assays (Dykstra et al.,

2006). Thus, HSCs with a short-term output activity exit quiescence more rapidly and complete a division sooner than those with longer-term output potentials (Bowie et al., 2007; Laurenti et al., 2015; Passegué et al., 2005). However, this correlation has been reported to break down when mouse HSCs from older donors were examined. As reviewed in Chapter 1, aging HSCs have several altered properties including an observed delay in aged mouse HSCs completing first and second divisions *in vitro* compared to their younger counterparts (Flach et al., 2014).

Interestingly, as also reviewed in Chapter 1, the products of a large number of genes have now been reported to be significant intrinsic contributors to the regulation of adult HSC self-renewal responses to proliferative stimuli (Wilkinson et al., 2020), including some that are developmentally controlled (such as *Sox17*; Kim et al., 2007) and the *Lin28-Let7-Hmga2* axis (Cesana et al., 2018; Copley et al., 2013). Nevertheless, very little is known about the mechanisms responsible for changes that accompany the onset of “old” age, particularly in humans. This paucity of human information is partially attributable to the very low number of HSCs (phenotypically characterized here as *CD49f*⁺ cells) that can be practically isolated from a single donor source. This coupled with the large heterogeneity that has thus far been observed in these cells (Belluschi et al., 2018; Knapp et al., 2016, 2017, 2018, 2019; Notta et al., 2016; Velten et al., 2017) then requires the need for systems that would allow their sequential proliferative and dynamic molecular responses to be tracked at a single-cell level. To overcome these hurdles, we used a system that enabled the proliferative responses of thousands of individual *CD49f*⁺ cells to be tracked over several days coupled with the development of a procedure for linking cell-cycle stage with multiplexed molecular single-cell analysis. We then assessed the GF requirements for survival and proliferation timing with advancing age and specific signaling pathway activation.

4.2 Results

4.2.1 Demonstration of a progressive age-related delay in the GF-stimulated kinetics of *CD49f*⁺ cell division *in vitro*

To compare responses of *CD49f*⁺ cells from different sample sources from donors of increasing age, we again grouped and defined them as neonatal (CB), from young adults (mPB or BM) for donors 18-45 yr old, and from aged adults (mPB or BM) for donors >50 yr old. To compare the GF-dependent survival and mitogenic responses of *CD49f*⁺ cells from these 3 different age groups, single FACS-purified cells were deposited into the individual wells of Terasaki plates preloaded with SFM + 300 µg/mL SF + 300 µg/mL FLT3L + 60 µg/mL IL3 (SFM + 3GF, Fig. 4.1A), a condition previously shown to maximally stimulate the subsequent proliferation of adult BM CD34⁺CD38⁻ cells with maximum retention of 6-week LTC-IC activity (Zandstra et al., 1997). In the present experiments, high levels of survival over a 7 day monitoring period were displayed by all sources of *CD49f*⁺ cells cultured under these conditions (85% by CB and young adult cells and 72% by cells from aged adults; Fig. 4.1B). In contrast, the time preceding the first division of the same cells demonstrated a highly significant and progressive increase with increasing donor age (Fig. 4.1C, all pairwise Holm-corrected $P < 1 \times 10^{-23}$). Specifically, the median time to a first division displayed by the CB *CD49f*⁺ cells was 57 hr, increasing to 75 hr for the young adult cells, and to 90 hr for those from adults >50 yr. Notably, this age-associated delay in the initial mitogenic response of isolated *CD49f*⁺ cells was not restricted to the first division, but was also evident as an 8 hr increase in the median time to complete a second and third division when the results for CB *CD49f*⁺ cells were compared to those for *CD49f*⁺ cells isolated from young or aged adult donors (Fig. 2.4D/E; Holm-corrected

Wilcox tests $P < 1 \times 10^{-19}$). However, there was no continuing difference between the young adult or aged adult *CD49f*⁺ cells. Taken together, these findings are consistent with the expectation of an early postnatal alteration in the cycling dynamics of HSCs (Baerlocher et al., 2007; Bowie et al., 2006, 2007; Copley et al., 2013; Sidorov et al., 2009) and suggest on-going alterations to cycling regulation during aging.

4.2.2 Development of a system for monitoring paired cell cycle state and molecular changes in individually tracked cells

We next sought to define the kinetics of cell cycle entry and progression associated with the different times to sequential divisions exhibited by individual *CD49f*⁺ cells isolated from donors of different ages. To this end, we developed a system that would allow for multiple-parameter phenotyping on single cells after defined periods of culture in SFM + 3GF using an approach for tethering nonadherent cells to a SA-coated plate surface via an interaction with a biotinylated antibody targeting a prominent antigen on the cells of interest (Loeffler et al., 2018). Here the antibody used was an α -CD44 antibody which we found allowed viable *CD49f*⁺ cells from all sources to be captured and retained post-fixation on the bottom of the wells of 384 well plates through multiple manipulations. Preliminary experiments showed that this capture strategy would remain stable through at least 3 rounds of fluorescent imaging with different antibodies labeled with the same Alexa Fluor dyes that could be quenched in between each round of labeling and imaging (Fig. 4.2 A/B) by exposure of the cells to a non-denaturing base-catalyzed oxidation of the Alexa Fluor structure (Lin et al., 2015). However, as a consequence of multiple rounds of imaging, small alterations in the location of each event were introduced due to minor variations in plate positioning in the holding adapter of the microscope stage. Therefore, to

ensure that the molecular information from sequential images were applied to the same events, we used landmark features identified in each well by the SIFT algorithm in FiJI to calculate well-specific affine transformations to be applied to correct the coordinates of events in the sequential imaging panels and finally link these together with the same events in the original imaging cycle by identifying nearest neighbour pairs in Euclidian space (Fig. 4.2C). Events were matched only a single time and high match quality was maintained by setting maximum distances for which event matching was possible. Events lost between imaging cycles (such as a cell that became detached) were removed from downstream analysis, such that fluorescent information from every imaging cycle was available for all events included in the final analyses.

Resultant fluorescence profiles for each individual event were then scaled within each experiment and converted to a flow cytometry-like data structure to allow for visualization and 2D gating of populations. This conversion allowed for the removal of cell-sized debris from analysis by first calculating an ‘autofluorescence’ and ‘circularity’ parameter for each event and removing outliers. Cells were then further enriched based on DAPI (DNA content) and CD45 fluorescence (Fig. 4.2D). Use of these features showed the proportion of cells retained at each imaging cycle in relation to the initial imaging cycle was still very high after the second and third imaging cycles (95% and 86%, respectively; Fig. 4.2E).

4.2.3 Adult CD49f+ cells display an elongated G₁-phase

Our multiple-parameter phenotyping system was then used to quantify the time-dependent changes in 7 features (DNA content, CD45, CDK2, CDK6, Ki67, pRb, and EdU) exhibited by 6850 individually analyzed cells obtained from a total of 6 donors (3 CB and 3

young adult BM; Table 4.1, Table 4.2). Since large differences were evident in the division kinetics of CB and young adult donors (Fig. 4.1B) we compared cells from these two age-groups with the assumption that differences detected would be maintained or amplified in cells from older donors. In these experiments the effects of exposing the cells to a high and low concentration of the same 3 GF cocktail were also examined (Fig 4.2A; discussed further in section 4.2.5). To visualize the movement of cells through the cell-cycle, the data was reduced to a 2D format using the UMAP algorithm (Becht et al., 2019; McInnes et al., 2018; Fig. 4.3A). Application of K-means clustering separated the data thus visualized into 3 regions (Fig. 4.3A *bottom-right*) that could then be assigned to the different phases of the cell-cycle based on the relative fluorescence of the markers defining them. For example, the region defined as G₀ was marked by a predominance of cells displaying very low levels of DAPI, Ki67, pRb, and EdU and the G₁ region as cells also with low levels of DAPI and EdU but showing increased levels of Ki67 and pRb. In contrast, the S/G₂/M region was defined by cells with significant levels of EdU fluorescence (indicative of active DNA replication) and increasing levels of DAPI, Ki67, and pRb. The proportion of cells in each of these 3 regions within this overall UMAP distribution were determined at each time point for each culture condition analyzed, and from this a time course pattern of the cell cycle progression exhibited by the *CD49f*⁺ and *CD34*⁺*CD38*⁻ cells obtained from the CB and young adult BM donors was generated (Fig. 4.3B). As expected from previous studies pointing to the common quiescent state of these cells at the time of their isolation (Laurenti et al., 2015; Wilpshaar et al., 2000), the majority of the *CD49f*⁺ and *CD34*⁺*CD38*⁻ cells used to initiate the present time-course cultures were found in the G₀ region of the general UMAP distribution (Fig. 4.3B). Within 24 hr of exposure to the highest 3GF concentration, approximately half of all the CB and young adult BM *CD49f*⁺ cells had

transitioned into G₁ but, after another 18 hr (a total of 42 hr), the majority of CB *CD49f*⁺ cells had progressed further into S/G₂/M whereas most of those obtained from young adults were still in G₁ (Fig. 4.3B *left*; Holm-corrected Kruskal-Wallis test $P=2.0 \times 10^{-9}$). However, within a further 22 hr (a total of 64 hr), most of these had transitioned to S/G₂/M indicating a prolongation of their first cell cycle transit time by 14-22 hr (Holm-corrected Kruskal-Wallis test $P=1.2 \times 10^{-8}$). These results agree with the overall observed time required for these cells to complete a first division as determined independently by direct visualization (Fig. 4.1C). Taken together, these results indicate that the longer time required by young adult *CD49f*⁺ cells to complete a first division in comparison to CB *CD49f*⁺ cells is due to an increased length in the time they require to complete G₁ rather than an increased time required for exiting G₀. Interestingly, the patterns for cell cycle progression kinetics were maintained between the *CD49f*⁺ and CD34⁺CD38⁻ cells (Fig. 4.3B *right*), suggesting that the prolonged cell cycle transit features of young adult cells seen in comparison to CB cells are developmentally and not differentiation state-determined.

We next asked if and how these observed developmentally associated differences in G₁ duration exhibited by *CD49f*⁺ cells under maximally stimulated mitogenic conditions might be related to differential changes in the levels of specific regulators. Among those examined, CDK6, a known regulator of the G₀ to G₁ transition of human HSCs (Laurenti et al., 2015) and early G₁ progression, maintained an equivalent or slightly higher median expression in young adult *CD49f*⁺ cells than in CB *CD49f*⁺ cells throughout a 64 hr period of follow-up, suggesting a difference in the priming requirements of CB and young adult for entry and progression through G₁ (Fig. 4.3C). Although the baseline level of Ki67 in young adult *CD49f*⁺ cells appeared higher than in CB *CD49f*⁺ cells, the levels of Ki67, pRb, and CDK2 (a regulator of the G₁ to S-phase transition), were all markedly lower in the young adult *CD49f*⁺ cells at 42 and 50

hr. Therefore, factors that control their expression appear to be involved in the mechanism that delays but does not arrest the ability of young adult *CD49f*⁺ cells to enter S-phase by comparison to CB *CD49f*⁺ cells. The differences in the patterns of expression of the same cell-cycle regulators exhibited by the CD34⁺CD38⁻ cells were also generally consistent with those displayed by the *CD49f*⁺ cells (Fig. 4.3D) This finding therefore reinforces the concept of a developmentally regulated change in the mechanism(s) that control cell cycle transitions that are operative in primitive human hematopoietic cells and extend downstream of the HSC compartment.

4.2.4 Proliferation but not survival responses of adult *CD49f*⁺ cells are more sensitive to reduced GF stimulation than CB *CD49f*⁺ cells

We next sought to determine whether the donor age of the *CD49f*⁺ cells would affect their mitogenic requirements and, if so, how these might correlate with changes in their rate of entry into and passage through a first cell cycle. For this, we chose to examine these parameters under conditions of decreasing 3GF concentrations over 5 orders of magnitude. In a first series of experiments, we simply tracked the survival and completion of sequential divisions undertaken by individual *CD49f*⁺ cells from CB and adult donors deposited into Terasaki plates over a 7-day period. Survival was maintained at high levels (>75%) for all sources of cells down to a 100-fold reduction in the highest 3GF concentration, but then steeply decreased as the 3GF concentration was further reduced (Fig. 4.4A). Although the aged adult cells had a small increase in their ED50 (0.19% 3GF compared to 0.11% and 0.09% for CB and young adult cells, respectively), the overall rate at which survival support was lost was very similar between the *CD49f*⁺ cells obtained from donors of different ages. In sharp contrast, the level of 3GFs

required to stimulate ≥ 1 *CD49f*⁺ cell division within 7 days was highly significantly different between the CB and adult (ED50 values differing ~3- to 5-fold for young and aged adults respectively ($P=1.7 \times 10^{-5}$ and 1.5×10^{-17}); Fig. 4.4B). However, no additional difference between the ED50 of young and aged adult *CD49f*⁺ cells was detected ($P=0.13$), suggesting that this change in the mechanisms regulating the mitogenic responses of primitive hematopoietic cells occurs developmentally prior to adulthood.

These experiments further revealed an even greater age-associated change in the time required by *CD49f*⁺ cells to complete a first division when exposed to reduced growth factors (Fig. 4.4C). For example, the 15-hr increase in time taken by CB *CD49f*⁺ cells to complete a first division when exposed to a 100-fold dilution of the 3GF cocktail (72 hr vs 57 hr), was increased to 39 hr (116 hrs vs 77 hrs) and to 58 hr (143 hrs vs 85 hrs) in the *CD49f*⁺ cells obtained from the young and older adults, respectively. However, this estimate for the older source of *CD49f*⁺ cells is likely an underestimate since less than 50% of the viable cells completed a division within 7 days in these reduced 3GF cultures. In fact, the number of divisions completed by all sources of *CD49f*⁺ cells cultured under high (Fig. 4.4D) and low (Fig. 4.4E) 3GF conditions remained heterogeneous. Nevertheless, the average values for the adult *CD49f*⁺ cells were consistently lower than those exhibited by the CB *CD49f*⁺ cells when these were compared for the same 3GF exposure conditions (Holm-corrected pairwise Kruskal-Wallis tests $P < 1 \times 10^{-17}$). For example, at the highest 3GF concentration tested, ~80% of the CB *CD49f*⁺ cells completed >5 divisions (>32 cells/clone) within 7 days, whereas only 20% of young or aged adult *CD49f*⁺ cells passed this threshold, and at the 1% 3GF condition, 77% of CB *CD49f*⁺ cells completed >2 divisions whereas this was reduced to 20% and 10% for the young and aged adult *CD49f*⁺ cells respectively.

Given the exaggerated differences in proliferation kinetics displayed by CB and adult *CD49f*⁺ cells at low 3GF, it was of interest to determine if this could be associated with specific effects on their rate of entry into or progression through the cell cycle. Accordingly, a parallel set of experiments were undertaken to analyze these parameters in *CD49f*⁺ and CD34⁺CD38⁻ cells exposed to a 1% 3GF concentration (Fig. 4.2A). The proportion of cells from each source present in the different regions of the 2D UMAP distribution (Fig. 4.3B) indicated that the majority of young adult *CD49f*⁺ cells exposed to the reduced 3GF cocktail were unable to transition into S/G₂/M even after 64 hr (Fig. 4.5A, *left*). Since ~70% of these cells (like their CB counterparts) were found to have entered G₁ within 24 hr, the delay in their completing a first division can be attributed to their failure to progress further for at least 40 additional hours. Moreover, even after 64 hr, 33% of the young adult *CD49f*⁺ cells continued to remain in G₀ compared to only 12% of CB *CD49f*⁺ cells. These numbers match well with the observed 29% of young adult *CD49f*⁺ cells that remained viable but did not divide within the full 7-day period of being tracked in the 1% 3GF cultures (Fig. 4.4B). Therefore, it appears that this level of 3GF stimulation is sufficient to maintain the viability of a prominent subset of young adult *CD49f*⁺ cells, but insufficient to induce their exit from G₀. Similar trends were observed in the co-examined CD34⁺CD38⁻ subset albeit with a greater proportion of young adult cells transitioning to S/G₂/M by 64 hrs (Fig. 4.5A, *right*). Parallel analyses of specific regulators showed the levels of CDK2, Ki67, and pRb were also consistently lower in young adult *CD49f*⁺ and CD34⁺CD38⁻ cells when compared to their similarly cultured CB counterparts between 42 and for up to 64 hr in cultures containing the 1% 3GF cocktail (Fig. 4.5B/C).

Together, these observations describe a model wherein adult *CD49f*⁺ cells exposed to a strong mitogenic stimulus exit G₀ at the same rate as CB *CD49f*⁺ cells but spend longer in G₁

before entering S-phase resulting in a ~20 hr longer median time to complete a first division than CB *CD49f*⁺ cells (Fig. 4.5D). Exposure to a minimal stimulus that sustains extensive viability, reveals an increasing age-associated vulnerability in the *CD49f*⁺ (and downstream *CD34*⁺*CD38*⁻) cells to mitogen-sensitive mechanisms that regulate progression through G₁ (Fig. 4.4C).

4.2.5 Adult *CD49f*⁺ cells display lower activation of AKT and β -catenin following exposure to a strong GF stimulus.

To further explore the mechanistic basis of the aging-associated differences in cell-cycle progression exhibited by CB and adult *CD49f*⁺ cells subjected to strong and weak mitogenic stimuli (high and low 3GF concentrations), we designed experiments to examine their matched levels of activation of multiple downstream signaling pathways. To this end, we cultured bulk suspensions of CB and young adult *CD34*⁺ cells in SFM for a total period of 3 hr during which the cells were also exposed to the 3GF cocktail for the last 0, 5, 15, or 30 min immediately prior to fixation (Fig. 4.6A). We also used a fluorescent barcoding system to label the cells exposed to each of these different conditions so that they could then be pooled prior to processing and analysis to reduce technical variability (Krutzik & Nolan, 2006; Fig. 4.6B). *CD49f*⁺ cells were identified as previously within each CB or young adult donor (Fig. 4.6C) and the relative median shift of each stimulation timepoint was compared to that of the corresponding unstimulated fraction contained within the same sample. Previous investigation of CB *CD49f*⁺ signaling activation in response to GF stimulation indicated the STAT5, ERK1/2, AKT, and β -catenin pathways would be anticipated targets (Knapp et al., 2016). *CD49f*⁺ cells from both CB and young adult donors displayed robust activation of AKT and STAT5 following 3GF stimulation

(Fig. 4.6D, bootstrapped P values <0.05). CB $CD49f^+$ cells displayed stronger activation of AKT at each examined timepoint than the young adult $CD49f^+$ cells, sustaining activation of this pathway above baseline for at least 30 min. Activation of ERK1/2 at the tested timepoints was low, with CB $CD49f^+$ cells showing only a small shift at 5 min. Interestingly, β -catenin activation was observed only in CB $CD49f^+$ cells within 30 min. Targeted activation of β -catenin (through inhibition of GSK3) was found previously to stimulate proliferation of CB $CD49f^+$ cells suggesting that activation of this pathway has a pro-mitogenic effect (Knapp et al., 2016). Given that some of the effects on cell-cycle transit were also present outside of the $CD49f^+$ compartment, we also examined the activation of these same pathways in CB and young adult $CD34^+CD38^-CD45RA^-$ cells (Fig. 4.6E). Patterns of activation were similar in this downstream population with CB cells having slightly higher and more sustained AKT activation. However, no significant activation of ERK1/2 or β -catenin was observed in either the CB or young adult donor sources of these predominantly more differentiated cell populations. STAT5 activation in them also occurred later than was observed in the $CD49f^+$ cells. These results suggest that the cell cycle control machinery in $CD49f^+$ cells from all sources may be more primed than the $CD34^+CD38^-CD45RA^-$ cells. In addition, the age-independent robust activation of STAT5 in $CD49f^+$ cells exposed to a stimulus that has profound effects on mitogenesis suggests this is likely not the key element of the exacerbated requirements of adult $CD49f^+$ cells. In contrast, the higher and more sustained activation of AKT and β -catenin within 30 min of 3GF stimulation of CB $CD49f^+$ cells may serve as a future clue to their different biological responses (Fig. 4.6F).

4.3 Discussion

Identification of the *CD49f*⁺ phenotype as one that is highly enriched in cells with the functional properties used to define human HSCs is allowing more direct measurements of the mechanisms that control the behaviour of these cells than has been previously possible. Here we exploited the use of this phenotype to undertake the first direct analyses of their age-associated responses to GF stimuli. We report a maintenance of *CD49f*⁺ survival programs and a progressive age-dependent delay in division kinetics and an associated age-determined decline in the rapidity with which they can initiate a mitogenic response due to alterations in the mechanisms that control their ability to transition from G₁ to S/G₂/M. These conclusions were derived from two related methodologies that were refined to enable thousands of single *CD49f*⁺ cells purified from different human blood and BM samples to be consecutively tracked for varying times under different conditions of GF stimulation. The first set-up was designed to enable sequential changes in the viability of the cells and their division timing over a 7-day period. The second was adapted from a previously described method for use with mouse HSCs (Loeffler et al., 2018) and adapted here for a larger scale analysis of the timed expression of multiple intrinsic markers that would discriminate human *CD49f*⁺ cells in different stages of the cell cycle. The GF conditions chosen for detailed analysis of aging-associated effects on their behaviour were such that survival was minimally affected across all groups compared.

The first tracking strategy enabled an 18 hr aging-associated prolongation of the time taken to complete a first division to be revealed between CB and young adult *CD49f*⁺ cells receiving a potent 3GF stimulus, one previously shown to optimize the retention of 6-week LTC-IC activity of cultured adult BM cells (Zandstra et al., 1997). Moreover, this 18 hr delay was

followed by a further 8 hr prolongation of the time taken by young adult *CD49f*⁺ cells to complete a second and third division. The *CD49f*⁺ cells from aged adults required an additional 15 hr than the young adult cells just to complete a first division. And when this GF stimulus was greatly reduced (to 1% of the maximum concentration tested), the delayed responses exhibited by CB *CD49f*⁺ cells were more than doubled by the responses obtained from the adult sources of *CD49f*⁺ cells.

These prolonged extensions of division times exhibited by quiescent human HSCs isolated from individuals spanning 7 decades of age are consistent with a previously documented elongation of the first division timing exhibited by HSCs isolated from young and old mice (Flach et al., 2014). However, the longest overall time required for adult mouse HSCs to complete a first division was found to be shorter than the fastest time displayed here by CB *CD49f*⁺ cells, and the difference in median first division timing between the young and old mouse HSCs was only 4 hr. In contrast, the overall difference in the same parameter reported here greatly exceeds the proportionality difference (Flach et al., 2014). Thus, the mechanisms regulating these differences in mice may not be identical with those affecting human HSCs and, from a practical perspective, it may be more difficult to pinpoint these in mice because of the much more restricted timing of their effects. It is also important to note that the duration of first division times can likewise be impacted by multiple variations in the culture conditions to which the cells are exposed (Belluschi et al., 2018; Knapp et al., 2017; Laurenti et al., 2015). Thus, the magnitude of aging-associated delays may be differently influenced by these condition-dependent variables which may also not be replicated between species. These issues have more than mechanistic relevance, given the important need for an improved understanding of HSC

proliferation control for the optimized development of *ex vivo* strategies for expanding HSCs from human donors of different ages for future clinical cell therapy applications.

To investigate where in the cell-cycle adult *CD49f*⁺ cells experienced delays in their progression by comparison to CB *CD49f*⁺ cells, we used a method that allows for a multiplexed analysis of small numbers of input cells by immunofluorescence. Here we used this approach to track hundreds of *CD49f*⁺ and thousands of CD34⁺CD38⁻ cells from normal CB and young adult donors as they entered and transited through the cell-cycle. However, the same principles underlying this methodology are highly adaptable and we thus anticipate its ready modification to investigate other processes currently difficult to assess at a single-cell level in a wide-range of nonadherent human cell types, such as the tracking of differentiation or division asymmetry. In the present study, this method was able to show an unexpected similarity in the proportion of *CD49f*⁺ cells from CB and young adults recruited from G₀ into G₁ within 24 hr of GF stimulation, given the large difference in the overall time taken to complete their respective first divisions. However, the associated marker analyses performed suggest this may be due, at least in part, to the slightly higher levels of CDK6 detected in the young adult *CD49f*⁺ cells. CDK6 has been previously identified as a candidate regulator of G₀ exit by human CB HSCs with those HSC phenotypes displaying more rapidly initiated and shorter-term regenerative activities being characterized by increased levels of CDK6 and shorter times spent in G₀ following exposure to a mitogenic stimulus (Laurenti et al., 2015). By analogy, this could suggest that young adult *CD49f*⁺ cells would be primed to counteract other mechanisms restraining their ability to quickly enter the cell-cycle when stimulated. However, analysis of additional timepoints prior to 24 hr would be required to determine the presence of small differences in the rate of G₀ exit

between *CD49f*⁺ cells from differently aged donors and their associated mechanistic underpinnings.

Also unexpected was the strikingly long time which young adult *CD49f*⁺ cells remained in G₁, with the majority remaining in this phase for at least 26 hr, compared to the <18 hr spent there by their CB counterparts. However, in this case, this finding could be more readily explained by the lower sustained levels of CDK2 expression by the young adult *CD49f*⁺ cells (compared to those in CB) for at least 50 hr. CDK2 regulates the G₁-S phase transition through its hyperphosphorylation of Rb and the timed activation of replication origins and hence DNA replication (Deegan & Diffley, 2016; Hume et al., 2020; Limas & Cook, 2019; Satyanarayana & Kaldis, 2009; Sherr, 2000). A delayed entry into S-phase by HSCs in aged mice has been linked to a heightened replication stress arising from a deficit in the MCM helicase components which are required both for activation of DNA replication origins and for unwinding DNA to allow its replication (Flach et al., 2014). Since aged mouse HSCs have been found to have increased levels of DNA damage that are resolved upon exiting G₀ (Beerman et al., 2014), it is possible that such a mechanism could be enhanced in HSCs from older donors. However, studies from the mouse suggest that the DNA damage response is not compromised in aged HSCs, with repair proceeding efficiently in both aged and younger HSCs (Moehrle et al., 2015). A combination of these processes inducing a moderate G₁ arrest in adult human *CD49f*⁺ cells could also arise from p53 activation of p21 which suppresses activity of CDK2, thereby preventing entrance into S-phase (Hume et al., 2020; Limas & Cook, 2019). Notably the more prolonged cell cycle duration times exhibited by adult *CD49f*⁺ cells were not limited to the first cell cycle they completed, it continued into the subsequent divisions of their immediate progeny. Future studies will therefore be of interest to determine the specific cell cycle-stage transitions that account for the extended

aging-associated effects observed here on the division kinetics exhibited by the progeny of *CD49f*⁺ cells and whether these are due to continued delays in transiting through G₁, a transient return to a more prolonged G₀, or via an additional unknown mechanism.

In addition to the delayed division kinetics displayed by adult *CD49f*⁺ cells (compared to CB *CD49f*⁺ cells) following their exposure to a potently mitogenic GF condition, a reduced GF stimulus caused a disproportionate further increase in the time required for the older *CD49f*⁺ cells to divide. A more detailed examination of the cell cycle phases most affected indicated that the most prominent effect was a further enhanced retention of the adult cells in G₁ and an increased proportion of those seen as failing to exit G₀. These findings suggest a rheostat mode of GF control of both the G₀-G₁ and G₁-S phase transitions and an aging-associated increase in the signaling events required to force these to occur. Progression into and through G₁ is also strongly related to the continued presence of mitogenic stimulation for example due to the relative instability of cyclin D family members and required continual translation downstream of mitogenic signaling to outcompete binding of CDK inhibitors with CDK4 and CDK6 ultimately arresting the cell in G₁ (García-Gutiérrez et al., 2019; Hume et al., 2020; Sherr, 1993, 2000; Yang et al., 2017). Signaling through the AKT pathway also has known pro-mitogenic effects in G₁ cells by downregulating FOXO transcription factors that otherwise inhibit the activity of cyclin E-CDK2 complexes through elevated levels of p21 and p27 (Massagué, 2004; Pietras et al., 2011). AKT also has a known role in phosphorylating and thereby inactivating GSK3 which, itself, acts as a negative regulator of β -catenin as well as increasing β -catenin activity through a direct phosphorylation mechanism (Sears & Nevins, 2002; Verheyen & Gottardi, 2010). It was previously shown that AKT and β -catenin are major regulators of both the survival and proliferation of CB *CD49f*⁺ cells (Knapp et al., 2016). In addition, both of these activities are

modulated in human HSCs by effects of miR126 on the same 2 pathways (Lechman et al., 2012). Interestingly, we did observe a lower increase and less sustained AKT activation in young adult *CD49f*⁺ cells and no activation of β -catenin after short-term *in vitro* stimulation with 3GF. The delayed transit through G₁ of young adult cells might thus be due to their insufficient AKT activity. We also observed that the elongated G₁-phase in adults shared by the more progenitor-enriched CD34⁺CD38⁻ population was similarly accompanied by the reduced ability of CD34⁺CD38⁻CD45RA⁻ cells to activate AKT. Although this effect was less pronounced than in the *CD49f*⁺ cells, it suggests that the key mechanisms persist downstream of the HSC compartment.

In summary, we provide the first evidence of a progressive postnatal age-related alteration in mechanisms that regulate the activation of quiescent human HSCs to progress through G₁ and transition into S-phase. We further show that with increasing age, the responses of these primitive hematopoietic cells are increasingly dependent on the level of GF-stimulation they require to progress through G₁ and that activation of AKT and β -catenin play a role in mediating the different responses obtained. Taken together, these findings suggest that efficient stimulation of adult HSCs may require specific tuning of conditions to increase AKT and β -catenin activation above what is necessary to optimize the stimulation of CB derived HSCs. Growing interest in using expanded HSCs for various clinical applications now heightens the importance of obtaining a further understanding of differences in the mechanisms regulating the effects of aging on GF-dependent survival and proliferation of human HSCs.

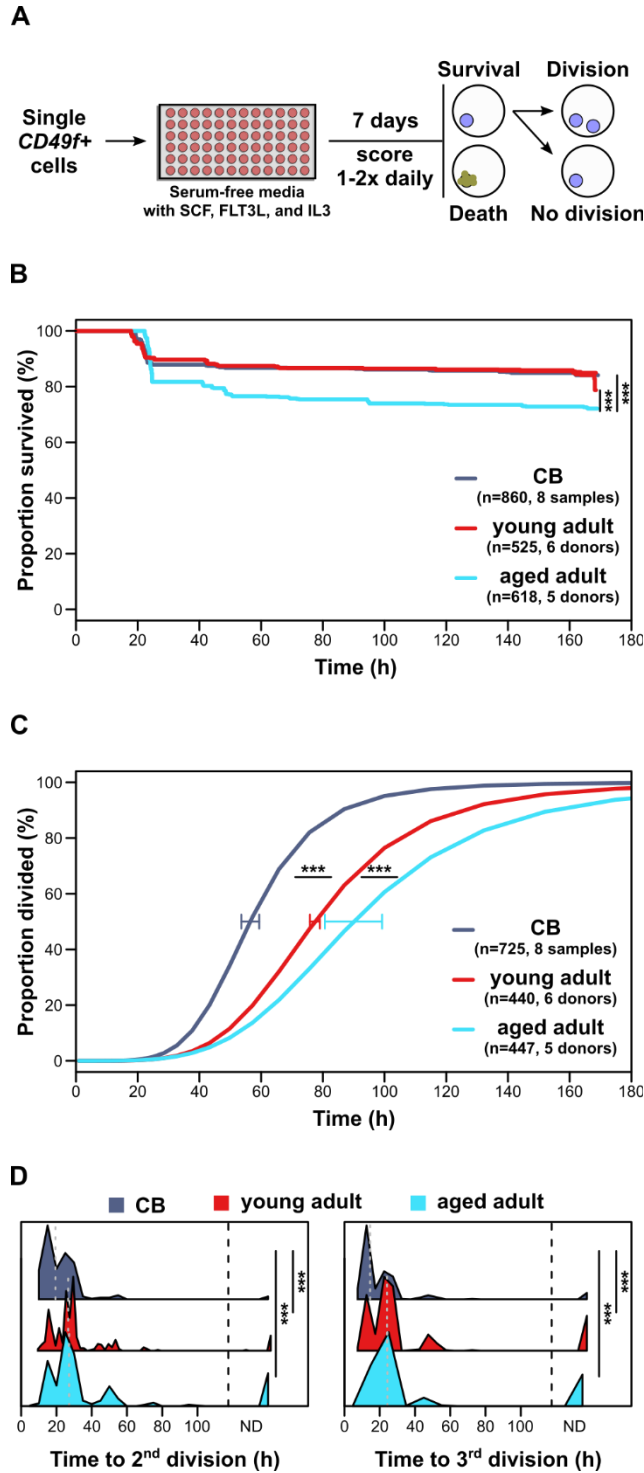


Figure 4.1 Identification of a progressive age-related delay in $CD49f+$ division kinetics *in vitro*. A) Single $CD49f+$ cell tracking design. B) Kaplan-Meier curves of $CD49f+$ survival (log-rank test, *** $P < 0.001$). C) Weighted dose-response curves of $CD49f+$ first division kinetics.

Curves reflect only *CD49f*⁺ cells which survived either until the end of the assay or past their first division. Error bars drawn at the median point of each curve indicate the standard error of the median division times of each sample (***P*<0.001). D) Time required for clones to complete a second (*left*) or third (*right*) division after completing their previous division. Clones which did not complete a subsequent division during the total observation period are counted as “not detected” (ND, ***P*<0.001, pairwise Holm-corrected Wilcoxon tests).

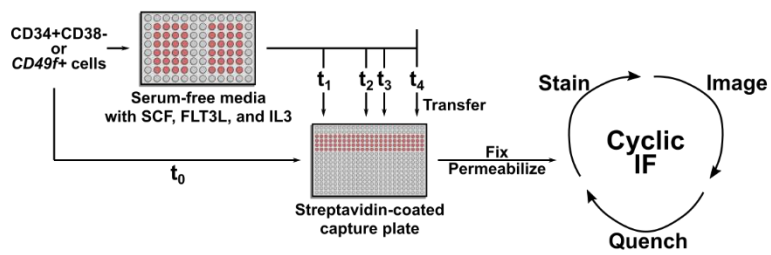
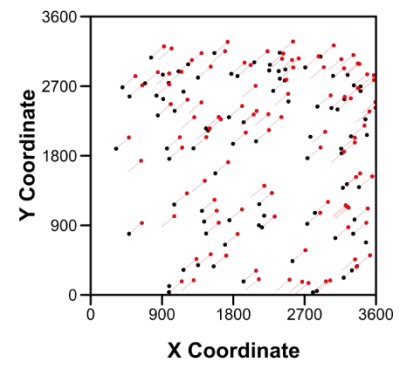
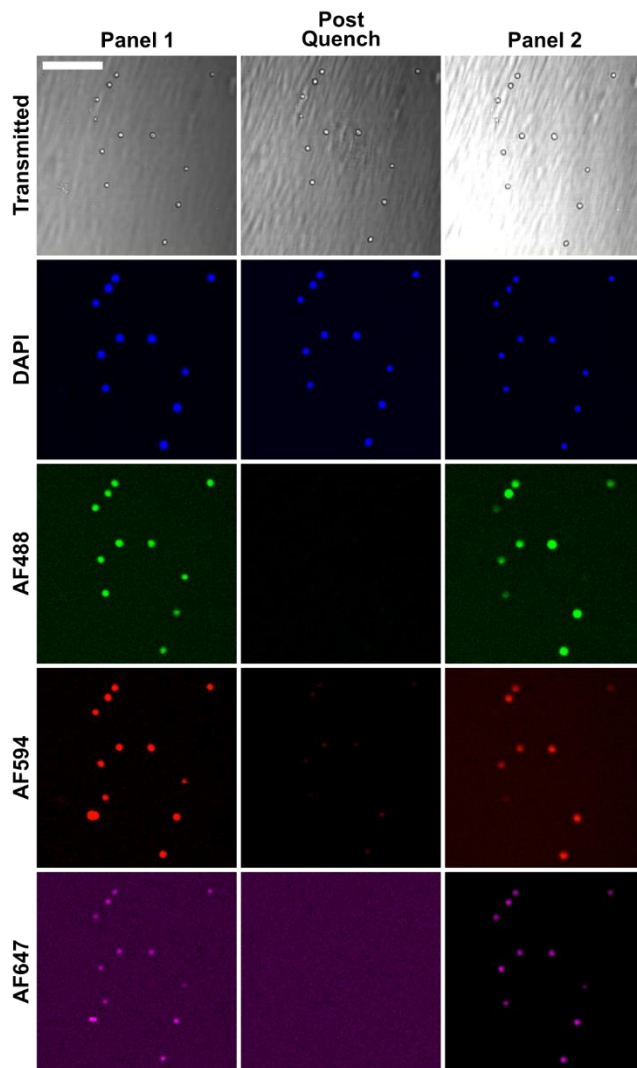
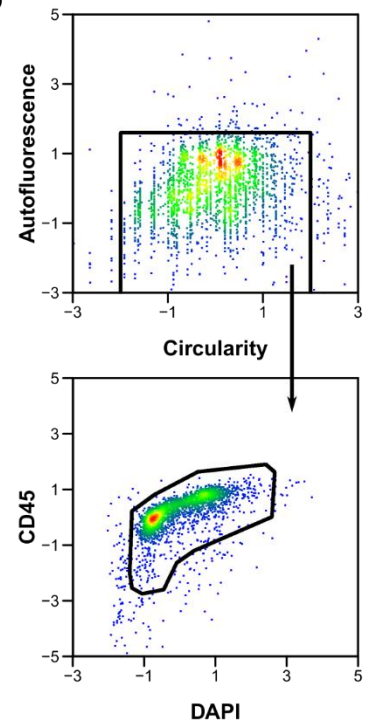
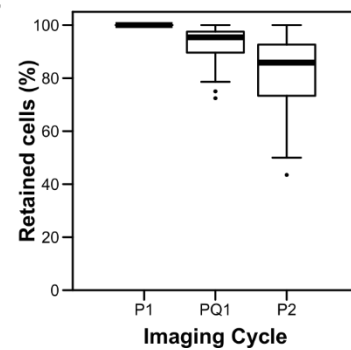
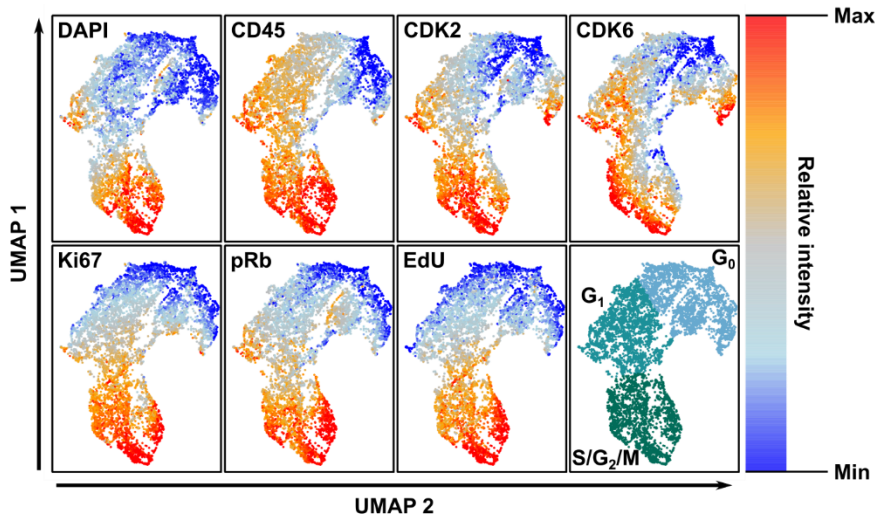
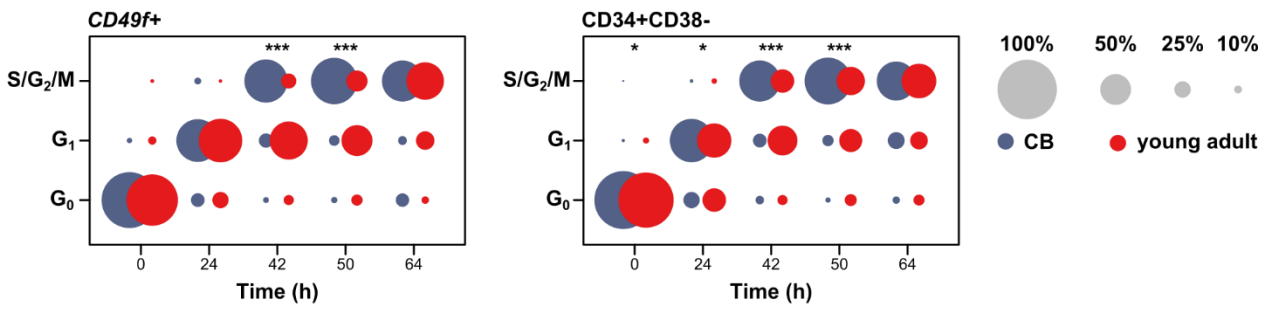
A**C****B****D****E**

Figure 4.2 Development of a system for monitoring paired cell-cycle state and molecular changes in individually tracked human blood cells. A) Experimental design of cell culture, cell capture, and cyclic immunofluorescence imaging. B) Representative images from the fluorescent microscopy analysis, scale bar = 100 μm . C) Representation of affine transformation correction of event drift between imaging cycles. Black dots represent events detected in a single well from the initial imaging cycle and red dots indicate events detected in a subsequent imaging cycle, red lines connect the adjusted position of the red dots to their unadjusted positions. Axes values indicate dimensions of the total stitched image tiling the well. D) Example 2D gating of events detected by microscopy. Axes values are the scaled (Z-scores) of the corresponding parameter. E) Proportion of cells maintained in each well between imaging cycles. Proportion is calculated as number of gated cells in the well for an imaging cycle divided by the number of gated cells in the same well detected in the first imaging cycle.

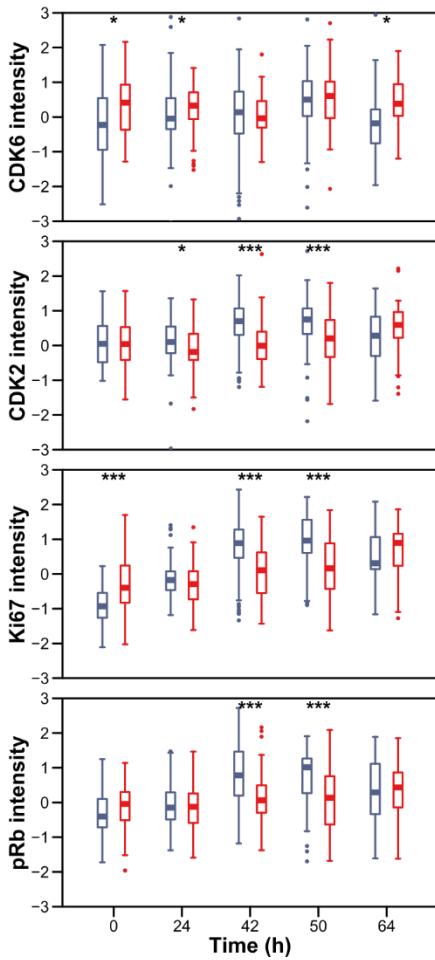
A



B



C



D

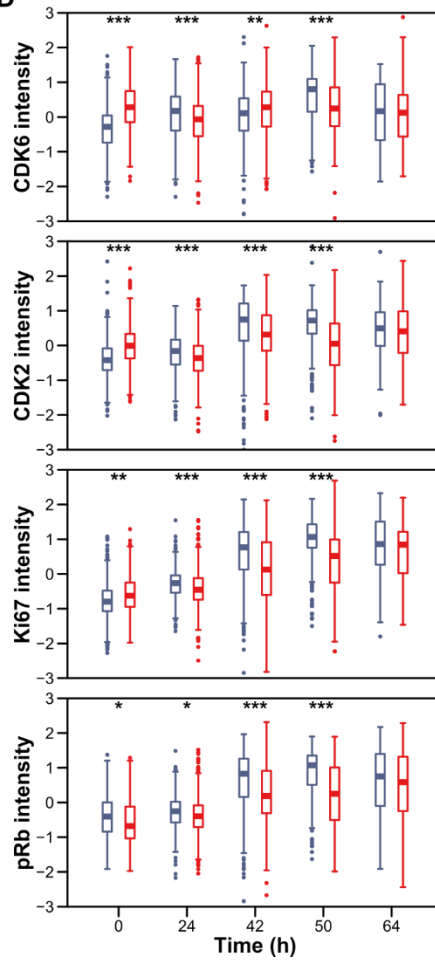


Figure 4.3 *CD49f+* and *CD34+CD38-* cells display an age-related elongation of G₁. A)

UMAP distribution of *CD49f+* and *CD34+CD38-* cells from CB and young adult BM cultured for 0, 24, 40, 52, or 64 hrs and analyzed by cyclic immunofluorescence. Assignment of regions of the UMAP distribution to phases of the cell-cycle by K-means clustering (*bottom-right*). B) Proportion of *CD49f+* cells (*left*) or *CD34+CD38-* cells (*right*) in different phases of the cell cycle by timepoint. The size of each circle represents the proportion of total CB or young adult cells in each phase for that timepoint (* $P < 0.05$, ** $P < 0.01$, *** $P < 0.001$, Holm-corrected Kruskal-Wallis tests). Scaled intensity (Z-scores) of CDK6, CDK2, Ki67, and pRb at each timepoint in *CD49f+* (C) or *CD34+CD38-* (D) cells (* $P < 0.05$, ** $P < 0.01$, *** $P < 0.001$, Holm-corrected Wilcox tests).

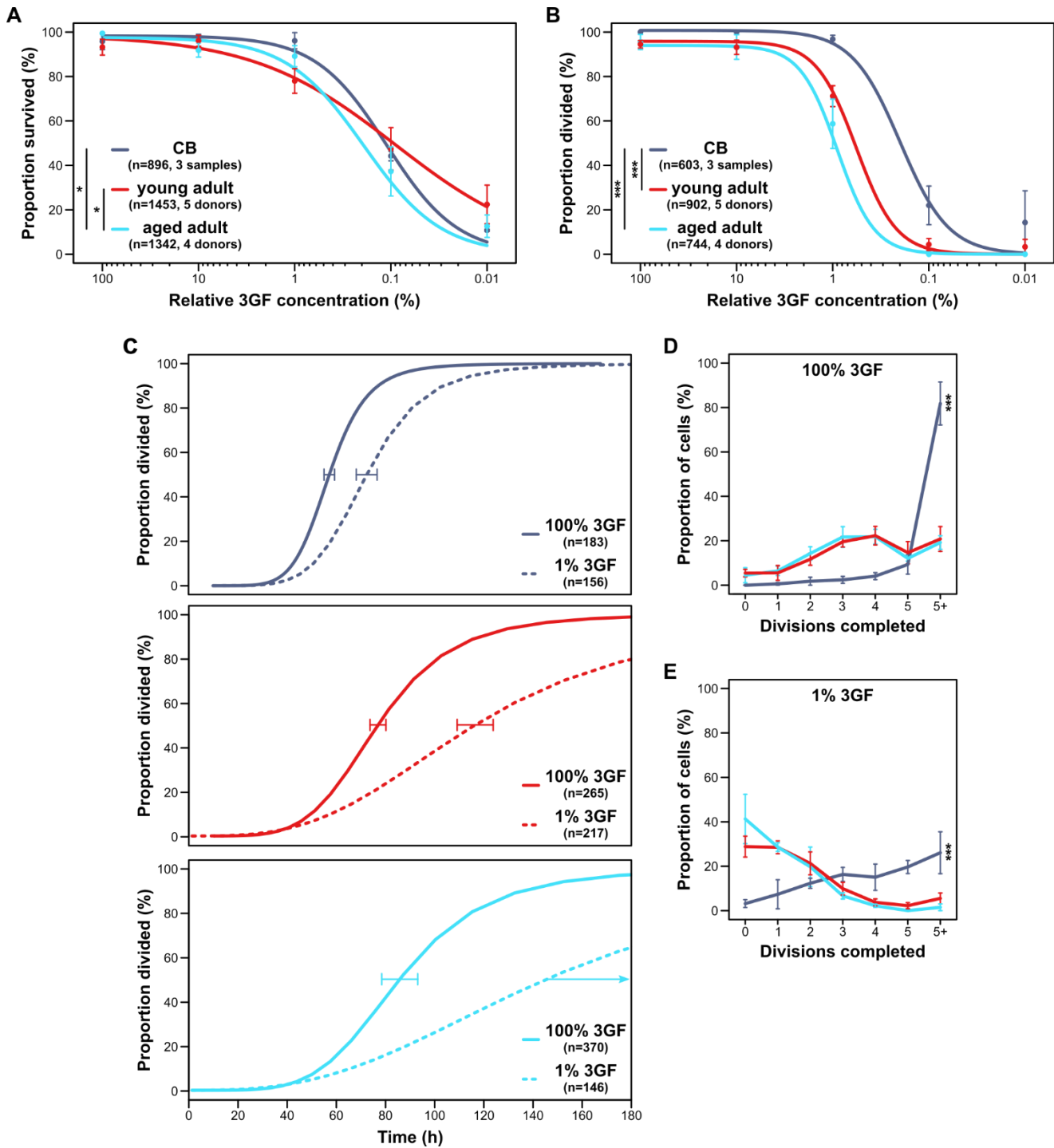


Figure 4.4 Stimulation of adult $CD49f^+$ cell proliferation requires higher levels of 3GF.

Weighted dose-response curves for $CD49f^+$ cell survival (A) and proliferation (B) at the

indicated concentrations of 3GF in SFM. Survival required cells to maintain high refractility and membrane integrity for 7 days and proliferation required a cell to divide at least once in the same time-period. Proliferation curves are normalized to cells which survived either until the end of the assay or past their first division. Points indicate the mean survival or proliferation response for each group at each concentration with error bars indicating the associated standard error (* $P < 0.05$, *** $P < 0.001$). C) Kinetics of first division timing of CB (*top*), young adult (*middle*), and aged adult (*bottom*) $CD49f^+$ cells at high (solid lines) and low (dotted lines) 3GF. Error bars indicate standard error of the median division timing between individual samples of each group. The arrow on the aged adult low 3GF condition indicates that the standard error of the median division timing extends beyond the observation timing (3/4 aged adult donors had $< 50\%$ of their surviving cells divide ≥ 1 time within 7 days in low 3GF). Number of divisions completed by $CD49f^+$ cells cultured at high (D) or low (E) 3GF for 7 days. Lines connect the observed mean proportion of cells completing the indicated number of divisions after 7 days. Error bars indicate standard error between individual donors (*** $P < 0.001$, pairwise Kruskal-Wallis tests).

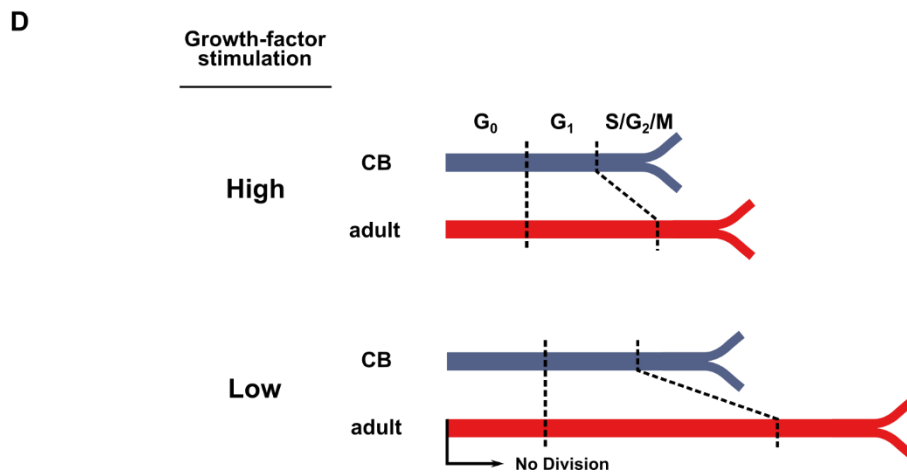
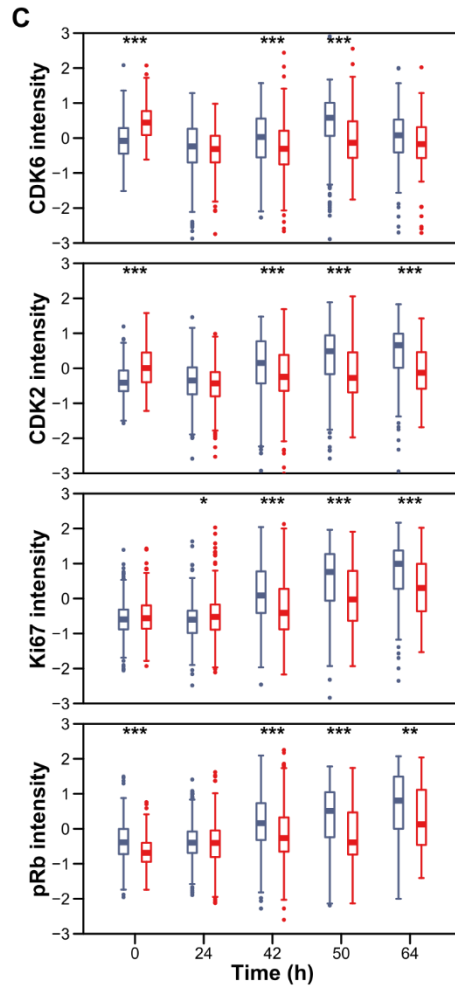
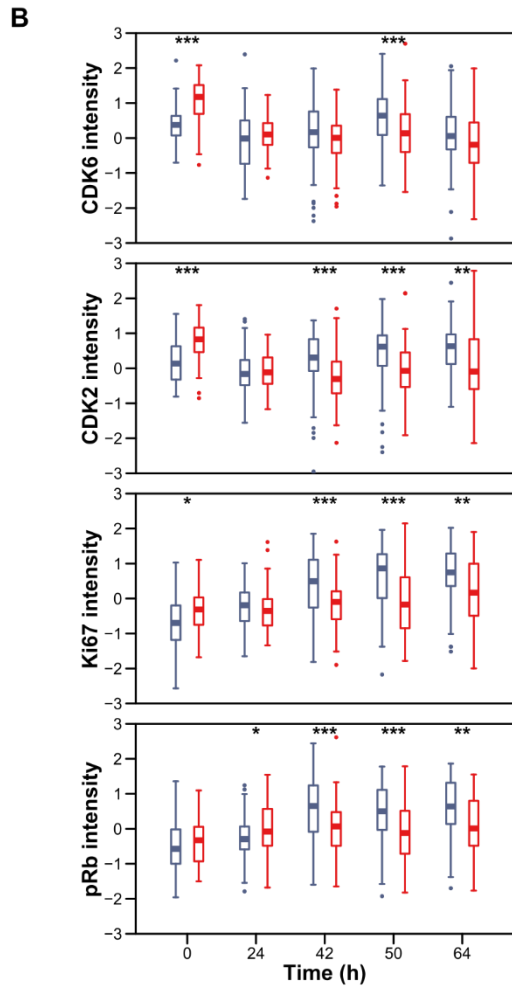
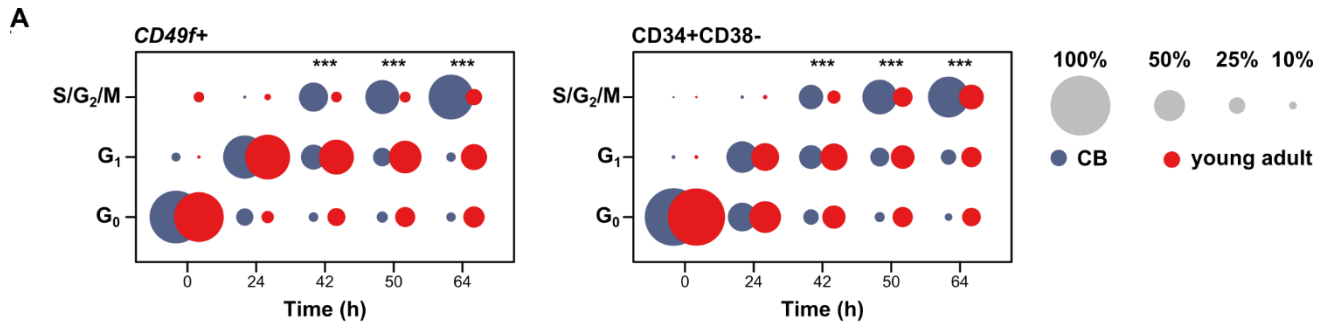


Figure 4.5 G₁ progression delay is exacerbated in adult cells under low 3GF stimulation. A)

Proportion of *CD49f*⁺ (*left*) or *CD34*⁺*CD38*⁻ (*right*) cells at each indicated phase of the cell-cycle at each timepoint. The size of each circle represents the proportion of total CB or young adult cells in each phase for that timepoint (**P*<0.05, ***P*<0.01, ****P*<0.001, Holm-corrected Kruskal-Wallis tests). Scaled intensity (Z-scores) of CDK6, CDK2, Ki67, and pRb at each timepoint in *CD49f*⁺ (C) or *CD34*⁺*CD38*⁻ (D) cells (**P*<0.05, ***P*<0.01, ****P*<0.001, Holm-corrected Wilcoxon tests). D) Summary model of age-related *CD49f*⁺ proliferation delays at high and low 3GF exposure. The length of the coloured lines indicates the relative time required to complete a first division (indicated by branched line end) with the dotted lines denoting relative lengths of time spent in the indicated phase of the cell-cycle.

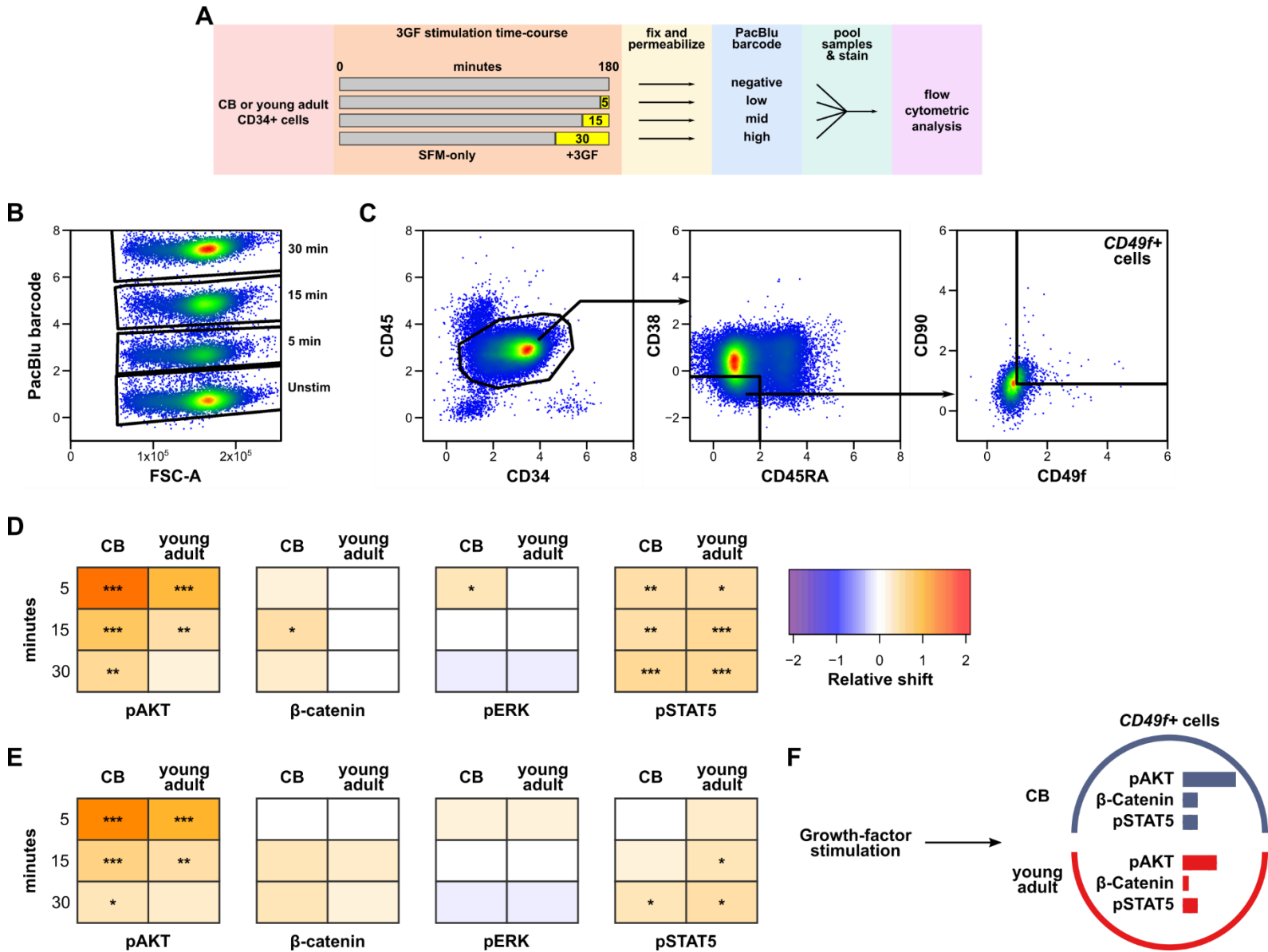


Figure 4.6 Reduced AKT and β -catenin activation in young adult stem and progenitor cells following short-term 3GF stimulation. A) Experimental design for the 3GF stimulation time-course and flow cytometric analysis. B) Representative gating of pooled Pacific Blue-barcoded samples. C) Representative gating of *CD49f*⁺ and *CD34*⁺*CD38*⁻*CD45RA*⁻ cells. Axes values apart from ‘FSC-A’ are in $\text{asinh}(x/150)$. Median relative shift in the intensity of the indicated marker from the corresponding unstimulated sample for *CD49f*⁺ (D) and *CD34*⁺*CD38*⁻

CD45RA- (E) cells. Asterisks indicate significant shifts away from the unstimulated samples (* $P < 0.05$, ** $P < 0.01$, *** $P < 0.001$, bootstrapped probabilities). F) Summary model of *CD49f*⁺ pathway activation following short-term 3GF stimulation. The length of the coloured bars indicates relative activation of the corresponding marker.

Table 4.1 Analyzed cells by timepoint for cell-cycle staging in 100% 3GF

Sample	Group	Phenotype	Number of cells				
			0 hrs	24 hrs	42 hrs	50 hrs	64 hrs
1	young	CD34+CD38-	NA	49	88	126	29
	adult BM	<i>CD49f</i> +	NA	24	13	40	23
2	CB	CD34+CD38-	NA	22	32	142	13
		<i>CD49f</i> +	NA	24	41	39	6
3	young	CD34+CD38-	99	111	88	88	59
	adult BM	<i>CD49f</i> +	33	31	36	41	33
4	CB	CD34+CD38-	182	110	114	86	31
		<i>CD49f</i> +	38	44	56	41	11
5	young	CD34+CD38-	64	206	203	48	7
	adult BM	<i>CD49f</i> +	31	21	21	18	17
6	CB	CD34+CD38-	243	141	196	122	52
		<i>CD49f</i> +	28	25	34	26	8

Table 4.2 Analyzed cells by timepoint for cell-cycle staging in 1% 3GF

Sample	Group	Phenotype	Number of cells				
			0 hrs	24 hrs	42 hrs	50 hrs	64 hrs
1	young	CD34+CD38-	NA	78	36	103	41
	adult BM	<i>CD49f</i> +	NA	15	13	44	27
2	CB	CD34+CD38-	NA	56	32	78	50
		<i>CD49f</i> +	NA	12	14	37	26
3	young	CD34+CD38-	91	87	96	100	56
	adult BM	<i>CD49f</i> +	40	4	46	31	26
4	CB	CD34+CD38-	146	115	111	92	44
		<i>CD49f</i> +	51	50	52	30	22
5	young	CD34+CD38-	NA	178	169	15	7
	adult BM	<i>CD49f</i> +	NA	31	20	27	19
6	CB	CD34+CD38-	222	144	156	157	71
		<i>CD49f</i> +	23	32	32	27	14

Chapter 5: Discussion

5.1 Major Contributions

The overall objective of the investigations described in this thesis was to interrogate the impact of normal aging on several functional properties of human HSCs and elucidate their underlying mechanisms. As a starting point, the *CD49f*⁺ phenotype was used to isolate a population previously shown to be enriched in HSCs from both neonatal and adult sources (Belluschi et al., 2018; Huntsman et al., 2015; Knapp et al., 2018; Notta et al., 2011; Wang et al., 2019). This population was isolated here from samples of healthy PB and BM donors spanning 7 decades of life and found to reproducibly contain a high frequency of cells able to generate differentiated lymphoid and myeloid progeny for many weeks *in vitro* in stromal cell-containing culture systems and for many months *in vivo* when transplanted into irradiated immunodeficient mice. More focused analysis on the proliferative response of these cells to GF stimulation revealed a postnatal change in the regulation of a mitogen-sensitive progression through the cell cycle which increased progressively with the age of the donor. Key to the generation of these findings was the development and validation of optimized methods to enable the variable biological and molecular features and responses of the rare *CD49f*⁺ cells to be measured at low numbers or individually.

In Chapter 3, phenotypic comparison of the CD34⁺ stem and progenitor compartment isolated from CB, adult BM, and adult mPB from donors aged 0-69 years revealed no differences that were consistent between the age or source of cells in the frequency of progenitor phenotypes that enrich for cells with specific differentiation abilities. This contrasts with results reported in

mice for which a decrease in lymphoid progenitors and an increase in phenotypic HSCs have been well documented (Beerman et al., 2010; de Haan et al., 1997; Dykstra et al., 2011; Flach et al., 2014; Morrison et al., 1996; Rossi et al., 2005; Sudo et al., 2000). In contrast, our studies did not detect any age-associated specific loss or decline in lymphoid output activity by adult *CD49f*⁺ cells either *in vitro* or *in vivo* suggesting an intrinsic retention of this capability in these cells during healthy human aging. However, we did not specifically analyze the T cell potential of these cells *in vitro*, whether this potential is also retained with aging is an area for future investigation.

In addition, we obtained evidence of a heterogeneous but nevertheless preserved longevity and magnitude of the *in vivo* repopulating ability by adult *CD49f*⁺ cells in immunodeficient mice; a finding that also stands in strong contrast to results of previous studies of mouse HSCs (Beerman et al., 2010; de Haan et al., 1997; Dykstra et al., 2011; Flach et al., 2014; Morrison et al., 1996; Rossi et al., 2005; Sudo et al., 2000). These observations also appear to differ from those reported previously for human HSCs (Huntsman et al., 2015; Pang et al., 2011; Wang et al., 2019). Important to note however is the absence of previous adult *CD49f*⁺ transplants to include co-injected CD34⁺ CB cells. Use of this co-transplantation model appeared beneficial to magnify the outputs of adult *CD49f*⁺ cells which was not observed for CB *CD49f*⁺ cells. Although the mechanism of this novel “helper effect” has yet to be elucidated, its use does serve to establish that the *CD49f*⁺ phenotype identifies a population enriched in HSCs with an intrinsic potential for high multi-lineage outputs of progeny which does not diminish significantly with donor age. Nevertheless, they do point to a change in the extrinsic stimulatory requirements to elicit this potential as was then pursued as described in Chapter 4.

In Chapter 4, initial studies were designed to compare the cell proliferation kinetics of *CD49f*⁺ cells from donors of different ages. Results from stromal cell-containing cultures first suggested a delay in the outputs of *CD49f*⁺ cells from older donors, and single-cell tracking experiments revealed a progressive age-related delay in their activation into and through a first and subsequent division cycles. Development of a system enabling the simultaneous tracking of the cell-cycle state and quantification of molecular regulators of this process at single-cell resolution indicated elongation of the G₁-phase in adult *CD49f*⁺ cells. This proliferative delay was also found to be highly exaggerated under conditions of reduced mitogenic stimuli with adult *CD49f*⁺ cells proving to require higher GF concentrations to elicit proliferation than those from CB. Mechanistically, GF stimulation of adult *CD49f*⁺ cells appeared to result in lower activation of AKT and β -catenin than was observed in CB. In addition, we similarly observed that the G₁ elongation and signaling responses extended into the CD34⁺CD38⁻(CD45RA⁻) fraction indicating that these mechanisms are not restricted to the adult HSC compartment. Combined, the results outlined in Chapters 3 and 4 identify several previously unknown aspects of aging human HSCs and dispute some of the features previously believed to accompany aging in this system.

5.1.1 Direct functional comparison of human *CD49f*⁺ cells across 7 decades of age

Identification of a phenotype capable of enriching functional human HSCs to ~10% purity in CB presented opportunities to explore the functional and molecular features of these cells at high resolution (Notta et al., 2011). Extension of this phenotype into adults has been minimally performed with some characterization of their molecular features (Buenrostro et al., 2018; Farlik et al., 2016; Notta et al., 2016; Velten et al., 2017). LDA transplants into

immunodeficient mice have also suggested a ~5-40-fold reduction in the purities of functionally defined human HSCs within the *CD49f*⁺ fraction (Huntsman et al., 2015; Wang et al., 2019). Our unexpected observation that *CD49f*⁺ cells from all donor age-groups display remarkably similar overall numbers of cells with LTC-IC capacity and lympho-myeloid differentiation potential suggests that historical models of human HSC aging require modification. Of particular interest was the observation that the CB *CD49f*⁺ compartment, in marked contrast to those in adult BM samples, contained a significant proportion of cells that only transiently generated progeny. Previous studies have shown that the *CD49f*⁺ compartment in CB is functionally heterogeneous and contains phenotypically identifiable subsets with reduced repopulating capacities (Belluschi et al., 2018; Knapp et al., 2018). It is therefore inviting to consider the possibility that analogous cells are not found in the aging adult *CD49f*⁺ samples because their activation or output potential is not detectable under the conditions of these assays. Alternatively, these cells may represent a fraction that is absent in the BM or reduced to frequencies below levels detectable in these assays. In support of this finding, we identified several phenotypic features of *CD49f*⁺ cells which differed not with donor age, but with the site from which the *CD49f*⁺ cells were isolated, strongly suggesting the composition of the *CD49f*⁺ compartment is site-dependant. This concept is strongly supported by a recent investigation which revealed the different molecular features and functional potentials of hematopoietic stem and progenitor cells found within human BM, PB, or the spleen (Mende et al., 2020).

Tracking of the survival and proliferation responses *in vitro* of *CD49f*⁺ cells from differently aged donors revealed a striking and progressive elongation of first division timing with increasing donor age. This was coupled with an additional 8 hr required to elicit subsequent divisions from the progeny of young and aged adult *CD49f*⁺ cells. These findings point to a

developmentally determined elongation of the overall cell cycle transit time that occurs postnatally, coupled with a progressively reduced rate at which quiescent *CD49f*⁺ cells can complete a division cycle. In the mouse a similar, albeit much less pronounced, aging-associated delay has been observed in the first and second division timings of HSCs which was attributed to a slower progression into and through S-phase due to decreased levels of MCM components and increased replication stress seen in the older HSCs (Flach et al., 2014). Other studies have also identified an accumulation of DNA damage in quiescent older mouse HSCs that is repaired following cycling (Beerman et al., 2014; Moehrle et al., 2015), thereby offering a potential explanation for the age-related increase in first division timing assuming that the damage progressively accumulated with age would require increasingly longer times to repair. However, this would not explain the switch from an ~16 hr to an ~24 hr requirement for each subsequent cycle as we observed between CB and young or aged adult *CD49f*⁺ cells. A model of division outlined in a recent review by Hume *et. al.* (2020) describes a process of checkpoints, the first of which occurs at a late stage of the mother cell cycle and influences each of the 2 progeny cells' subsequent cell cycles according to the level of mitogenic stimulation and replicative stress experienced. If the mitogenic stimulation is maintained, and the DNA damage from replication is low, the daughter cells can inherit hyperphosphorylated Rb (inactive) and low p21 and proceed into G₁ and efficiently into S-phase barring the introduction of new DNA damage. Conversely, if there is late withdrawal of mitogenic stimulation, or if replication stress is experienced in the mother cell past the point of commitment to division, the progeny inherit hypophosphorylated Rb (active) and high levels of p21 requiring re-entry into and through G₁ (Hume et al., 2020; Moser et al., 2018). This model could account for the increased cell cycle transit time required for subsequent divisions if the *CD49f*⁺ cells from young and aged adults both experience replication

stress in excess of that experienced by CB. Additionally, this would be influenced by whether the efficiency of DNA damage responses in human HSCs is similarly aging-independent as had been shown in the mouse (Moehrle et al., 2015). Future investigations into the impact of replication stress and repair in these cells could then serve to identify mechanisms that contribute to progressive acquisition of clones bearing somatic mutations during normal aging (CHIP).

5.1.2 Development of a high-resolution platform for multiplexed analysis of rare cells

The very low frequency of *CD49f*⁺ cells in typically available samples of normal human hematopoietic cells and their extensive heterogeneity mandates the need for techniques which are able to resolve single-cell information from small numbers of input cells. The method used here was based on one developed for mouse HSCs (Loeffler et al., 2018) and involved tethering the non-adherent cells to the bottom of 384-well plates so that they could be retained through multiple manipulations. Combination of this technique with a strategy that allows multiple rounds of sequential staining and immunofluorescence measurements to be made on the same cells (Lin et al., 2015) enabled establishment of the cell-cycle state and levels of several molecular regulators in individual *CD49f*⁺ cells from different sources. Additional bioinformatic strategies developed here made it possible to remove cell-sized debris and retain desired cell-specific information for downstream analysis through each cycle of immunofluorescence imaging. While this platform was used here for cell-cycle progression analyses, we anticipate this strategy will be well suited for many other investigations of rare subsets of nonadherent cells. For example, recent findings indicate that differentiation processes in the hematopoietic system involve continuous changes in key regulators, such as transcription factor expression levels and modulation of the epigenome, which are not as easily discretized into a step-wise

progression model as previously envisaged (Bock et al., 2012; Buenrostro et al., 2018; Karamitros et al., 2018; Knapp et al., 2019; Pellin et al., 2019; Velten et al., 2017; Zheng et al., 2018). While transcription factor expression dynamics are readily accessible in the mouse by generation of transgenic reporters (Hoppe et al., 2016), this strategy is more difficult to realize in primary sources of human cells. Use of the platform described here would enable direct quantification of multiple transcription factors in individual rare human cell subsets or across a single clone by antibody labeling. Analysis of division symmetry in human HSCs could similarly be analyzed in this way through fluorescent quantification of several markers recently associated with the asymmetric inheritance of functional properties in mouse and human HSCs (García-Pratt et al., 2021; Loeffler et al., 2019). Although relatively few cycles of quantification were reported here, this process could likely be repeated continuously as long as cell retention remains sufficient. Overall, this methodology presents as a highly adaptable and efficient method for the direct quantification of multiple markers in rare cells with known functional properties.

5.1.3 Identification of a mitogen-sensitive developmentally regulated G₁ transit delay

Use of our cell-capture and cyclic immunofluorescence system identified the first evidence of an age-dependent elongation of first division timing in primitive human hematopoietic cells to a delayed passage through G₁. Interestingly, the proportion of *CD49f*⁺ cells from CB and young adult BM which exited G₀ was equivalent after 24 hr, indicating a high responsiveness of these cells to the GF stimulus. Increased baseline levels of CDK6 in the adult *CD49f*⁺ cells may suggest differential priming of these cells to exit quiescence in response to mitogens, since this protein has been demonstrated to impact the kinetics of G₀/G₁ transition in human HSCs (Laurenti et al., 2015). However, CDK2 levels remained lower in adult *CD49f*⁺

cells for at least 50 hr suggesting that the G₁ delay occurs prior to CDK2 activation which canonically follows phosphorylation of Rb by CDK4/6 with cyclin D and inhibition of CDK inhibitors, including p21, p27, and p15 (García-Gutiérrez et al., 2019; Hume et al., 2020; Sherr, 2000). The non-proportional increased G₁ delay we observed in adult *CD49f*⁺ cells exposed to lower mitogen concentrations similarly points to progression being stalled at an early stage of G₁. Mitogen exposure in early G₁ drives signaling through the MAPK and AKT pathways and activates the transcription factor c-MYC which, in turn, exerts pro-division effects such as transcription of cyclin D (required for CDK4/CDK6 phosphorylation of Rb) and repression of p21, p27, and p15 (García-Gutiérrez et al., 2019; Hume et al., 2020; Sherr, 2000; Fig. 1.3). In addition to the pro-survival influence of AKT signaling, AKT also acts to push cells through G₁ through inactivating FOXO transcription factors and GSK3 to produce reduced levels of p21 and p27, and an increased level of cyclin D (Chang et al., 2003). Short-term stimulation with our 3GF cocktail revealed lower and less sustained activation of AKT and no activation of β-catenin (downstream of GSK3 inactivation) in the *CD49f*⁺ cells of young adult BM compared to CB. Taking these findings altogether then suggests a model in which adult cells have reduced stimulation of pro-mitogenic pathways operative in early G₁ leading to delayed activation of CDK2 and progression into S-phase. Importantly this does not preclude additional delays at other stages of cell-cycle progression control, including even at other points within G₁. Indeed, the finding of decreased MCM helicase levels in aged mouse HSCs compared to those of younger adult mice, as well as the increased replication stress experienced by these cells during S-phase, suggests that multiple points of the cell-cycle may be impacted (Flach et al., 2014). Future investigations into the mechanism proposed here may be facilitated by the finding that this G₁ delay also occurs in the more prominent CD34⁺CD38⁻ subset of adult BM cells.

The observation that a large fraction of adult *CD49f*⁺ cells remain in G₀ when exposed to low levels of 3GF, with ~30% remaining viable but undivided for 7 days, implicates that a significant proportion of adult *CD49f*⁺ cells have increased mitogen requirements to even exit G₀. Whether this represents a distinct functional subset will be an interesting avenue of future investigation.

5.2 Implications and future directions

A higher mitogenic barrier for cell-cycle entry in the adult system suggests an additional or altered regulatory mechanism that acts to maintain adult HSCs in a predominantly quiescent state to avoid exhausting their numbers. The interaction of this mechanism with the altered cytokine milieu in the aging adult BM, including increased levels of inflammatory cytokines, and the increasing rate of CHIP and overt leukemias present important areas of future investigation. Additionally, our findings *in vitro* and *in vivo* of similar output potentials and repopulating abilities of *CD49f*⁺ cells from CB or adult samples indicate that their intrinsic potentials are largely maintained through aging but may require highly optimized conditions to induce their appearance. For example, studies of mice have demonstrated improvements to lymphoid output from aged hematopoietic cells when transplanted into younger hosts suggesting this typical aging-associated phenotype can be extrinsically driven (Ergen et al., 2012; Young et al., 2021). Furthermore, our observation of a high correlation of *in vivo* repopulating activity of adult *CD49f*⁺ cells with the output of co-transplanted CB CD34⁺ cells, and the lack of a similar correlation for CB *CD49f*⁺ cells, implies that current immunodeficient mouse models are lacking factors that are required to elicit the full reconstituting activity of adult human HSCs. In connection with the model proposed above, this could be lower levels of mitogenic signals

interpretable by the human receptors which are sufficient for activating CB *CD49f*⁺ cells but insufficient for those from the adult. It would be of interest to explore whether this particular observation arises specifically from the co-transplantation of CB CD34⁺ cells or if this effect is reproducible using CD34⁺ cells from adult sources.

Additionally, attempts to robustly and consistently expand HSC numbers *in vitro* for clinical transplantation purposes has prompted much interest in the analysis of HSC responses to various extrinsic factors *in vitro*. While these studies have had varying levels of success, CB sources have emerged as a front-runner for the limited cell expansions now achievable due to their relatively high availability, ability to engraft in allogeneic recipients, and low HSC yield per single CB sample (Rocha, 2016). Single matched adult allogeneic or autologous donors can still provide an adequate collection of cells sufficient for most transplant-dependent therapies (Rocha, 2016) and autologous transplants remain the gold standard for gene therapy approaches (Naldini, 2019). But conditions optimized for maintenance of adult HSC functionality during *ex vivo* manipulation remain of huge clinical interest.

Interestingly, limited research has been performed to investigate the potential differential requirements that development or aging impose on HSC proliferation *ex vivo*. In the mouse, fetal HSC self-renewal was found to be more sensitive to SCF than adult HSCs (Audet et al., 2002; Bowie et al., 2007). A study in human CD34⁺CD38⁻ cells found lower expansion of LTC-ICs from CB than adult BM donors using the 3GF cocktail also used here, suggesting a differential responsiveness of the cells producing the expanded LTC-ICs between these sources (Petzer et al., 1996; Zandstra et al., 1998, 1997). However, it is important to note that the majority of LTC-ICs are not functionally equivalent to HSCs and may have different expansion requirements as

was seen to achieve expansion of the even more differentiated CFCs (Petzer et al., 1996; Zandstra et al., 1997). It is then likely that conditions for *ex vivo* expansion of human hematopoietic cells will not be defined as a one-size-fits-all for cells from donors of different ages. Rather specific protocols will need to be optimized for the cells being cultured and the outcome desired, whether it be expansion, maintenance, or maximization of gene transfer.

5.3 Limitations of the current work

While this work presents a novel aging-related regulatory mechanism in G₁ progression and intrinsic retention of several functional potentials in human *CD49f*⁺ cells, considerations of the systems used should coincide with interpretation. As mentioned throughout this thesis, the *CD49f*⁺ subset consistently identifies a population that is enriched for HSCs. Nevertheless, it remains a heterogenous and impure subset. Identification of decreased AKT and β -catenin activation and slower cycling in this population in addition to the downstream CD34⁺CD38⁻ cells suggests that this developmental mechanism persists into closely related subsets of primitive human hematopoietic cells, but does not necessarily reflect control systems operative in functionally defined HSCs. However, the functional purity of the *CD49f*⁺ subset is intertwined with the ability of current immunodeficient mouse models to elicit their repopulation potential. In contrast to the human system, mouse HSCs can be obtained at purities of up to ~50% (Benz et al., 2012; Kent et al., 2009). It thus remains unclear as to whether this difference in detectable purities between mouse and human HSCs is a reflection of differences in their contents of functionally equivalent cells or in their ability to be detected in syngeneic as compared to a xenogeneic host. Continued advancement in ‘humanizing’ mouse models may be able to bridge this gap. For instance, mice bearing human ossicles from transplanted BM

mesenchymal cells could serve to provide necessary human factors insufficiently supplied by the mouse (Reinisch et al., 2017).

Additionally, while most apparent changes reported here occurred between CB and young adult donors, the cycling delay and GF requirement for *in vitro* proliferation appeared to be progressive with age. Molecular characterizations of the G₁ delay and reduced AKT/ β -catenin signaling would then be expected to be more severe in cells isolated from older donors. Also important to note is the reliance here on adult sources coming from healthy individuals donating hematopoietic material for transplantation into patients thereby limiting the upper age to adults in their 60's. Analysis of these mechanisms in donors of more advanced ages could have important parallels with the rapid accumulation of CHIP with increasing age since many of these clones are believed to originate in the HSC compartment due to their long-term persistence (Jaiswal & Ebert, 2019). Since these somatic mutation-bearing clones grow to dominate the hematopoietic compartment, an impact on the proliferation of early cells or increased expansion downstream are implicated.

Finally, molecular characterization of regulators involved in the signaling and cycling differences obviously represent a subset of many players involved in these processes. Nevertheless, they do indicate an impact on a mitogen-sensitive early G₁-phase mechanism. Regulatory changes at other points of the cell cycle or alternative signaling pathways will require additional analysis and could also indicate co-operative or separate developmental mechanisms controlling proliferation. For example, assessing the level of replication stress experienced by *CD49f*⁺ cells of different ages might suggest mechanisms that promote the acquisition of mutations leading to CHIP or overt malignancy with advancing age.

5.4 Concluding remarks

The clinical utility and biological importance of HSCs as a developmental model relies on an understanding of the mechanisms regulating these cells. In this thesis, we report a developmental alteration which regulates G₁ progression in highly primitive human hematopoietic cells that is accompanied by an aging-associated altered sensitivity to mitogenic stimulation. This finding has immediate implications for *in vitro* and *in vivo* systems that can be anticipated to require optimization to further characterize and successfully manipulate HSCs isolated from differently aged human donors. It will be of future interest to determine if this mechanism is unique to the blood system, or whether it represents a fundamental mechanism regulating the cycling of many adult tissue stem cells, such as those in the skin or gut epithelium.

Bibliography

- AbuSamra, D. B., Aleisa, F. A., Al-Amoodi, A. S., Jalal Ahmed, H. M., Chin, C. J., Abuelela, A. F., Bergam, P., Sougrat, R., & Merzaban, J. S. (2017). Not just a marker: CD34 on human hematopoietic stem/progenitor cells dominates vascular selectin binding along with CD44. *Blood Advances*, *1*(27), 2799–2816. <https://doi.org/10.1182/bloodadvances.2017004317>
- Aiuti, A., Biasco, L., Scaramuzza, S., Ferrua, F., Cicalese, M. P., Baricordi, C., Dionisio, F., Calabria, A., Giannelli, S., Castiello, M. C., Bosticardo, M., Evangelio, C., Assanelli, A., Casiraghi, M., Nunzio, S. D., Callegaro, L., Benati, C., Rizzardi, P., Pellin, D., ... Naldini, L. (2013). Lentiviral Hematopoietic Stem Cell Gene Therapy in Patients with Wiskott-Aldrich Syndrome. *Science*, *341*(6148), 1233151. <https://doi.org/10.1126/science.1233151>
- Aleem, E., Kiyokawa, H., & Kaldis, P. (2005). Cdc2–cyclin E complexes regulate the G1/S phase transition. *Nature Cell Biology*, *7*(8), 831–836. <https://doi.org/10.1038/ncb1284>
- Allsopp, R. C., Morin, G. B., DePinho, R., Harley, C. B., & Weissman, I. L. (2003). Telomerase is required to slow telomere shortening and extend replicative lifespan of HSCs during serial transplantation. *Blood*, *102*(2), 517–520. <https://doi.org/10.1182/blood-2002-07-2334>
- Antonchuk, J., Sauvageau, G., & Humphries, R. K. (2002). HOXB4-Induced Expansion of Adult Hematopoietic Stem Cells Ex Vivo. *Cell*, *109*(1), 39–45. [https://doi.org/10.1016/S0092-8674\(02\)00697-9](https://doi.org/10.1016/S0092-8674(02)00697-9)
- Aubert, G., & Lansdorp, P. M. (2008). Telomeres and Aging. *Physiol Rev*, *88*, 23.

Audet, J., Miller, C. L., Eaves, C. J., & Piret, J. M. (2002). Common and distinct features of cytokine effects on hematopoietic stem and progenitor cells revealed by dose-response surface analysis. *Biotechnology and Bioengineering*, *80*(4), 393–404. <https://doi.org/10.1002/bit.10399>

Babovic, S., & Eaves, C. J. (2014). Hierarchical organization of fetal and adult hematopoietic stem cells. *Experimental Cell Research*, *329*(2), 185–191.

<https://doi.org/10.1016/j.yexcr.2014.08.005>

Baerlocher, G. M., Rice, K., Vulto, I., & Lansdorp, P. M. (2007). Longitudinal data on telomere length in leukocytes from newborn baboons support a marked drop in stem cell turnover around 1 year of age. *Aging Cell*, *6*(1), 121–123. <https://doi.org/10.1111/j.1474-9726.2006.00254.x>

Barker, T. H., Grenett, H. E., MacEwen, M. W., Tilden, S. G., Fuller, G. M., Settleman, J., Woods, A., Murphy-Ullrich, J., & Hagood, J. S. (2004). Thy-1 regulates fibroblast focal adhesions, cytoskeletal organization and migration through modulation of p190 RhoGAP and Rho GTPase activity. *Experimental Cell Research*, *295*(2), 488–496.

<https://doi.org/10.1016/j.yexcr.2004.01.026>

Baum, C. M., Weissman, I. L., Tsukamoto, A. S., Buckle, A. M., & Peault, B. (1992). Isolation of a candidate human hematopoietic stem-cell population. *Proceedings of the National Academy of Sciences*, *89*(7), 2804–2808. <https://doi.org/10.1073/pnas.89.7.2804>

Becht, E., McInnes, L., Healy, J., Dutertre, C.-A., Kwok, I. W. H., Ng, L. G., Ginhoux, F., & Newell, E. W. (2019). Dimensionality reduction for visualizing single-cell data using UMAP. *Nature Biotechnology*, *37*(1), 38–44. <https://doi.org/10.1038/nbt.4314>

Becker, A. J., McCulloch, E. A., Siminovitch, L., & Till, J. E. (1965). The Effect of Differing Demands for Blood Cell Production on DNA Synthesis by Hematopoietic Colony-Forming Cells of Mice. *Blood*, *26*, 296–308.

Becker, A. J., McCulloch, E. A., & Till, J. E. (1963). Cytological Demonstration of the Clonal Nature of Spleen Colonies Derived from Transplanted Mouse Marrow Cells. *Nature*, *197*(4866), 452–454. <https://doi.org/10.1038/197452a0>

Beerman, I., Bock, C., Garrison, B. S., Smith, Z. D., Gu, H., Meissner, A., & Rossi, D. J. (2013). Proliferation-Dependent Alterations of the DNA Methylation Landscape Underlie Hematopoietic Stem Cell Aging. *Cell Stem Cell*, *12*(4), 413–425. <https://doi.org/10.1016/j.stem.2013.01.017>

Beerman, I., Maloney, W. J., Weissmann, I. L., & Rossi, D. J. (2010). Stem cells and the aging hematopoietic system. *Current Opinion in Immunology*, *22*(4), 500–506. <https://doi.org/10.1016/j.coi.2010.06.007>

Beerman, I., Seita, J., Inlay, M. A., Weissman, I. L., & Rossi, D. J. (2014). Quiescent Hematopoietic Stem Cells Accumulate DNA Damage during Aging that Is Repaired upon Entry into Cell Cycle. *Cell Stem Cell*, *15*(1), 37–50. <https://doi.org/10.1016/j.stem.2014.04.016>

Belluschi, S., Calderbank, E. F., Ciaurro, V., Pijuan-Sala, B., Santoro, A., Mende, N., Diamanti, E., Sham, K. Y. C., Wang, X., Lau, W. W. Y., Jawaid, W., Göttgens, B., & Laurenti, E. (2018). Myelo-lymphoid lineage restriction occurs in the human haematopoietic stem cell compartment before lymphoid-primed multipotent progenitors. *Nature Communications*, *9*(1). <https://doi.org/10.1038/s41467-018-06442-4>

Benz, C., Copley, M. R., Kent, D. G., Wohrer, S., Cortes, A., Aghaeepour, N., Ma, E., Mader, H., Rowe, K., Day, C., Treloar, D., Brinkman, R. R., & Eaves, C. J. (2012). Hematopoietic Stem

Cell Subtypes Expand Differentially during Development and Display Distinct Lymphopoietic Programs. *Cell Stem Cell*, 10(3), 273–283. <https://doi.org/10.1016/j.stem.2012.02.007>

Bhatia, M., Wang, J. C. Y., Kapp, U., Bonnet, D., & Dick, J. E. (1997). Purification of primitive human hematopoietic cells capable of repopulating immune-deficient mice. *Proceedings of the National Academy of Sciences*, 94(10), 5320–5325. <https://doi.org/10.1073/pnas.94.10.5320>

Biasco, L., Pellin, D., Scala, S., Dionisio, F., Basso-Ricci, L., Leonardelli, L., Scaramuzza, S., Baricordi, C., Ferrua, F., Cicalese, M. P., Giannelli, S., Neduva, V., Dow, D. J., Schmidt, M., Von Kalle, C., Roncarolo, M. G., Ciceri, F., Vicard, P., Wit, E., ... Aiuti, A. (2016). In Vivo Tracking of Human Hematopoiesis Reveals Patterns of Clonal Dynamics during Early and Steady-State Reconstitution Phases. *Cell Stem Cell*, 19(1), 107–119. <https://doi.org/10.1016/j.stem.2016.04.016>

Biffi, A., Montini, E., Lorioli, L., Cesani, M., Fumagalli, F., Plati, T., Baldoli, C., Martino, S., Calabria, A., Canale, S., Benedicenti, F., Vallanti, G., Biasco, L., Leo, S., Kabbara, N., Zanetti, G., Rizzo, W. B., Mehta, N. A. L., Cicalese, M. P., ... Naldini, L. (2013). Lentiviral Hematopoietic Stem Cell Gene Therapy Benefits Metachromatic Leukodystrophy. *Science*, 341(6148), 1233158. <https://doi.org/10.1126/science.1233158>

Blasco, Maria A. (2005). Telomeres and human disease: Ageing, cancer and beyond. *Nature Reviews Genetics*, 6(8), 611–622. <https://doi.org/10.1038/nrg1656>

Blasco, María A, Lee, H.-W., Hande, M. P., Samper, E., Lansdorp, P. M., DePinho, R. A., & Greider, C. W. (1997). Telomere Shortening and Tumor Formation by Mouse Cells Lacking Telomerase RNA. *Cell*, 91(1), 25–34. [https://doi.org/10.1016/S0092-8674\(01\)80006-4](https://doi.org/10.1016/S0092-8674(01)80006-4)

Blokzijl, F., de Ligt, J., Jager, M., Sasselli, V., Roerink, S., Sasaki, N., Huch, M., Boymans, S., Kuijk, E., Prins, P., Nijman, I. J., Martincorena, I., Mokry, M., Wiegerinck, C. L., Middendorp, S., Sato, T., Schwank, G., Nieuwenhuis, E. E. S., Verstegen, M. M. A., ... van Boxtel, R. (2016). Tissue-specific mutation accumulation in human adult stem cells during life. *Nature*, 538(7624), 260–264. <https://doi.org/10.1038/nature19768>

Bock, C., Beerman, I., Lien, W.-H., Smith, Z. D., Gu, H., Boyle, P., Gnirke, A., Fuchs, E., Rossi, D. J., & Meissner, A. (2012). DNA Methylation Dynamics during In Vivo Differentiation of Blood and Skin Stem Cells. *Molecular Cell*, 47(4), 633–647. <https://doi.org/10.1016/j.molcel.2012.06.019>

Boitano, A. E., Wang, J., Romeo, R., Bouchez, L. C., Parker, A. E., Sutton, S. E., Walker, J. R., Flaveny, C. A., Perdew, G. H., Denison, M. S., Schultz, P. G., & Cooke, M. P. (2010). Aryl Hydrocarbon Receptor Antagonists Promote the Expansion of Human Hematopoietic Stem Cells. *Science*, 329(5997), 1345–1348. <https://doi.org/10.1126/science.1191536>

Bonnet, D., Lemoine, F. M., Najman, A., & Guigon, M. (1995). Comparison of the inhibitory effect of AcSDKP, TNF-alpha, TGF-beta, and MIP-1 alpha on marrow-purified CD34+ progenitors. *Experimental Hematology*, 23(6), 551–556.

Bowie, M. B., Kent, D. G., Dykstra, B., McKnight, K. D., McCaffrey, L., Hoodless, P. A., & Eaves, C. J. (2007). Identification of a new intrinsically timed developmental checkpoint that reprograms key hematopoietic stem cell properties. *Proceedings of the National Academy of Sciences*, 104(14), 5878–5882. <https://doi.org/10.1073/pnas.0700460104>

Bowie, M. B., McKnight, K. D., Kent, D. G., McCaffrey, L., Hoodless, P. A., & Eaves, C. J. (2006). Hematopoietic stem cells proliferate until after birth and show a reversible phase-specific

engraftment defect. *Journal of Clinical Investigation*, 116(10), 2808–2816.

<https://doi.org/10.1172/JCI28310>

Bowie, Michelle B., Kent, D. G., Copley, M. R., & Eaves, C. J. (2007). Steel factor responsiveness regulates the high self-renewal phenotype of fetal hematopoietic stem cells.

Blood, 109(11), 5043–5048. <https://doi.org/10.1182/blood-2006-08-037770>

Bradfute, S. B., Graubert, T. A., & Goodell, M. A. (2005). Roles of Sca-1 in hematopoietic stem/progenitor cell function. *Experimental Hematology*, 33(7), 836–843.

<https://doi.org/10.1016/j.exphem.2005.04.001>

Bruce, W. R., Meeker, B. E., & Valeriote, F. A. (1966). Comparison of the Sensitivity of Normal Hematopoietic and Transplanted Lymphoma Colony-Forming Cells to Chemotherapeutic Agents Administered In Vivo. *JOURNAL OF THE NATIONAL CANCER INSTITUTE*, 37, 233–245.

Buenrostro, J. D., Corces, M. R., Lareau, C. A., Beijing, W., Schep, A. N., Aryee, M. J., Majeti, R., Chang, H. Y., & Greenleaf, W. J. (2018). Integrated Single-Cell Analysis Maps the Continuous Regulatory Landscape of Human Hematopoietic Differentiation. *Cell*, 173, 1535–1548. <https://doi.org/10.1016/j.cell.2018.03.074>

Busch, K., Klapproth, K., Barile, M., Flossdorf, M., Holland-Letz, T., Schlenner, S. M., Reth, M., Höfer, T., & Rodewald, H.-R. (2015). Fundamental properties of unperturbed haematopoiesis from stem cells in vivo. *Nature*, 518(7540), 542–546.

<https://doi.org/10.1038/nature14242>

Campbell, V., Legendre, P., & Lapointe, F.-J. (2011). The performance of the Congruence Among Distance Matrices (CADM) test in phylogenetic analysis. *BMC Evolutionary Biology*, 11(1), 64. <https://doi.org/10.1186/1471-2148-11-64>

Carrelha, J., Meng, Y., Kettyle, L. M., Luis, T. C., Norfo, R., Alcolea, V., Boukarabila, H., Grasso, F., Gambardella, A., Grover, A., Högstrand, K., Lord, A. M., Sanjuan-Pla, A., Woll, P. S., Nerlov, C., & Jacobsen, S. E. W. (2018). Hierarchically related lineage-restricted fates of multipotent haematopoietic stem cells. *Nature*, *554*(7690), 106–111.

<https://doi.org/10.1038/nature25455>

Carrero, D., Soria-Valles, C., & López-Otín, C. (2016). Hallmarks of progeroid syndromes: Lessons from mice and reprogrammed cells. *Disease Models & Mechanisms*, *9*(7), 719–735.

<https://doi.org/10.1242/dmm.024711>

Cashman, J., Clark-Lewis, I., Eaves, A., & Eaves, C. (2002). Stromal-derived factor 1 inhibits the cycling of very primitive human hematopoietic cells in vitro and in NOD/SCID mice. *Blood*, *99*(3), 792–799. <https://doi.org/10.1182/blood.V99.3.792>

Cashman, J. D., Eaves, C. J., Sarris, A. H., & Eaves, A. C. (1998). MCP-1, not MIP-1, Is the Endogenous Chemokine That Cooperates With TGF- β to Inhibit the Cycling of Primitive Normal but not Leukemic (CML) Progenitors in Long-Term Human Marrow Cultures. *Blood*, *92*(7), 2338–2344.

Cesana, M., Guo, M. H., Cacchiarelli, D., Wahlster, L., Barragan, J., Doulatov, S., Vo, L. T., Salvatori, B., Trapnell, C., Clement, K., Cahan, P., Tsanov, K. M., Sousa, P. M., Tazon-Vega, B., Bolondi, A., Giorgi, F. M., Califano, A., Rinn, J. L., Meissner, A., ... Daley, G. Q. (2018). A CLK3-HMGA2 Alternative Splicing Axis Impacts Human Hematopoietic Stem Cell Molecular Identity throughout Development. *Cell Stem Cell*, *22*(4), 575-588.e7.

<https://doi.org/10.1016/j.stem.2018.03.012>

Chagraoui, J., Girard, S., Spinella, J.-F., Simon, L., Bonneil, E., Mayotte, N., MacRae, T., Coulombe-Huntington, J., Bertomeu, T., Moison, C., Tomellini, E., Thibault, P., Tyers, M., Marinier, A., & Sauvageau, G. (2021). UM171 Preserves Epigenetic Marks that Are Reduced in Ex Vivo Culture of Human HSCs via Potentiation of the CLR3-KBTBD4 Complex. *Cell Stem Cell*, 28(1), 48-62.e6. <https://doi.org/10.1016/j.stem.2020.12.002>

Chagraoui, J., Lehnertz, B., Girard, S., Spinella, J. F., Fares, I., Tomellini, E., Mayotte, N., Corneau, S., MacRae, T., Simon, L., & Sauvageau, G. (2019). UM171 induces a homeostatic inflammatory-detoxification response supporting human HSC self-renewal. *PLOS ONE*, 14(11), e0224900. <https://doi.org/10.1371/journal.pone.0224900>

Challen, G. A., Sun, D., Jeong, M., Luo, M., Jelinek, J., Berg, J. S., Bock, C., Vasanthakumar, A., Gu, H., Xi, Y., Liang, S., Lu, Y., Darlington, G. J., Meissner, A., Issa, J.-P. J., Godley, L. A., Li, W., & Goodell, M. A. (2012). Dnmt3a is essential for hematopoietic stem cell differentiation. *Nature Genetics*, 44(1), 23–31. <https://doi.org/10.1038/ng.1009>

Champion, K. M., Gilbert, J. G. R., Asimakopoulos, F. A., Hinshelwood, S., & Green, A. R. (1997). Clonal haemopoiesis in normal elderly women: Implications for the myeloproliferative disorders and myelodysplastic syndromes. *British Journal of Haematology*, 97(4), 920–926. <https://doi.org/10.1046/j.1365-2141.1997.1933010.x>

Chang, F., Lee, J. T., Navolanic, P. M., Steelman, L. S., Shelton, J. G., Blalock, W. L., Franklin, R. A., & McCubrey, J. A. (2003). Involvement of PI3K/Akt pathway in cell cycle progression, apoptosis, and neoplastic transformation: A target for cancer chemotherapy. *Leukemia*, 17(3), 590–603. <https://doi.org/10.1038/sj.leu.2402824>

Charbord, P., Tavian, M., Humeau, L., & Peault, B. (1996). Early ontogeny of the human marrow from long bones: An immunohistochemical study of hematopoiesis and its microenvironment [see comments]. *Blood*, *87*(10), 4109–4119.

<https://doi.org/10.1182/blood.V87.10.4109.bloodjournal87104109>

Cheng, T., Rodrigues, N. P., Shen, H., Yang, Y., Dombkowski, D., Sykes, M., & Scadden, D. T. (2000). Hematopoietic Stem Cell Quiescence Maintained by p21cip1/waf1. *Science*, *287*(5459), 1804–1808. <https://doi.org/10.1126/science.287.5459.1804>

Cheshier, S. H., Morrison, S. J., Liao, X., & Weissman, I. L. (1999). In vivo proliferation and cell cycle kinetics of long-term self-renewing hematopoietic stem cells. *Proceedings of the National Academy of Sciences*, *96*(6), 3120–3125. <https://doi.org/10.1073/pnas.96.6.3120>

Cheung, A. M. S., Nguyen, L. V., Carles, A., Beer, P., Miller, P. H., Knapp, D. J. H. F., Dhillon, K., Hirst, M., & Eaves, C. J. (2013). Analysis of the clonal growth and differentiation dynamics of primitive barcoded human cord blood cells in NSG mice. *Blood*, *122*(18), 3129–3137.

<https://doi.org/10.1182/blood-2013-06-508432>

Cheung, T. H., & Rando, T. A. (2013). Molecular regulation of stem cell quiescence. *Nature Reviews Molecular Cell Biology*, *14*(6), 329–340. <https://doi.org/10.1038/nrm3591>

Cho, R. H., Sieburg, H. B., & Muller-Sieburg, C. E. (2008). A new mechanism for the aging of hematopoietic stem cells: Aging changes the clonal composition of the stem cell compartment but not individual stem cells. *Blood*, *111*(12), 5553–5561. <https://doi.org/10.1182/blood-2007-11-123547>

Copley, M. R., Babovic, S., Benz, C., Knapp, D. J. H. F., Beer, P. A., Kent, D. G., Wohrer, S., Treloar, D. Q., Day, C., Rowe, K., Mader, H., Kuchenbauer, F., Humphries, R. K., & Eaves, C.

J. (2013). The Lin28b–let-7–Hmga2 axis determines the higher self-renewal potential of fetal haematopoietic stem cells. *Nature Cell Biology*, *15*(8), 916–925. <https://doi.org/10.1038/ncb2783>

Cosgun, K. N., Rahmig, S., Mende, N., Reinke, S., Hauber, I., Schäfer, C., Petzold, A., Weisbach, H., Heidkamp, G., Purbojo, A., Cesnjevar, R., Platz, A., Bornhäuser, M., Schmitz, M., Dudziak, D., Hauber, J., Kirberg, J., & Waskow, C. (2014). Kit Regulates HSC Engraftment across the Human-Mouse Species Barrier. *Cell Stem Cell*, *15*(2), 227–238.

<https://doi.org/10.1016/j.stem.2014.06.001>

Crane, G. M., Jeffery, E., & Morrison, S. J. (2017). Adult haematopoietic stem cell niches. *Nature Reviews Immunology*, *17*(9), 573–590. <https://doi.org/10.1038/nri.2017.53>

Csaszar, E., Kirouac, D. C., Yu, M., Wang, W., Qiao, W., Cooke, M. P., Boitano, A. E., Ito, C., & Zandstra, P. W. (2012). Rapid Expansion of Human Hematopoietic Stem Cells by Automated Control of Inhibitory Feedback Signaling. *Cell Stem Cell*, *10*(2), 218–229.

<https://doi.org/10.1016/j.stem.2012.01.003>

de Haan, G., Nijhof, W., & Van Zant, G. (1997). Mouse Strain-Dependent Changes in Frequency and Proliferation of Hematopoietic Stem Cells During Aging: Correlation Between Lifespan and Cycling Activity. *Blood*, *89*(5), 1543–1550. <https://doi.org/10.1182/blood.V89.5.1543>

de Pater, E., Kaimakis, P., Vink, C. S., Yokomizo, T., Yamada-Inagawa, T., van der Linden, R., Kartalaei, P. S., Camper, S. A., Speck, N., & Dzierzak, E. (2013). Gata2 is required for HSC generation and survival. *Journal of Experimental Medicine*, *210*(13), 2843–2850.

<https://doi.org/10.1084/jem.20130751>

Deegan, T. D., & Diffley, J. F. (2016). MCM: One ring to rule them all. *Current Opinion in Structural Biology*, *37*, 145–151. <https://doi.org/10.1016/j.sbi.2016.01.014>

Doulatov, S., Notta, F., Eppert, K., Nguyen, L. T., Ohashi, P. S., & Dick, J. E. (2010). Revised map of the human progenitor hierarchy shows the origin of macrophages and dendritic cells in early lymphoid development. *Nature Immunology*, *11*(7), 585–593.

<https://doi.org/10.1038/ni.1889>

Doulatov, S., Notta, F., Laurenti, E., & Dick, J. E. (2012). Hematopoiesis: A Human Perspective. *Cell Stem Cell*, *10*(2), 120–136. <https://doi.org/10.1016/j.stem.2012.01.006>

Dykstra, B., Ramunas, J., Kent, D., McCaffrey, L., Szumsky, E., Kelly, L., Farn, K., Blaylock, A., Eaves, C., & Jarvis, E. (2006). High-resolution video monitoring of hematopoietic stem cells cultured in single-cell arrays identifies new features of self-renewal. *Proceedings of the National Academy of Sciences*, *103*(21), 8185–8190. <https://doi.org/10.1073/pnas.0602548103>

Dykstra, Brad, Kent, D., Bowie, M., McCaffrey, L., Hamilton, M., Lyons, K., Lee, S.-J., Brinkman, R., & Eaves, C. (2007). Long-Term Propagation of Distinct Hematopoietic Differentiation Programs In Vivo. *Cell Stem Cell*, *1*(2), 218–229.

<https://doi.org/10.1016/j.stem.2007.05.015>

Dykstra, Brad, Olthof, S., Schreuder, J., Ritsema, M., & de Haan, G. (2011). Clonal analysis reveals multiple functional defects of aged murine hematopoietic stem cells. *Journal of Experimental Medicine*, *208*(13), 2691–2703. <https://doi.org/10.1084/jem.20111490>

Eaves, C. J. (2015). Hematopoietic stem cells: Concepts, definitions, and the new reality. *Blood*, *125*(17), 2605–2613. <https://doi.org/10.1182/blood-2014-12-570200>

Ergen, A. V., Boles, N. C., & Goodell, M. A. (2012). Rantes/Ccl5 influences hematopoietic stem cell subtypes and causes myeloid skewing. *Blood*, *119*(11), 2500–2509.

<https://doi.org/10.1182/blood-2011-11-391730>

Ernst, T., Chase, A. J., Score, J., Hidalgo-Curtis, C. E., Bryant, C., Jones, A. V., Waghorn, K., Zoi, K., Ross, F. M., Reiter, A., Hochhaus, A., Drexler, H. G., Duncombe, A., Cervantes, F., Oscier, D., Boultonwood, J., Grand, F. H., & Cross, N. C. P. (2010). Inactivating mutations of the histone methyltransferase gene EZH2 in myeloid disorders. *Nature Genetics*, *42*(8), 722–726. <https://doi.org/10.1038/ng.621>

Escribano, L., Ocqueteaub, M., Almeida, J., Orfao, A., & Migue, J. F. S. (1998). Expression of the c-kit (CD117) Molecule in Normal and Malignant Hematopoiesis. *Leukemia & Lymphoma*, *30*(5–6), 459–466. <https://doi.org/10.3109/10428199809057558>

Fares, I., Chagraoui, J., Gareau, Y., Gingras, S., Ruel, R., Mayotte, N., Csaszar, E., Knapp, D. J. H. F., Miller, P., Ngom, M., Imren, S., Roy, D.-C., Watts, K. L., Kiem, H.-P., Herrington, R., Iscove, N. N., Humphries, R. K., Eaves, C. J., Cohen, S., ... Sauvageau, G. (2014). Pyrimidoindole derivatives are agonists of human hematopoietic stem cell self-renewal. *Science*, *345*(6203), 1509–1512. <https://doi.org/10.1126/science.1256337>

Fares, I., Chagraoui, J., Lehnertz, B., MacRae, T., Mayotte, N., Tomellini, E., Aubert, L., Roux, P. P., & Sauvageau, G. (2017). EPCR expression marks UM171-expanded CD34+ cord blood stem cells. *Blood*, *129*(25), 3344–3351. <https://doi.org/10.1182/blood-2016-11-750729>

Farlik, M., Halbritter, F., Müller, F., Choudry, F. A., Ebert, P., Klughammer, J., Farrow, S., Santoro, A., Ciaurro, V., Mathur, A., Uppal, R., Stunnenberg, H. G., Ouwehand, W. H., Laurenti, E., Lengauer, T., Frontini, M., & Bock, C. (2016). DNA Methylation Dynamics of Human Hematopoietic Stem Cell Differentiation. *Cell Stem Cell*, *19*(6), 808–822. <https://doi.org/10.1016/j.stem.2016.10.019>

Fey, M., Liechti-Gallati, S., von Rohr, A., Borisch, B., Theilkas, L., Schneider, V., Oestreicher, M., Nagel, S., Ziemiecki, A., & Tobler, A. (1994). Clonality and X-inactivation patterns in hematopoietic cell populations detected by the highly informative M27 beta DNA probe [see comments]. *Blood*, *83*(4), 931–938. <https://doi.org/10.1182/blood.V83.4.931.931>

Finke, J., Schmoor, C., Bethge, W. A., Ottinger, H. D., Stelljes, M., Zander, A. R., Volin, L., Heim, D. A., Schwerdtfeger, R., Kolbe, K., Mayer, J., Maertens, J. A., Linkesch, W., Holler, E., Koza, V., Bornhäuser, M., Einsele, H., Bertz, H., Grishina, O., & Socié, G. (2012). Prognostic Factors Affecting Outcome after Allogeneic Transplantation for Hematological Malignancies from Unrelated Donors: Results from a Randomized Trial. *Biology of Blood and Marrow Transplantation*, *18*(11), 1716–1726. <https://doi.org/10.1016/j.bbmt.2012.06.001>

Flach, J., Bakker, S. T., Mohrin, M., Conroy, P. C., Pietras, E. M., Reynaud, D., Alvarez, S., Diolaiti, M. E., Ugarte, F., Forsberg, E. C., Le Beau, M. M., Stohr, B. A., Méndez, J., Morrison, C. G., & Passegué, E. (2014). Replication stress is a potent driver of functional decline in ageing haematopoietic stem cells. *Nature*, *512*(7513), 198–202. <https://doi.org/10.1038/nature13619>

Florian, M. C., Dörr, K., Niebel, A., Daria, D., Schrezenmeier, H., Rojewski, M., Filippi, M.-D., Hasenberg, A., Gunzer, M., Scharffetter-Kochanek, K., Zheng, Y., & Geiger, H. (2012). Cdc42 Activity Regulates Hematopoietic Stem Cell Aging and Rejuvenation. *Cell Stem Cell*, *10*(5), 520–530. <https://doi.org/10.1016/j.stem.2012.04.007>

Ford, E., Hamerton, L., Barnes, D. W. H., & Loutit, F. (1956). Cytological Identification of Radiation-Chimeras. *Nature*, *177*, 452–454.

- Foudi, A., Hochedlinger, K., Van Buren, D., Schindler, J. W., Jaenisch, R., Carey, V., & Hock, H. (2009). Analysis of histone 2B-GFP retention reveals slowly cycling hematopoietic stem cells. *Nature Biotechnology*, *27*(1), 84–90. <https://doi.org/10.1038/nbt.1517>
- Franceschi, C., Bonafè, M., Valensin, S., Olivieri, F., De Luca, M., Ottaviani, E., & De Benedictis, G. (2006). Inflamm-aging: An Evolutionary Perspective on Immunosenescence. *Annals of the New York Academy of Sciences*, *908*(1), 244–254. <https://doi.org/10.1111/j.1749-6632.2000.tb06651.x>
- Franceschi, C., Garagnani, P., Parini, P., Giuliani, C., & Santoro, A. (2018). Inflammaging: A new immune–metabolic viewpoint for age-related diseases. *Nature Reviews Endocrinology*, *14*(10), 576–590. <https://doi.org/10.1038/s41574-018-0059-4>
- Frelin, C., Herrington, R., Janmohamed, S., Barbara, M., Tran, G., Paige, C. J., Benveniste, P., Zuñiga-Pflücker, J.-C., Souabni, A., Busslinger, M., & Iscove, N. N. (2013). GATA-3 regulates the self-renewal of long-term hematopoietic stem cells. *Nature Immunology*, *14*(10), 1037–1044. <https://doi.org/10.1038/ni.2692>
- Gao, Y., Yang, P., Shen, H., Yu, H., Song, X., Zhang, L., Zhang, P., Cheng, H., Xie, Z., Hao, S., Dong, F., Ma, S., Ji, Q., Bartlow, P., Ding, Y., Wang, L., Liu, H., Li, Y., Cheng, H., ... Xie, X.-Q. (2015). Small-molecule inhibitors targeting INK4 protein p18INK4C enhance ex vivo expansion of haematopoietic stem cells. *Nature Communications*, *6*(1), 6328. <https://doi.org/10.1038/ncomms7328>
- García-Gutiérrez, L., Delgado, M. D., & León, J. (2019). MYC Oncogene Contributions to Release of Cell Cycle Brakes. *Genes*, *10*(3), 244. <https://doi.org/10.3390/genes10030244>

García-Pratt, L., Kaufmann, K. B., Schneiter, F., Voisin, V., Murison, A., Chen, J., Chan-Seng-Yue, M., Gan, O., McLeod, J., Smith, S., Shoong, M., Paris, D., Pan, K., Zeng, A., Krivdova, G., Gupta, K., Takayanagi, S.-I., Wagenblast, E., Wang, W., ... Dick, J. E. (2021). Dichotomous regulation of lysosomes by MYC and TFEB controls hematopoietic stem cell fate. *Bioarxiv*.

Geiger, H., de Haan, G., & Florian, M. C. (2013). The ageing haematopoietic stem cell compartment. *Nature Reviews Immunology*, *13*(5), 376–389. <https://doi.org/10.1038/nri3433>

Genovese, G., Kähler, A. K., Handsaker, R. E., Lindberg, J., Rose, S. A., Bakhoum, S. F., Chambert, K., Mick, E., Neale, B. M., Fromer, M., Purcell, S. M., Svantesson, O., Landén, M., Höglund, M., Lehmann, S., Gabriel, S. B., Moran, J. L., Lander, E. S., Sullivan, P. F., ...

McCarroll, S. A. (2014). Clonal Hematopoiesis and Blood-Cancer Risk Inferred from Blood DNA Sequence. *New England Journal of Medicine*, *371*(26), 2477–2487.

<https://doi.org/10.1056/NEJMoa1409405>

Giustacchini, A., Thongjuea, S., Barkas, N., Woll, P. S., Povinelli, B. J., Booth, C. A. G., Sopp, P., Norfo, R., Rodriguez-Meira, A., Ashley, N., Jamieson, L., Vyas, P., Anderson, K.,

Segerstolpe, Å., Qian, H., Olsson-Strömberg, U., Mustjoki, S., Sandberg, R., Jacobsen, S. E. W., & Mead, A. J. (2017). Single-cell transcriptomics uncovers distinct molecular signatures of stem cells in chronic myeloid leukemia. *Nature Medicine*, *23*(6), 692–702.

<https://doi.org/10.1038/nm.4336>

Görgens, A., Radtke, S., Möllmann, M., Cross, M., Dürig, J., Horn, P. A., & Giebel, B. (2013). Revision of the Human Hematopoietic Tree: Granulocyte Subtypes Derive from Distinct Hematopoietic Lineages. *Cell Reports*, *3*(5), 1539–1552.

<https://doi.org/10.1016/j.celrep.2013.04.025>

Goyama, S., Yamamoto, G., Shimabe, M., Sato, T., Ichikawa, M., Ogawa, S., Chiba, S., & Kurokawa, M. (2008). Evi-1 Is a Critical Regulator for Hematopoietic Stem Cells and Transformed Leukemic Cells. *Cell Stem Cell*, 3(2), 207–220.

<https://doi.org/10.1016/j.stem.2008.06.002>

Grover, A., Sanjuan-Pla, A., Thongjuea, S., Carrelha, J., Giustacchini, A., Gambardella, A., Macaulay, I., Mancini, E., Luis, T. C., Mead, A., Jacobsen, S. E. W., & Nerlov, C. (2016). Single-cell RNA sequencing reveals molecular and functional platelet bias of aged haematopoietic stem cells. *Nature Communications*, 7(1), 11075.

<https://doi.org/10.1038/ncomms11075>

Guralnik, J. M., Eisenstaedt, R. S., Ferrucci, L., Klein, H. G., & Woodman, R. C. (2004). Prevalence of anemia in persons 65 years and older in the United States: Evidence for a high rate of unexplained anemia. *Blood*, 104(8), 2263–2268. <https://doi.org/10.1182/blood-2004-05-1812>

Hahne, F., LeMeur, N., Brinkman, R. R., Ellis, B., Haaland, P., Sarkar, D., Spidlen, J., Strain, E., & Gentleman, R. (2009). flowCore: A Bioconductor package for high throughput flow cytometry. *BMC Bioinformatics*, 10(1), 106. <https://doi.org/10.1186/1471-2105-10-106>

Hao, S., Chen, C., & Cheng, T. (2016). Cell cycle regulation of hematopoietic stem or progenitor cells. *International Journal of Hematology*, 103(5), 487–497. <https://doi.org/10.1007/s12185-016-1984-4>

He, S., Kim, I., Lim, M. S., & Morrison, S. J. (2011). Sox17 expression confers self-renewal potential and fetal stem cell characteristics upon adult hematopoietic progenitors. *Genes & Development*, 25(15), 1613–1627. <https://doi.org/10.1101/gad.2052911>

Ho, T. T., Warr, M. R., Adelman, E. R., Lansinger, O. M., Flach, J., Verovskaya, E. V., Figueroa, M. E., & Passegué, E. (2017). Autophagy maintains the metabolism and function of young and old stem cells. *Nature*, *543*(7644), 205–210. <https://doi.org/10.1038/nature21388>

Hock, H., Hamblen, M. J., Rooke, H. M., Schindler, J. W., Saleque, S., Fujiwara, Y., & Orkin, S. H. (2004). Gfi-1 restricts proliferation and preserves functional integrity of haematopoietic stem cells. *Nature*, *431*(7011), 1002–1007. <https://doi.org/10.1038/nature02994>

Hogge, D., Lansdorp, P., Reid, D., Gerhard, B., & Eaves, C. (1996). Enhanced detection, maintenance, and differentiation of primitive human hematopoietic cells in cultures containing murine fibroblasts engineered to produce human stem cell factor, interleukin-3, and granulocyte colony-stimulating factor. *Blood*, *88*(10), 3765–3773. <https://doi.org/10.1182/blood.V88.10.3765.bloodjournal88103765>

Holyoake, T., Nicolini, F. E., & Eaves, C. J. (1999). Functional differences between transplantable human hematopoietic stem cells from fetal liver, cord blood, and adult marrow. *Experimental Hematology*, *27*(9), 1418–1427. [https://doi.org/10.1016/S0301-472X\(99\)00078-8](https://doi.org/10.1016/S0301-472X(99)00078-8)

Hoppe, P. S., Schwarzfischer, M., Loeffler, D., Kokkaliaris, K. D., Hilsenbeck, O., Moritz, N., Endele, M., Filipczyk, A., Gambardella, A., Ahmed, N., Eitzrodt, M., Coutu, D. L., Rieger, M. A., Marr, C., Strasser, M. K., Schauburger, B., Burtscher, I., Ermakova, O., Bürger, A., ... Schroeder, T. (2016). Early myeloid lineage choice is not initiated by random PU.1 to GATA1 protein ratios. *Nature*, *535*(7611), 299–302. <https://doi.org/10.1038/nature18320>

Howard, A., & Pelc, S. R. (1951). Synthesis of Nucleoprotein in Bean Root Cells. *Nature*, *167*, 599–600.

Huber, W., Carey, V. J., Gentleman, R., Anders, S., Carlson, M., Carvalho, B. S., Bravo, H. C., Davis, S., Gatto, L., Girke, T., Gottardo, R., Hahne, F., Hansen, K. D., Irizarry, R. A., Lawrence, M., Love, M. I., MacDonald, J., Obenchain, V., Oleś, A. K., ... Morgan, M. (2015).

Orchestrating high-throughput genomic analysis with Bioconductor. *Nature Methods*, *12*(2), 115–121. <https://doi.org/10.1038/nmeth.3252>

Hui, T., Cao, Q., Wegrzyn-Woltosz, J., O'Neill, K., Hammond, C. A., Knapp, D. J. H. F., Laks, E., Moksa, M., Aparicio, S., Eaves, C. J., Karsan, A., & Hirst, M. (2018). High-Resolution Single-Cell DNA Methylation Measurements Reveal Epigenetically Distinct Hematopoietic Stem Cell Subpopulations. *Stem Cell Reports*, *11*(2), 578–592.

<https://doi.org/10.1016/j.stemcr.2018.07.003>

Hume, S., Dianov, G. L., & Ramadan, K. (2020). A unified model for the G1/S cell cycle transition. *Nucleic Acids Research*, *48*(22), 12483–12501. <https://doi.org/10.1093/nar/gkaa1002>

Huntsman, H. D., Bat, T., Cheng, H., Cash, A., Cheruku, P. S., Fu, J.-F., Keyvanfar, K., Childs, R. W., Dunbar, C. E., & Larochelle, A. (2015). Human hematopoietic stem cells from mobilized peripheral blood can be purified based on CD49f integrin expression. *Blood*, *126*(13), 1631–1633. <https://doi.org/10.1182/blood-2015-07-660670>

Ikuta, K., & Weissman, I. L. (1992). Evidence that hematopoietic stem cells express mouse c-kit but do not depend on steel factor for their generation. *Proceedings of the National Academy of Sciences*, *89*(4), 1502–1506. <https://doi.org/10.1073/pnas.89.4.1502>

Imren, S., Heuser, M., Gasparetto, M., Beer, P. A., Norddahl, G. L., Xiang, P., Chen, L., Berg, T., Rhyasen, G. W., Rosten, P., Park, G., Moon, Y., Weng, A. P., Eaves, C. J., & Humphries, R.

K. (2014). Modeling de novo leukemogenesis from human cord blood with MN1 and NUP98HOXD13. *Blood*, *124*(24), 3608–3612. <https://doi.org/10.1182/blood-2014-04-564666>

Ivanovs, A., Rybtsov, S., Ng, E. S., Stanley, E. G., Elefanty, A. G., & Medvinsky, A. (2017). Human haematopoietic stem cell development: From the embryo to the dish. *Development*, *144*(13), 2323–2337. <https://doi.org/10.1242/dev.134866>

Iwama, A., Oguro, H., Negishi, M., Kato, Y., Morita, Y., Tsukui, H., Ema, H., Kamijo, T., Katoh-Fukui, Y., Koseki, H., van Lohuizen, M., & Nakauchi, H. (2004). Enhanced Self-Renewal of Hematopoietic Stem Cells Mediated by the Polycomb Gene Product Bmi-1. *Immunity*, *21*, 843–851.

Jacobson, L. O., Simmons, E. L., Marks, E. K., & Eldredge, J. H. (1951). Recovery from Radiation Injury. *Science*, *113*(2940), 510–511. <https://doi.org/10.1126/science.113.2940.510>

Jaiswal, S., & Ebert, B. L. (2019). Clonal hematopoiesis in human aging and disease. *Science*, *366*(6465), eaan4673. <https://doi.org/10.1126/science.aan4673>

Jaiswal, S., Fontanillas, P., Flannick, J., Manning, A., Grauman, P. V., Mar, B. G., Lindsley, R. C., Mermel, C. H., Burt, N., Chavez, A., Higgins, J. M., Moltchanov, V., Kuo, F. C., Kluk, M. J., Henderson, B., Kinnunen, L., Koistinen, H. A., Ladenvall, C., Getz, G., ... Ebert, B. L. (2014). Age-Related Clonal Hematopoiesis Associated with Adverse Outcomes. *New England Journal of Medicine*, *371*(26), 2488–2498. <https://doi.org/10.1056/NEJMoa1408617>

Janzen, V., Forkert, R., Fleming, H. E., Saito, Y., Waring, M. T., Dombkowski, D. M., Cheng, T., DePinho, R. A., Sharpless, N. E., & Scadden, D. T. (2006). Stem-cell ageing modified by the cyclin-dependent kinase inhibitor p16INK4a. *Nature*, *443*(7110), 421–426.

<https://doi.org/10.1038/nature05159>

Jeong, M., Park, H. J., Celik, H., Ostrander, E. L., Reyes, J. M., Guzman, A., Rodriguez, B., Lei, Y., Lee, Y., Ding, L., Guryanova, O. A., Li, W., Goodell, M. A., & Challen, G. A. (2018). Loss of Dnmt3a immortalizes hematopoietic stem cells in vivo. *Cell Reports*, *23*(1), 1–10.

<https://doi.org/10.1016/j.celrep.2018.03.025>

Karamitros, D., Stoilova, B., Aboukhalil, Z., Hamey, F., Reinisch, A., Samitsch, M., Quek, L., Otto, G., Repapi, E., Doondea, J., Usukhbayar, B., Calvo, J., Taylor, S., Goardon, N., Six, E., Pflumio, F., Porcher, C., Majeti, R., Göttgens, B., & Vyas, P. (2018). Single-cell analysis reveals the continuum of human lympho-myeloid progenitor cells. *Nature Immunology*, *19*(1), 85.

<https://doi.org/10.1038/s41590-017-0001-2>

Kent, D., Copley, M., Benz, C., Dykstra, B., Bowie, M., & Eaves, C. (2008). Regulation of Hematopoietic Stem Cells by the Steel Factor/KIT Signaling Pathway: Fig. 1. *Clinical Cancer Research*, *14*(7), 1926–1930. <https://doi.org/10.1158/1078-0432.CCR-07-5134>

Kent, D. G., Copley, M. R., Benz, C., Wöhrer, S., Dykstra, B. J., Ma, E., Cheyne, J., Zhao, Y., Bowie, M. B., Zhao, Y., Gasparetto, M., Delaney, A., Smith, C., Marra, M., & Eaves, C. J. (2009). Prospective isolation and molecular characterization of hematopoietic stem cells with durable self-renewal potential. *Blood*, *113*(25), 6342–6350. <https://doi.org/10.1182/blood-2008-12-192054>

Kiel, M. J., He, S., Ashkenazi, R., Gentry, S. N., Teta, M., Kushner, J. A., Jackson, T. L., & Morrison, S. J. (2007). Haematopoietic stem cells do not asymmetrically segregate chromosomes or retain BrdU. *Nature*, *449*(7159), 238–242. <https://doi.org/10.1038/nature06115>

Kim, I., Saunders, T. L., & Morrison, S. J. (2007). Sox17 Dependence Distinguishes the Transcriptional Regulation of Fetal from Adult Hematopoietic Stem Cells. *Cell*, 130(3), 470–483. <https://doi.org/10.1016/j.cell.2007.06.011>

Kimura, S., Roberts, A. W., Metcalf, D., & Alexander, W. S. (1998). Hematopoietic stem cell deficiencies in mice lacking c-Mpl, the receptor for thrombopoietin. *Proceedings of the National Academy of Sciences*, 95(3), 1195–1200. <https://doi.org/10.1073/pnas.95.3.1195>

Knapp, D. J. H. F., Hammond, C. A., Aghaeepour, N., Miller, P. H., Pellacani, D., Beer, P. A., Sachs, K., Qiao, W., Wang, W., Humphries, R. K., Sauvageau, G., Zandstra, P. W., Bendall, S. C., Nolan, G. P., Hansen, C., & Eaves, C. J. (2016). Distinct signaling programs control human hematopoietic stem cell survival and proliferation. *Blood*, blood-2016-09-740654. <https://doi.org/10.1182/blood-2016-09-740654>

Knapp, D. J. H. F., Hammond, C. A., Hui, T., Loenhout, M. T. J. van, Wang, F., Aghaeepour, N., Miller, P. H., Moksa, M., Rabu, G. M., Beer, P. A., Pellacani, D., Humphries, R. K., Hansen, C., Hirst, M., & Eaves, C. J. (2018). Single-cell analysis identifies a CD33 + subset of human cord blood cells with high regenerative potential. *Nature Cell Biology*, 20(6), 710. <https://doi.org/10.1038/s41556-018-0104-5>

Knapp, D. J. H. F., Hammond, C. A., Miller, P. H., Rabu, G. M., Beer, P. A., Ricicova, M., Lecault, V., Costa, D. D., VanInsberghe, M., Cheung, A. M., Pellacani, D., Piret, J., Hansen, C., & Eaves, C. J. (2017). Dissociation of Survival, Proliferation, and State Control in Human Hematopoietic Stem Cells. *Stem Cell Reports*, 8(1), 152–162. <https://doi.org/10.1016/j.stemcr.2016.12.003>

Knapp, D. J. H. F., Hammond, C. A., Wang, F., Aghaeepour, N., Miller, P. H., Beer, P. A., Pellacani, D., VanInsberghe, M., Hansen, C., Bendall, S. C., Nolan, G. P., & Eaves, C. J. (2019). A topological view of human CD34+ cell state trajectories from integrated single-cell output and proteomic data. *Blood*, *133*(9), 927–939. <https://doi.org/10.1182/blood-2018-10-878025>

Knapp, D. J. H. F., Kannan, N., Pellacani, D., & Eaves, C. J. (2017). Mass Cytometric Analysis Reveals Viable Activated Caspase-3+ Luminal Progenitors in the Normal Adult Human Mammary Gland. *Cell Reports*, *21*(4), 1116–1126. <https://doi.org/10.1016/j.celrep.2017.09.096>

Kollman, C., Howe, C. W. S., Anasetti, C., Antin, J. H., Davies, S. M., Filipovich, A. H., Hegland, J., Kamani, N., Kernan, N. A., King, R., Ratanatharathorn, V., Weisdorf, D., & Confer, D. L. (2001). Donor characteristics as risk factors in recipients after transplantation of bone marrow from unrelated donors: The effect of donor age. *Blood*, *98*(7), 2043–2051. <https://doi.org/10.1182/blood.V98.7.2043>

Kollman, C., Spellman, S. R., Zhang, M.-J., Hassebroek, A., Anasetti, C., Antin, J. H., Champlin, R. E., Confer, D. L., DiPersio, J. F., Fernandez-Viña, M., Hartzman, R. J., Horowitz, M. M., Hurley, C. K., Karanes, C., Maiers, M., Mueller, C. R., Perales, M.-A., Setterholm, M., Woolfrey, A. E., ... Eapen, M. (2016). The effect of donor characteristics on survival after unrelated donor transplantation for hematologic malignancy. *Blood*, *127*(2), 260–267. <https://doi.org/10.1182/blood-2015-08-663823>

Kowalczyk, M. S., Tirosh, I., Heckl, D., Rao, T. N., Dixit, A., Haas, B. J., Schneider, R. K., Wagers, A. J., Ebert, B. L., & Regev, A. (2015). Single-cell RNA-seq reveals changes in cell cycle and differentiation programs upon aging of hematopoietic stem cells. *Genome Research*, *25*(12), 1860–1872. <https://doi.org/10.1101/gr.192237.115>

Kozar, K., Ciemerych, M. A., Rebel, V. I., Shigematsu, H., Zagozdzon, A., Sicinska, E., Geng, Y., Yu, Q., Bhattacharya, S., Bronson, R. T., Akashi, K., & Sicinski, P. (2004). Mouse Development and Cell Proliferation in the Absence of D-Cyclins. *Cell*, *118*(4), 477–491.

<https://doi.org/10.1016/j.cell.2004.07.025>

Krutzik, P. O., & Nolan, G. P. (2006). Fluorescent cell barcoding in flow cytometry allows high-throughput drug screening and signaling profiling. *Nature Methods*, *3*(5), 361–368.

<https://doi.org/10.1038/nmeth872>

Ku, C.-J., Hosoya, T., Maillard, I., & Engel, J. D. (2012). GATA-3 regulates hematopoietic stem cell maintenance and cell-cycle entry. *Blood*, *119*(10), 2242–2251. <https://doi.org/10.1182/blood-2011-07-366070>

Kuranda, K., Vargaftig, J., de la Rochere, P., Dosquet, C., Charron, D., Bardin, F., Tonnelles, C., Bonnet, D., & Goodhardt, M. (2011). Age-related changes in human hematopoietic stem/progenitor cells: Aging of human HSC. *Aging Cell*, *10*(3), 542–546.

<https://doi.org/10.1111/j.1474-9726.2011.00675.x>

Kuribayashi, W., Oshima, M., Itokawa, N., Koide, S., Nakajima-Takagi, Y., Yamashita, M., Yamazaki, S., Rahmutulla, B., Miura, F., Ito, T., Kaneda, A., & Iwama, A. (2021). Limited rejuvenation of aged hematopoietic stem cells in young bone marrow niche. *Journal of Experimental Medicine*, *218*(3), e20192283. <https://doi.org/10.1084/jem.20192283>

Lara-Astiaso, D., Weiner, A., Lorenzo-Vivas, E., Zaretzky, I., Jaitin, D. A., David, E., Keren-Shaul, H., Mildner, A., Winter, D., Jung, S., Friedman, N., & Amit, I. (2014). Chromatin state dynamics during blood formation. *Science*, *345*(6199), 943–949.

Laurenti, E., Frelin, C., Xie, S., Ferrari, R., Dunant, C. F., Zandi, S., Neumann, A., Plumb, I., Doulatov, S., Chen, J., April, C., Fan, J.-B., Iscove, N., & Dick, J. E. (2015). CDK6 Levels Regulate Quiescence Exit in Human Hematopoietic Stem Cells. *Cell Stem Cell*, *16*(3), 302–313. <https://doi.org/10.1016/j.stem.2015.01.017>

Laurenti, E., & Göttgens, B. (2018). From haematopoietic stem cells to complex differentiation landscapes. *Nature*, *553*(7689), 418–426. <https://doi.org/10.1038/nature25022>

Lechman, E. R., Gentner, B., van Galen, P., Giustacchini, A., Saini, M., Boccalatte, F. E., Hiramatsu, H., Restuccia, U., Bachi, A., Voisin, V., Bader, G. D., Dick, J. E., & Naldini, L. (2012). Attenuation of miR-126 Activity Expands HSC In Vivo without Exhaustion. *Cell Stem Cell*, *11*(6), 799–811. <https://doi.org/10.1016/j.stem.2012.09.001>

Lee, H.-W., Blasco, M. A., Gottlieb, G. J., Horner, J. W., Greider, C. W., & DePinho, R. A. (1998). Essential role of mouse telomerase in highly proliferative organs. *Nature*, *392*(6676), 569–574. <https://doi.org/10.1038/33345>

Liles, W. C., Broxmeyer, H. E., Rodger, E., Wood, B., Hübel, K., Cooper, S., Hangan, G., Bridger, G. J., Henson, G. W., Calandra, G., & Dale, D. C. (2003). Mobilization of hematopoietic progenitor cells in healthy volunteers by AMD3100, a CXCR4 antagonist. *Blood*, *102*(8), 2728–2730. <https://doi.org/10.1182/blood-2003-02-0663>

Limas, J. C., & Cook, J. G. (2019). Preparation for DNA replication: The key to a successful S phase. *FEBS Letters*, *593*(20), 2853–2867. <https://doi.org/10.1002/1873-3468.13619>

Lin, J.-R., Fallahi-Sichani, M., & Sorger, P. K. (2015). Highly multiplexed imaging of single cells using a high-throughput cyclic immunofluorescence method. *Nature Communications*, *6*(1), 8390. <https://doi.org/10.1038/ncomms9390>

Ljungman, P., Bregni, M., Brune, M., Cornelissen, J., Witte, T. de, Dini, G., Einsele, H., Gaspar, H. B., Gratwohl, A., Passweg, J., Peters, C., Rocha, V., Saccardi, R., Schouten, H., Sureda, A., Tichelli, A., Velardi, A., & Niederwieser, D. (2010). Allogeneic and autologous transplantation for haematological diseases, solid tumours and immune disorders: Current practice in Europe 2009. *Bone Marrow Transplantation*, *45*(2), 219–234. <https://doi.org/10.1038/bmt.2009.141>

Loeffler, D., Wang, W., Hopf, A., Hilsenbeck, O., Bourguine, P. E., Rudolf, F., Martin, I., & Schroeder, T. (2018). Mouse and human HSPC immobilization in liquid culture by CD43- or CD44-antibody coating. *Blood*, *131*(13), 1425–1429. <https://doi.org/10.1182/blood-2017-07-794131>

Loeffler, D., Wehling, A., Schneider, F., Zhang, Y., Müller-Böttcher, N., Hoppe, P. S., Hilsenbeck, O., Kokkaliaris, K. D., Endele, M., & Schroeder, T. (2019). Asymmetric lysosome inheritance predicts activation of haematopoietic stem cells. *Nature*, *573*(7774), 426–429. <https://doi.org/10.1038/s41586-019-1531-6>

López-Otín, C., Blasco, M. A., Partridge, L., Serrano, M., & Kroemer, G. (2013). The Hallmarks of Aging. *Cell*, *153*(6), 1194–1217. <https://doi.org/10.1016/j.cell.2013.05.039>

Lorenz, E., Uphoff, D., Reid, T. R., & Shelton, E. (1951). Modification of Irradiation Injury in Mice and Guinea Pigs by Bone Marrow Injections. *JNCI: Journal of the National Cancer Institute*, *12*, 197–201. <https://doi.org/10.1093/jnci/12.1.197>

Lu, R., Neff, N. F., Quake, S. R., & Weissman, I. L. (2011). Tracking single hematopoietic stem cells in vivo using high-throughput sequencing in conjunction with viral genetic barcoding. *Nature Biotechnology*, *29*(10), 928–933. <https://doi.org/10.1038/nbt.1977>

Malumbres, M., Sotillo, R., Santamaría, D., Galán, J., Cerezo, A., Ortega, S., Dubus, P., & Barbacid, M. (2004). Mammalian Cells Cycle without the D-Type Cyclin-Dependent Kinases Cdk4 and Cdk6. *Cell*, *118*(4), 493–504. <https://doi.org/10.1016/j.cell.2004.08.002>

Mann, M., Mehta, A., de Boer, C. G., Kowalczyk, M. S., Lee, K., Haldeman, P., Rogel, N., Knecht, A. R., Farouq, D., Regev, A., & Baltimore, D. (2018). Heterogeneous Responses of Hematopoietic Stem Cells to Inflammatory Stimuli Are Altered with Age. *Cell Reports*, *25*(11), 2992-3005.e5. <https://doi.org/10.1016/j.celrep.2018.11.056>

Manz, M. G., Miyamoto, T., Akashi, K., & Weissman, I. L. (2002). Prospective isolation of human clonogenic common myeloid progenitors. *Proceedings of the National Academy of Sciences*, *99*(18), 11872–11877. <https://doi.org/10.1073/pnas.172384399>

Martincorena, I., Roshan, A., Gerstung, M., Ellis, P., Van Loo, P., McLaren, S., Wedge, D. C., Fullam, A., Alexandrov, L. B., Tubio, J. M., Stebbings, L., Menzies, A., Widaa, S., Stratton, M. R., Jones, P. H., & Campbell, P. J. (2015). High burden and pervasive positive selection of somatic mutations in normal human skin. *Science*, *348*(6237), 880–886. <https://doi.org/10.1126/science.aaa6806>

Martincorena, Iñigo, Fowler, J. C., Wabik, A., Lawson, A. R. J., Abascal, F., Hall, M. W. J., Cagan, A., Murai, K., Mahbubani, K., Stratton, M. R., Fitzgerald, R. C., Handford, P. A., Campbell, P. J., Saeb-Parsy, K., & Jones, P. H. (2018). Somatic mutant clones colonize the human esophagus with age. *Science*, *362*(6417), 911–917. <https://doi.org/10.1126/science.aau3879>

Massagué, J. (2004). G1 cell-cycle control and cancer. *Nature*, *432*(7015), 298–306. <https://doi.org/10.1038/nature03094>

Matsumoto, A., Takeishi, S., Kanie, T., Susaki, E., Onoyama, I., Tateishi, Y., Nakayama, K., & Nakayama, K. I. (2011). P57 Is Required for Quiescence and Maintenance of Adult Hematopoietic Stem Cells. *Cell Stem Cell*, 9(3), 262–271.

<https://doi.org/10.1016/j.stem.2011.06.014>

Matsuoka, S., Tsuji, K., Hisakawa, H., Xu, M., Ebihara, Y., Ishii, T., Sugiyama, D., Manabe, A., Tanaka, R., Ikeda, Y., Asano, S., & Nakahata, T. (2001). Generation of definitive hematopoietic stem cells from murine early yolk sac and paraaortic splanchnopleures by aorta-gonad-mesonephros region-derived stromal cells. *Blood*, 98(1), 6–12.

<https://doi.org/10.1182/blood.V98.1.6>

Mayani, H., & Lansdorp, P. (1994). Thy-1 expression is linked to functional properties of primitive hematopoietic progenitor cells from human umbilical cord blood. *Blood*, 83(9), 2410–2417. <https://doi.org/10.1182/blood.V83.9.2410.2410>

Mayani, H., Little, M. T., Dragowska, W., Thornbury, G., & Lansdorp, P. M. (1995). Differential effects of the hematopoietic inhibitors MIP-1 alpha, TGF-beta, and TNF-alpha on cytokine-induced proliferation of subpopulations of CD34+ cells purified from cord blood and fetal liver. *Experimental Hematology*, 23(5), 422–427.

McCabe, M. T., Graves, A. P., Ganji, G., Diaz, E., Halsey, W. S., Jiang, Y., Smitheman, K. N., Ott, H. M., Pappalardi, M. B., Allen, K. E., Chen, S. B., Della Pietra, A., Dul, E., Hughes, A. M., Gilbert, S. A., Thrall, S. H., Tummino, P. J., Kruger, R. G., Brandt, M., ... Creasy, C. L. (2012). Mutation of A677 in histone methyltransferase EZH2 in human B-cell lymphoma promotes hypertrimethylation of histone H3 on lysine 27 (H3K27). *Proceedings of the National Academy of Sciences*, 109(8), 2989–2994. <https://doi.org/10.1073/pnas.1116418109>

McCulloch, E. A., Siminovitch, L., Till, J. E., Russell, E. S., & Bernstein, S. E. (1965). The Cellular Basis of the Genetically Determined Hemopoietic Defect in Anemic Mice of Genotype Sl/Sl^d. *Blood*, *26*(4), 399–410. <https://doi.org/10.1182/blood.V26.4.399.399>

McCulloch, E. A., & Till, J. E. (1960). The Radiation Sensitivity of Normal Mouse Bone Marrow Cells, Determined by Quantitative Marrow Transplantation into Irradiated Mice. *Radiation Research*, *13*(1), 115. <https://doi.org/10.2307/3570877>

McInnes, L., Healy, J., Saul, N., & Großberger, L. (2018). UMAP: Uniform Manifold Approximation and Projection. *Journal of Open Source Software*, *3*(29), 861. <https://doi.org/10.21105/joss.00861>

McIntosh, B. E., Brown, M. E., Duffin, B. M., Maufort, J. P., Vereide, D. T., Slukvin, I. I., & Thomson, J. A. (2015). Nonirradiated NOD,B6.SCID Il2 $\gamma^{-/-}$ KitW41/W41 (NBSGW) Mice Support Multilineage Engraftment of Human Hematopoietic Cells. *Stem Cell Reports*, *4*(2), 171–180. <https://doi.org/10.1016/j.stemcr.2014.12.005>

McKerrell, T., Park, N., Moreno, T., Grove, C. S., Ponstingl, H., Stephens, J., Crawley, C., Craig, J., Scott, M. A., Hodgkinson, C., Baxter, J., Rad, R., Forsyth, D. R., Quail, M. A., Zeggini, E., Ouwehand, W., Varela, I., & Vassiliou, G. S. (2015). Leukemia-Associated Somatic Mutations Drive Distinct Patterns of Age-Related Clonal Hemopoiesis. *Cell Reports*, *10*(8), 1239–1245. <https://doi.org/10.1016/j.celrep.2015.02.005>

Mende, N., Bastos, H. P., Santoro, A., Sham, K., Mahbubani, K. T., Curd, A., Takizawa, H., Wilson, N. K., Göttgens, B., Saeb-Parsy, K., & Laurenti, E. (2020). *Quantitative and molecular differences distinguish adult human medullary and extramedullary haematopoietic stem and progenitor cell landscapes* [Preprint]. *Cell Biology*. <https://doi.org/10.1101/2020.01.26.919753>

Miller, C. L., Rebel, V. I., Lemieux, M. E., Helgason, C. D., Lansdorp, P. M., & Eaves, C. J. (1996). Studies of W mutant mice provide evidence for alternate mechanisms capable of activating hematopoietic stem cells. *Experimental Hematology*, *24*(2), 185–194.

Miller, P. H., Rabu, G., MacAldaz, M., Knapp, D. J. H. F., Cheung, A. M. S., Dhillon, K., Nakamichi, N., Beer, P. A., Shultz, L. D., Humphries, R. K., & Eaves, C. J. (2017). Analysis of parameters that affect human hematopoietic cell outputs in mutant c-kit-immunodeficient mice. *Experimental Hematology*, *48*, 41–49. <https://doi.org/10.1016/j.exphem.2016.12.012>

Moehrle, B. M., Nattamai, K., Brown, A., Florian, M. C., Ryan, M., Vogel, M., Bliederaeuser, C., Soller, K., Prows, D. R., Abdollahi, A., Schleimer, D., Walter, D., Milsom, M. D., Stambrook, P., Porteus, M., & Geiger, H. (2015). Stem Cell-Specific Mechanisms Ensure Genomic Fidelity within HSCs and upon Aging of HSCs. *Cell Reports*, *13*(11), 2412–2424. <https://doi.org/10.1016/j.celrep.2015.11.030>

Moran-Crusio, K., Reavie, L., Shih, A., Abdel-Wahab, O., Ndiaye-Lobry, D., Lobry, C., Figueroa, M. E., Vasanthakumar, A., Patel, J., Zhao, X., Perna, F., Pandey, S., Madzo, J., Song, C., Dai, Q., He, C., Ibrahim, S., Beran, M., Zavadil, J., ... Levine, R. L. (2011). Tet2 Loss Leads to Increased Hematopoietic Stem Cell Self-Renewal and Myeloid Transformation. *Cancer Cell*, *20*(1), 11–24. <https://doi.org/10.1016/j.ccr.2011.06.001>

Morcos, M. N. F., Zerjatke, T., Glauche, I., Munz, C. M., Ge, Y., Petzold, A., Reinhardt, S., Dahl, A., Anstee, N. S., Bogeska, R., Milsom, M. D., Säwén, P., Wan, H., Bryder, D., Roers, A., & Gerbault, A. (2020). Continuous mitotic activity of primitive hematopoietic stem cells in adult mice. *Journal of Experimental Medicine*, *217*(6), e20191284.

<https://doi.org/10.1084/jem.20191284>

Morrison, S. J., Wright, D. E., & Weissman, I. L. (1997). Cyclophosphamide/granulocyte colony-stimulating factor induces hematopoietic stem cells to proliferate prior to mobilization.

Proceedings of the National Academy of Sciences, 94(5), 1908–1913.

<https://doi.org/10.1073/pnas.94.5.1908>

Morrison, Sean J., Wandycz, A. M., Akashi, K., Globerson, A., & Weissman, I. L. (1996). The aging of hematopoietic stem cells. *Nature Medicine*, 2(9), 1011–1016.

<https://doi.org/10.1038/nm0996-1011>

Moser, J., Miller, I., Carter, D., & Spencer, S. L. (2018). Control of the Restriction Point by Rb and p21. *Proceedings of the National Academy of Sciences*, 115(35), E8219–E8227.

<https://doi.org/10.1073/pnas.1722446115>

Muller-Sieburg, C. E., Cho, R. H., Karlsson, L., Huang, J.-F., & Sieburg, H. B. (2004). Myeloid-biased hematopoietic stem cells have extensive self-renewal capacity but generate diminished lymphoid progeny with impaired IL-7 responsiveness. *Blood*, 103(11), 4111–4118.

<https://doi.org/10.1182/blood-2003-10-3448>

Nakauchi, H., Osawa, M., Sudo, K., & Ema, H. (2000). Isolation and Characterization of CD34-Low/Negative Mouse Hematopoietic Stem Cells. In Y. Ikeda, J. Hata, S. Koyasu, Y. Kawakami, & Y. Hattori (Eds.), *Cell Therapy* (pp. 95–103). Springer Japan. https://doi.org/10.1007/978-4-431-68506-7_8

Naldini, L. (2019). Genetic engineering of hematopoiesis: Current stage of clinical translation and future perspectives. *EMBO Molecular Medicine*, 11(3).

<https://doi.org/10.15252/emmm.201809958>

Nicolini, F. E., Holyoake, T. L., Cashman, J. D., Chu, P. P. Y., Lambie, K., & Eaves, C. J. (1999). Unique Differentiation Programs of Human Fetal Liver Stem Cells Shown Both In Vitro and In Vivo in NOD/SCID Mice. *Blood*, *94*(8), 2686–2695. https://doi.org/10.1182/blood.V94.8.2686.420k15_2686_2695

Nijnik, A., Woodbine, L., Marchetti, C., Dawson, S., Lambe, T., Liu, C., Rodrigues, N. P., Crockford, T. L., Cabuy, E., Vindigni, A., Enver, T., Bell, J. I., Slijepcevic, P., Goodnow, C. C., Jeggo, P. A., & Cornall, R. J. (2007). DNA repair is limiting for haematopoietic stem cells during ageing. *Nature*, *447*(7145), 686–690. <https://doi.org/10.1038/nature05875>

Nilsson, A. R., Soneji, S., Adolfsson, S., Bryder, D., & Pronk, C. J. (2016). Human and Murine Hematopoietic Stem Cell Aging Is Associated with Functional Impairments and Intrinsic Megakaryocytic/Erythroid Bias. *PLOS ONE*, *20*.

Notta, F., Doulatov, S., Laurenti, E., Poeppl, A., Jurisica, I., & Dick, J. E. (2011). Isolation of Single Human Hematopoietic Stem Cells Capable of Long-Term Multilineage Engraftment. *Science*, *333*(6039), 218–221. <https://doi.org/10.1126/science.1201219>

Notta, F., Zandi, S., Takayama, N., Dobson, S., Gan, O. I., Wilson, G., Kaufmann, K. B., McLeod, J., Laurenti, E., Dunant, C. F., McPherson, J. D., Stein, L. D., Dror, Y., & Dick, J. E. (2016). Distinct routes of lineage development reshape the human blood hierarchy across ontogeny. *Science*, *351*(6269), aab2116. <https://doi.org/10.1126/science.aab2116>

O’Byrne, S., Elliott, N., Rice, S., Buck, G., Fordham, N., Garnett, C., Godfrey, L., Crump, N. T., Wright, G., Inglott, S., Hua, P., Psaila, B., Povinelli, B., Knapp, D. J. H. F., Agraz-Doblas, A., Bueno, C., Varela, I., Bennett, P., Koohy, H., ... Roy, A. (2019). Discovery of a CD10-negative

B-progenitor in human fetal life identifies unique ontogeny-related developmental programs. *Blood*, 134(13), 1059–1071. <https://doi.org/10.1182/blood.2019001289>

Ogawa, T., Kitagawa, M., & Hirokawa, K. (2000). Age-related changes of human bone marrow: A histometric estimation of proliferative cells, apoptotic cells, T cells, B cells and macrophages. *Mechanisms of Ageing and Development*, 117(1–3), 57–68. [https://doi.org/10.1016/S0047-6374\(00\)00137-8](https://doi.org/10.1016/S0047-6374(00)00137-8)

Oguro, H., Yuan, J., Ichikawa, H., Ikawa, T., Yamazaki, S., Kawamoto, H., Nakauchi, H., & Iwama, A. (2010). Poised Lineage Specification in Multipotential Hematopoietic Stem and Progenitor Cells by the Polycomb Protein Bmi1. *Cell Stem Cell*, 6(3), 279–286. <https://doi.org/10.1016/j.stem.2010.01.005>

Ohta, H., Sekulovic, S., Bakovic, S., Eaves, C. J., Pineault, N., Gasparetto, M., Smith, C., Sauvageau, G., & Humphries, R. K. (2007). Near-maximal expansions of hematopoietic stem cells in culture using NUP98-HOX fusions. *Experimental Hematology*, 35(5), 817–830. <https://doi.org/10.1016/j.exphem.2007.02.012>

Osawa, M., Hanada, K. -i., Hamada, H., & Nakauchi, H. (1996). Long-Term Lymphohematopoietic Reconstitution by a Single CD34-Low/Negative Hematopoietic Stem Cell. *Science*, 273(5272), 242–245. <https://doi.org/10.1126/science.273.5272.242>

Panch, S. R., Szymanski, J., Savani, B. N., & Stroncek, D. F. (2017). Sources of Hematopoietic Stem and Progenitor Cells and Methods to Optimize Yields for Clinical Cell Therapy. *Biology of Blood and Marrow Transplantation*, 23(8), 1241–1249. <https://doi.org/10.1016/j.bbmt.2017.05.003>

Pang, W. W., Price, E. A., Sahoo, D., Beerman, I., Maloney, W. J., Rossi, D. J., Schrier, S. L., & Weissman, I. L. (2011). Human bone marrow hematopoietic stem cells are increased in frequency and myeloid-biased with age. *Proceedings of the National Academy of Sciences*, *108*(50), 20012–20017. <https://doi.org/10.1073/pnas.1116110108>

Park, I., Qian, D., Kiel, M., Becker, M. W., Pihalja, M., Weissman, I. L., Morrison, S. J., & Clarke, M. F. (2003). Bmi-1 is required for maintenance of adult self-renewing haematopoietic stem cells. *Nature*, *423*(6937), 302–305. <https://doi.org/10.1038/nature01587>

Passegué, E., Wagers, A. J., Giuriato, S., Anderson, W. C., & Weissman, I. L. (2005). Global analysis of proliferation and cell cycle gene expression in the regulation of hematopoietic stem and progenitor cell fates. *Journal of Experimental Medicine*, *202*(11), 1599–1611. <https://doi.org/10.1084/jem.20050967>

Pellin, D., Loperfido, M., Baricordi, C., Wolock, S. L., Montepeloso, A., Weinberg, O. K., Biffi, A., Klein, A., & Biasco, L. (2019). A comprehensive single cell transcriptional landscape of human hematopoietic progenitors. *Nature Communications*, *10*(2395), 1–15.

Petzer, A. L., Zandstra, P. W., Piret, J. M., & Eaves, C. J. (1996). Differential Cytokine Effects on Primitive (CD34⁺CD38⁻) Human Hematopoietic Cells: Novel Responses to Flt3-Ligand and Thrombopoietin. *Journal of Experimental Medicine*, *183*, 2551–2558.

Pietras, E. M., Mirantes-Barbeito, C., Fong, S., Loeffler, D., Kovtonyuk, L. V., Zhang, S., Lakshminarasimhan, R., Chin, C. P., Techner, J.-M., Will, B., Nerlov, C., Steidl, U., Manz, M. G., Schroeder, T., & Passegué, E. (2016). Chronic interleukin-1 exposure drives haematopoietic stem cells towards precocious myeloid differentiation at the expense of self-renewal. *Nature Cell Biology*, *18*(6), 607–618. <https://doi.org/10.1038/ncb3346>

Pietras, E. M., Warr, M. R., & Passegué, E. (2011). Cell cycle regulation in hematopoietic stem cells. *The Journal of Cell Biology*, *195*(5), 709–720. <https://doi.org/10.1083/jcb.201102131>

Ponchio, L., Conneally, E., & Eaves, C. (1995). Quantitation of the quiescent fraction of long-term culture-initiating cells in normal human blood and marrow and the kinetics of their growth factor-stimulated entry into S-phase in vitro. *Blood*, *86*(9), 3314–3321.

<https://doi.org/10.1182/blood.V86.9.3314.bloodjournal8693314>

Prasher, J. M., Lalai, A. S., Heijmans-Antonissen, C., Ploemacher, R. E., Hoeijmakers, J. H. J., Touw, I. P., & Niedernhofer, L. J. (2005). Reduced hematopoietic reserves in DNA interstrand crosslink repair-deficient *Ercc1*^{-/-} mice. *The EMBO Journal*, *24*(4), 861–871.

<https://doi.org/10.1038/sj.emboj.7600542>

Qian, H., Buza-Vidas, N., Hyland, C. D., Jensen, C. T., Antonchuk, J., Månsson, R., Thoren, L. A., Ekblom, M., Alexander, W. S., & Jacobsen, S. E. W. (2007). Critical Role of Thrombopoietin in Maintaining Adult Quiescent Hematopoietic Stem Cells. *Cell Stem Cell*, *1*(6), 671–684. <https://doi.org/10.1016/j.stem.2007.10.008>

Randall, T., Lund, F., Howard, M., & Weissman, I. (1996). Expression of murine CD38 defines a population of long-term reconstituting hematopoietic stem cells. *Blood*, *87*(10), 4057–4067.

<https://doi.org/10.1182/blood.V87.10.4057.bloodjournal87104057>

Ravin, S. S. D., Wu, X., Moir, S., Kardava, L., Anaya-O'Brien, S., Kwatema, N., Littel, P., Theobald, N., Choi, U., Su, L., Marquesen, M., Hilligoss, D., Lee, J., Buckner, C. M., Zarembek, K. A., O'Connor, G., McVicar, D., Kuhns, D., Throm, R. E., ... Malech, H. L. (2016). Lentiviral hematopoietic stem cell gene therapy for X-linked severe combined immunodeficiency. *Science Translational Medicine*, *8*(335), 335ra57–335ra57. <https://doi.org/10.1126/scitranslmed.aad8856>

Rebel, V. I., Miller, C. L., Eaves, C. J., & Lansdorp, P. M. (1996). The Repopulation Potential of Fetal Liver Hematopoietic Stem Cells in Mice Exceeds That of Their Adult Bone Marrow Counterparts. *Blood*, *87*(8), 3500–3507.

Reinisch, A., Hernandez, D. C., Schallmoser, K., & Majeti, R. (2017). Generation and use of a humanized bone-marrow-ossicle niche for hematopoietic xenotransplantation into mice. *Nature Protocols*, *12*(10), 2169–2188. <https://doi.org/10.1038/nprot.2017.088>

Rezvani, A. R., Storer, B. E., Guthrie, K. A., Schoch, H. G., Maloney, D. G., Sandmaier, B. M., & Storb, R. (2015). Impact of Donor Age on Outcome after Allogeneic Hematopoietic Cell Transplantation. *Biology of Blood and Marrow Transplantation*, *21*(1), 105–112. <https://doi.org/10.1016/j.bbmt.2014.09.021>

Ritz, C., Baty, F., Streibig, J. C., & Gerhard, D. (2015). Dose-Response Analysis Using R. *PLOS ONE*, *10*(12), e0146021. <https://doi.org/10.1371/journal.pone.0146021>

Rocha, V. (2016). Umbilical cord blood cells from unrelated donor as an alternative source of hematopoietic stem cells for transplantation in children and adults. *Seminars in Hematology*, *53*(4), 237–245. <https://doi.org/10.1053/j.seminhematol.2016.08.002>

Rodrigues, Neil P., Janzen, V., Forkert, R., Dombkowski, D. M., Boyd, A., Orkin, S., Enver, T., Vyas, P., & Scadden, D. (2005). Haploinsufficiency of GATA-2 perturbs adult hematopoietic stem-cell homeostasis. *Blood*, *106*(2), 477–484. <https://doi.org/10.1182/blood-2004-08-2989>

Rodrigues, Neil P., Tipping, A. J., Wang, Z., & Enver, T. (2012). GATA-2 mediated regulation of normal hematopoietic stem/progenitor cell function, myelodysplasia and myeloid leukemia. *The International Journal of Biochemistry & Cell Biology*, *44*(3), 457–460.

<https://doi.org/10.1016/j.biocel.2011.12.004>

Rossi, D. J., Bryder, D., Zahn, J. M., Ahlenius, H., Sonu, R., Wagers, A. J., & Weissman, I. L. (2005). Cell intrinsic alterations underlie hematopoietic stem cell aging. *Proceedings of the National Academy of Sciences*, *102*(26), 9194–9199. <https://doi.org/10.1073/pnas.0503280102>

Rossi, Derrick J., Bryder, D., Seita, J., Nussenzweig, A., Hoeijmakers, J., & Weissman, I. L. (2007). Deficiencies in DNA damage repair limit the function of haematopoietic stem cells with age. *Nature*, *447*(7145), 725–729. <https://doi.org/10.1038/nature05862>

Rowe, R. G., Mandelbaum, J., Zon, L. I., & Daley, G. Q. (2016). Engineering Hematopoietic Stem Cells: Lessons from Development. *Cell Stem Cell*, *18*(6), 707–720. <https://doi.org/10.1016/j.stem.2016.05.016>

Sanjuan-Pla, A., Macaulay, I. C., Jensen, C. T., Woll, P. S., Luis, T. C., Mead, A., Moore, S., Carella, C., Matsuoka, S., Jones, T. B., Chowdhury, O., Stenson, L., Lutteropp, M., Green, J. C. A., Facchini, R., Boukarabila, H., Grover, A., Gambardella, A., Thongjuea, S., ... Jacobsen, S. E. W. (2013). Platelet-biased stem cells reside at the apex of the haematopoietic stem-cell hierarchy. *Nature*, *502*(7470), 232–236. <https://doi.org/10.1038/nature12495>

Satyanarayana, A., & Kaldis, P. (2009). Mammalian cell-cycle regulation: Several Cdks, numerous cyclins and diverse compensatory mechanisms. *Oncogene*, *28*(33), 2925–2939. <https://doi.org/10.1038/onc.2009.170>

Sauvageau, G., Thorsteinsdottir, U., Eaves, C. J., Lawrence, H. J., Langman, C., Lansdorp, P. M., & Humphries, R. K. (1995). Overexpression of HOXB4 in hematopoietic cells causes the selective expansion of more primitive populations in vitro and in vivo. *Genes & Development*, *9*, 1753–1765.

Sawai, C. M., Babovic, S., Upadhaya, S., Knapp, D. J. H. F., Lavin, Y., Lau, C. M., Goloborodko, A., Feng, J., Fujisaki, J., Ding, L., Mirny, L. A., Merad, M., Eaves, C. J., & Reizis, B. (2016). Hematopoietic Stem Cells Are the Major Source of Multilineage Hematopoiesis in Adult Animals. *Immunity*, *45*(3), 597–609. <https://doi.org/10.1016/j.immuni.2016.08.007>

Sears, R. C., & Nevins, J. R. (2002). Signaling Networks That Link Cell Proliferation and Cell Fate. *Journal of Biological Chemistry*, *277*(14), 11617–11620. <https://doi.org/10.1074/jbc.R100063200>

Sherr, C. J. (1993). Mammalian G1 Cyclins. *Cell*, *73*, 1059–1065.

Sherr, C. J. (2000). The Pezcoller Lecture: Cancer Cell Cycles Revisited. *Cancer Research*, *60*, 3689–3695.

Sherr, C. J. (2012). Ink4-Arf locus in cancer and aging. *Wiley Interdisciplinary Reviews: Developmental Biology*, *1*(5), 731–741. <https://doi.org/10.1002/wdev.40>

Sidorov, I., Kimura, M., Yashin, A., & Aviv, A. (2009). Leukocyte telomere dynamics and human hematopoietic stem cell kinetics during somatic growth. *Experimental Hematology*, *37*(4), 514–524. <https://doi.org/10.1016/j.exphem.2008.11.009>

Sieburg, H. B., Cho, R. H., Dykstra, B., Uchida, N., Eaves, C. J., & Muller-Sieburg, C. E. (2006). The hematopoietic stem compartment consists of a limited number of discrete stem cell subsets. *Blood*, *107*(6), 2311–2316. <https://doi.org/10.1182/blood-2005-07-2970>

Siminovitch, L., McCulloch, E. A., & Till, J. E. (1963). The distribution of colony-forming cells among spleen colonies. *Journal of Cellular and Comparative Physiology*, *62*(3), 327–336. <https://doi.org/10.1002/jcp.1030620313>

Singh, K. P., Casado, F. L., Opanashuk, L. A., & Gasiewicz, T. A. (2009). The aryl hydrocarbon receptor has a normal function in the regulation of hematopoietic and other stem/progenitor cell populations. *Biochemical Pharmacology*, *77*(4), 577–587.

<https://doi.org/10.1016/j.bcp.2008.10.001>

Sloma, I., Imren, S., Beer, P. A., Zhao, Y., Lecault, V., Leung, D., Raghuram, K., Brimacombe, C., Lambie, K., Piret, J. M., Hansen, C., Humphries, R. K., & Eaves, C. J. (2013). Ex vivo expansion of normal and chronic myeloid leukemic stem cells without functional alteration using a NUP98HOXA10homeodomain fusion gene. *Leukemia*, *27*, 159–169.

Suda, K., Nakaoka, H., Yoshihara, K., Ishiguro, T., Tamura, R., Mori, Y., Yamawaki, K., Adachi, S., Takahashi, T., Kase, H., Tanaka, K., Yamamoto, T., Motoyama, T., Inoue, I., & Enomoto, T. (2018). Clonal Expansion and Diversification of Cancer-Associated Mutations in Endometriosis and Normal Endometrium. *Cell Reports*, *24*(7), 1777–1789.

<https://doi.org/10.1016/j.celrep.2018.07.037>

Sudo, K., Ema, H., Morita, Y., & Nakauchi, H. (2000). Age-Associated Characteristics of Murine Hematopoietic Stem Cells. *Journal of Experimental Medicine*, *192*(9), 1273–1280.

<https://doi.org/10.1084/jem.192.9.1273>

Sugiyama, T., Kohara, H., Noda, M., & Nagasawa, T. (2006). Maintenance of the Hematopoietic Stem Cell Pool by CXCL12-CXCR4 Chemokine Signaling in Bone Marrow Stromal Cell Niches. *Immunity*, *25*(6), 977–988. <https://doi.org/10.1016/j.immuni.2006.10.016>

Sun, D., Luo, M., Jeong, M., Rodriguez, B., Xia, Z., Hannah, R., Wang, H., Le, T., Faull, K. F., Chen, R., Gu, H., Bock, C., Meissner, A., Göttgens, B., Darlington, G. J., Li, W., & Goodell, M. A. (2014). Epigenomic Profiling of Young and Aged HSCs Reveals Concerted Changes during

Aging that Reinforce Self-Renewal. *Cell Stem Cell*, 14(5), 673–688.

<https://doi.org/10.1016/j.stem.2014.03.002>

Sun, J., Ramos, A., Chapman, B., Johnnidis, J. B., Le, L., Ho, Y.-J., Klein, A., Hofmann, O., & Camargo, F. D. (2014). Clonal dynamics of native haematopoiesis. *Nature*, 514(7522), 322–327.

<https://doi.org/10.1038/nature13824>

Sutherland, D. J. A., Till, J. E., & McCulloch, E. A. (1970). A kinetic study of the genetic control of hemopoietic progenitor cells assayed in culture and In vivo. *Journal of Cellular Physiology*, 75(3), 267–274. <https://doi.org/10.1002/jcp.1040750302>

Sutherland, H., Eaves, C. J., Eaves, A. C., Dragowska, W., & Lansdorp, P. (1989).

Characterization and Partial Purification of Human Marrow Cells Capable of Initiating Long-Term Hematopoiesis In Vitro. *Blood*, 74(5), 1563–1570.

Thomas, E. D., Lochte, H. L., Cannon, J. H., Sahler, O. D., & Ferrebee, J. W. (1959). Supralethal Whole Body Irradiation and Isologous Marrow Transplantation in Man. *Journal of Clinical Investigation*, 38(10 Pt 1-2), 1709–1716. <https://doi.org/10.1172/JCI103949>

Thorén, L. A., Liuba, K., Bryder, D., Nygren, J. M., Jensen, C. T., Qian, H., Antonchuk, J., & Jacobsen, S.-E. W. (2008). Kit Regulates Maintenance of Quiescent Hematopoietic Stem Cells. *The Journal of Immunology*, 180(4), 2045–2053. <https://doi.org/10.4049/jimmunol.180.4.2045>

Till, J. E., & McCulloch, E. A. (1961). A Direct Measurement of the Radiation Sensitivity of Normal Mouse Bone Marrow Cells. *Radiation Research*, 14(2), 213–222.

Trowbridge, J. J., Snow, J. W., Kim, J., & Orkin, S. H. (2009). DNA Methyltransferase 1 Is Essential for and Uniquely Regulates Hematopoietic Stem and Progenitor Cells. *Cell Stem Cell*, 5(4), 442–449. <https://doi.org/10.1016/j.stem.2009.08.016>

Tsutsui, T., Hesabi, B., Moons, D. S., Pandolfi, P. P., Hansel, K. S., Koff, A., & Kiyokawa, H. (1999). Targeted Disruption of CDK4 Delays Cell Cycle Entry with Enhanced p27Kip1 Activity. *Molecular and Cellular Biology*, 19(10), 7011–7019. <https://doi.org/10.1128/MCB.19.10.7011>

Tzeng, Y.-S., Li, H., Kang, Y.-L., Chen, W.-C., Cheng, W.-C., & Lai, D.-M. (2011). Loss of Cxcl12/Sdf-1 in adult mice decreases the quiescent state of hematopoietic stem/progenitor cells and alters the pattern of hematopoietic regeneration after myelosuppression. *Blood*, 117(2), 429–439. <https://doi.org/10.1182/blood-2010-01-266833>

Velten, L., Haas, S. F., Raffel, S., Blaszkiewicz, S., Islam, S., Hennig, B. P., Hirche, C., Lutz, C., Buss, E. C., Nowak, D., Boch, T., Hofmann, W.-K., Ho, A. D., Huber, W., Trumpp, A., Essers, M. A. G., & Steinmetz, L. M. (2017). Human haematopoietic stem cell lineage commitment is a continuous process. *Nature Cell Biology*, 19(4), 271–281. <https://doi.org/10.1038/ncb3493>

Verheyen, E. M., & Gottardi, C. J. (2010). Regulation of Wnt/ β -catenin signaling by protein kinases. *Developmental Dynamics*, 239(1), 34–44. <https://doi.org/10.1002/dvdy.22019>

Wang, K., Guzman, A. K., Yan, Z., Zhang, S., Hu, M. Y., Hamaneh, M. B., Yu, Y.-K., Tolu, S., Zhang, J., Kanavy, H. E., Ye, K., Bartholdy, B., & Bouhassira, E. E. (2019). Ultra-High-Frequency Reprogramming of Individual Long-Term Hematopoietic Stem Cells Yields Low Somatic Variant Induced Pluripotent Stem Cells. *Cell Reports*, 26(10), 2580-2592.e7. <https://doi.org/10.1016/j.celrep.2019.02.021>

- Wang, K., Yan, Z., Zhang, S., Bartholdy, B., Eaves, C. J., & Bouhassira, E. E. (2020). Clonal origin in normal adults of all blood lineages and circulating hematopoietic stem cells. *Experimental Hematology*, S0301472X20300254. <https://doi.org/10.1016/j.exphem.2020.01.005>
- Wilkinson, A. C., Igarashi, K. J., & Nakauchi, H. (2020). Haematopoietic stem cell self-renewal in vivo and ex vivo. *Nature Reviews Genetics*. <https://doi.org/10.1038/s41576-020-0241-0>
- Wilpshaar, J., Falkenburg, J. H. F., Tong, X., Noort, W. A., Breese, R., Heilman, D., Kanhai, H., Orschell-Traycoff, C. M., & Srour, E. F. (2000). Similar repopulating capacity of mitotically active and resting umbilical cord blood CD34+ cells in NOD/SCID mice. *Blood*, 96(6), 2100–2107. <https://doi.org/10.1182/blood.V96.6.2100>
- Wilson, A., Laurenti, E., Oser, G., van der Wath, R. C., Blanco-Bose, W., Jaworski, M., Offner, S., Dunant, C. F., Eshkind, L., Bockamp, E., Lió, P., MacDonald, H. R., & Trumpp, A. (2008). Hematopoietic Stem Cells Reversibly Switch from Dormancy to Self-Renewal during Homeostasis and Repair. *Cell*, 135(6), 1118–1129. <https://doi.org/10.1016/j.cell.2008.10.048>
- Wilson, N. K., Calero-Nieto, F. J., Ferreira, R., & Göttgens, B. (2011). Transcriptional regulation of haematopoietic transcription factors. *Stem Cell Research & Therapy*, 2(1), 6. <https://doi.org/10.1186/scrt47>
- Woolthuis, C. M., Mariani, N., Verkaik-Schakel, R. N., Brouwers-Vos, A. Z., Schuringa, J. J., Vellenga, E., de Wolf, J. T. M., & Huls, G. (2014). Aging Impairs Long-Term Hematopoietic Regeneration after Autologous Stem Cell Transplantation. *Biology of Blood and Marrow Transplantation*, 20(6), 865–871. <https://doi.org/10.1016/j.bbmt.2014.03.001>
- Wright, D. E. (2001). Physiological Migration of Hematopoietic Stem and Progenitor Cells. *Science*, 294(5548), 1933–1936. <https://doi.org/10.1126/science.1064081>

Wu, A. M., Till, J. E., Siminovitch, L., & McCulloch, E. A. (1967). A cytological study of the capacity for differentiation of normal hemopoietic colony-forming cells. *Journal of Cellular Physiology*, *69*(2), 177–184. <https://doi.org/10.1002/jcp.1040690208>

Wu, A. M., Till, J. E., Siminovitch, L., & McCulloch, E. A. (1968). Cytological Evidence for a Relationship Between Normal Hematopoietic Colony-Forming Cells and Cells of the Lymphoid System. *Journal of Experimental Medicine*, *127*(3), 455–464.
<https://doi.org/10.1084/jem.127.3.455>

Yahata, T., Takanashi, T., Mugeruma, Y., Ibrahim, A. A., Matsuzawa, H., Uno, T., Sheng, Y., Onizuka, M., Ito, M., Kato, S., & Ando, K. (2011). Accumulation of oxidative DNA damage restricts the self-renewal capacity of human hematopoietic stem cells. *Blood*, *118*(11), 2941–2950. <https://doi.org/10.1182/blood-2011-01-330050>

Yamamoto, R., Morita, Y., Ooehara, J., Hamanaka, S., Onodera, M., Rudolph, K. L., Ema, H., & Nakauchi, H. (2013). Clonal Analysis Unveils Self-Renewing Lineage-Restricted Progenitors Generated Directly from Hematopoietic Stem Cells. *Cell*, *154*(5), 1112–1126.
<https://doi.org/10.1016/j.cell.2013.08.007>

Yamamoto, R., Wilkinson, A. C., Ooehara, J., Lan, X., Lai, C.-Y., Nakauchi, Y., Pritchard, J. K., & Nakauchi, H. (2018). Large-Scale Clonal Analysis Resolves Aging of the Mouse Hematopoietic Stem Cell Compartment. *Cell Stem Cell*, *22*(4), 600-607.e4.
<https://doi.org/10.1016/j.stem.2018.03.013>

Yang, H. W., Chung, M., Kudo, T., & Meyer, T. (2017). Competing memories of mitogen and p53 signalling control cell-cycle entry. *Nature*, *549*(7672), 404–408.
<https://doi.org/10.1038/nature23880>

Yizhak, K., Aguet, F., Kim, J., Hess, J. M., Kübler, K., Grimsby, J., Frazer, R., Zhang, H., Haradhvala, N. J., Rosebrock, D., Livitz, D., Li, X., Arich-Landkof, E., Shores, N., Stewart, C., Segrè, A. V., Branton, P. A., Polak, P., Ardlie, K. G., & Getz, G. (2019). RNA sequence analysis reveals macroscopic somatic clonal expansion across normal tissues. *Science*, *364*(6444), eaaw0726. <https://doi.org/10.1126/science.aaw0726>

Young, A. L., Challen, G. A., Birmann, B. M., & Druley, T. E. (2016). Clonal haematopoiesis harbouring AML-associated mutations is ubiquitous in healthy adults. *Nature Communications*, *7*(1), 12484. <https://doi.org/10.1038/ncomms12484>

Young, K., Eudy, E., Bell, R., Loberg, M. A., Stearns, T., Sharma, D., Velten, L., Haas, S., Filippi, M.-D., & Trowbridge, J. J. (2021). Decline in IGF1 in the bone marrow microenvironment initiates hematopoietic stem cell aging. *Cell Stem Cell*, S1934590921001235. <https://doi.org/10.1016/j.stem.2021.03.017>

Yu, K.-R., Espinoza, D. A., Wu, C., Truitt, L., Shin, T.-H., Chen, S., Fan, X., Yabe, I. M., Panch, S., Hong, S. G., Koelle, S., Lu, R., Bonifacino, A., Krouse, A., Metzger, M., Donahue, R. E., & Dunbar, C. E. (2018). The impact of aging on primate hematopoiesis as interrogated by clonal tracking. *Blood*, *131*(11), 1195–1205. <https://doi.org/10.1182/blood-2017-08-802033>

Yu, V. W. C., Yusuf, R. Z., Oki, T., Wu, J., Saez, B., Wang, X., Cook, C., Baryawno, N., Ziller, M. J., Lee, E., Gu, H., Meissner, A., Lin, C. P., Kharchenko, P. V., & Scadden, D. T. (2016). Epigenetic Memory Underlies Cell-Autonomous Heterogeneous Behavior of Hematopoietic Stem Cells. *Cell*, *167*(5), 1310-1322.e17. <https://doi.org/10.1016/j.cell.2016.10.045>

Yuan, Y., Shen, H., Franklin, D. S., Scadden, D. T., & Cheng, T. (2004). In vivo self-renewing divisions of haematopoietic stem cells are increased in the absence of the early G1-phase inhibitor, p18INK4C. *Nature Cell Biology*, 6(5), 436–442. <https://doi.org/10.1038/ncb1126>

Yurino, A., Takenaka, K., Yamauchi, T., Nunomura, T., Uehara, Y., Jinnouchi, F., Miyawaki, K., Kikushige, Y., Kato, K., Miyamoto, T., Iwasaki, H., Kunisaki, Y., & Akashi, K. (2016). Enhanced Reconstitution of Human Erythropoiesis and Thrombopoiesis in an Immunodeficient Mouse Model with Kit Wv Mutations. *Stem Cell Reports*, 7(3), 425–438. <https://doi.org/10.1016/j.stemcr.2016.07.002>

Zandstra, Conneally, Piret, & Eaves. (1998). Ontogeny-associated changes in the cytokine responses of primitive human haematopoietic cells. *British Journal of Haematology*, 101(4), 770–778. <https://doi.org/10.1046/j.1365-2141.1998.00777.x>

Zandstra, P. W., Conneally, E., Petzer, A. L., Piret, J. M., & Eaves, C. J. (1997). Cytokine manipulation of primitive human hematopoietic cell self-renewal. *Proceedings of the National Academy of Sciences*, 94(9), 4698–4703. <https://doi.org/10.1073/pnas.94.9.4698>

Zeng, H., Yücel, R., Kosan, C., Klein-Hitpass, L., & Möröy, T. (2004). Transcription factor Gfi1 regulates self-renewal and engraftment of hematopoietic stem cells. *The EMBO Journal*, 23(20), 4116–4125. <https://doi.org/10.1038/sj.emboj.7600419>

Zhang, Y., Stehling-Sun, S., Lezon-Geyda, K., Juneja, S. C., Coillard, L., Chatterjee, G., Wuertz, C. A., Camargo, F., & Perkins, A. S. (2011). PR-domain-containing Mds1-Evi1 is critical for long-term hematopoietic stem cell function. *Blood*, 118(14), 3853–3861. <https://doi.org/10.1182/blood-2011-02-334680>

Zhao, X., Gao, S., Wu, Z., Kajigaya, S., Feng, X., Liu, Q., Townsley, D. M., Cooper, J., Chen, J., Keyvanfar, K., Fernandez Ibanez, M. del P., Wang, X., & Young, N. S. (2017). Single-cell RNA-seq reveals a distinct transcriptome signature of aneuploid hematopoietic cells. *Blood*, *130*(25), 2762–2773. <https://doi.org/10.1182/blood-2017-08-803353>

Zheng, S., Papalexi, E., Butler, A., Stephenson, W., & Satija, R. (2018). Molecular transitions in early progenitors during human cord blood hematopoiesis. *Molecular Systems Biology*, *14*(3), e8041. <https://doi.org/10.15252/msb.20178041>